6-16-2011

Solar Warning Architecture for Manned Missions to Mars

James S. Bohren

John K. Howard

SOLAR WARNING ARCHITECTURE FOR MANNED MISSIONS TO MARS

THESIS

James S. Bohren
Major, USAF

John K. Howard
Major USAF

AFIT/GSE/ENV/11-J01DL

DEPARTMENT OF THE AIR FORCE
AIR UNIVERSITY

AIR FORCE INSTITUTE OF TECHNOLOGY

Wright-Patterson Air Force base, Ohio

AFIT/GSE/ENV/11-J01DL

SOLAR WARNING ARCHITECTURE FOR MANNED MISSIONS TO MARS

THESIS

Presented to the faculty

Department of Systems and Engineering Management

Graduate School of Engineering and Management

Air University

Air Education and Training Command

In partial Fulfillment of the Requirements for the

Degree of Master of Science in Systems Engineering

James S. Bohren
Major, USAF

John K. Howard
Major USAF

June 2011

AFIT/GSE/ENV/11-J01DL

SOLAR WARNING ARCHITECTURE FOR MANNED MISSIONS TO MARS

James S. Bohren
Major, USAF

John K. Howard
Major USAF

Approved:

_____	_____
John M. Colombi, Ph.D. (Chairman)	Date
_____	_____
Michael E. Miller, Ph.D. (Member)	Date
_____	_____
Joseph J. Pignatiello, Ph.D. (Member)	Date

Abstract

Solar radiation storms present a significant threat to future manned missions to Mars and other bodies within the solar system. Due to the radiation storm hazard to both Earth-orbit missions and terrestrial infrastructures, an international solar monitoring and forecasting architecture has been established. When monitoring indicates a solar storm is imminent, forecasters issue alerts so that terrestrial entities and operations have time to activate protective measures, such as placing at-risk satellites in "safe" operating modes. Space forecasters have made great strides in protecting Earth-based activities from solar weather, but little analysis has been documented on how to protect interplanetary manned missions, such as the one planned to Mars in the 2030's timeframe.

With the renewed interest in sending astronauts to Mars within the next 30 years, there is a clear mandate to develop radiation protection systems, a key aspect of which is the timely provision of solar storm warnings to the potentially threatened spacecraft throughout its entire mission. Analyzing concepts for solar warning architectures holds merit for three reasons: the requirement is foundational, prerequisite, and achievable. An effective solar warning architecture is foundational as a baseline requirement for any active protection measures; prerequisite because the design must be defined and integrated into the manned mission before embarkation; and achievable in that mankind currently has the technology and capability. Lastly, protection of astronauts is a national imperative.

The project's primary objective was to develop a solar warning architecture that provides coverage for a potential manned mission to Mars. The Mars scenario was selected due to its relatively high likelihood, the robust body of background data available, and the adaptability of the analytic methods, concepts, and trade spaces to other planetary missions. Relying on the industry-standard Satellite Tool Kit (STK) for modeling and simulation, a series of models were developed to assess the feasibility, cost, and effectiveness of 14 candidate solar warning architectures. Candidates were measured and compared according to two performance metrics: warning time and solar coverage. The cost of each architecture was also assessed by estimating the total dry mass of all required components. Correlation of the performance metric of each architecture to its estimated cost enabled construction of an efficient frontier which illustrated the relative cost-benefit merits of each candidate. Efficient frontiers analysis indicated clusters of candidates with strong or weak performance and provided insights into overarching performance characteristics within certain architecture families. Finally, value modeling was applied to identify an overall "best-value" architecture solution.

Acknowledgments

First and foremost, I would like to thank Maj "Sig" Bohren for embarking on this adventure with me; there were many times we did not know "how" or "if" it would turn out. I would also like to thank our advisor, Dr. Colombi, for his patience and insight, and for giving me kindly-worded kicks in the pants whenever I lost momentum. Most importantly I'm grateful to my wife and hero, who sacrificed tremendous amounts of time and energy for me. Additional thanks go to the following people: Dr. Black for providing us with a never-ending supply of STK licenses, Lt Col Ross Balestreri who taught me all about efficient frontiers analysis and started me on the Systems Engineering path, and my 3rd-grade daughter, who reminded her old Dad how to do technical writing by teaching him all about T-charts.

- Maj John Howard

Top of this list I must thank Maj John Howard for all the work, brainstorming, debates, and discussion that made this thesis what it is. I would also like to thank Dr. John Colombi, our thesis advisor who's ability to both get us focused and to always know the right time to check up on us was invaluable, and without which we would never have completed this effort. Additional thanks go to Dr. Black who was always encouraging when dealing with STK neophytes; Jennifer Jahn, Kristen Jones, and Lynn Curtis who have provided outstanding support throughout the entire program in keeping a wayward distance learning student on track with all the AFIT paperwork; and the team at the AFIT Library: Patrick Colucci, Kathi French, and Amanda Lindsey for their invaluable support in finding and acquiring the documents to support this research. Finally, and most importantly, as the foundation of it all I wish to thank my wife: life partner and best friend. Without your Love, support, and encouragement I could never have succeeded in this. You make me a better person.

- Maj James "Sig" Bohren

Table of Contents

Page

Page

List of Figures

Page

List of Tables

SOLAR WARNING ARCHITECTURE FOR MANNED MISSIONS TO MARS

1.0 Introduction

1.1 Background

Between 11:18 a.m. and 11:23 a.m., on September 1st, 1859, Richard Carrington of the Royal Astronomical Society witnessed "two patches of intensely bright and white light" appear and then fade while observing the sun and recording sunspots (Carrington 1860). See Figure 1-1 from this day. This event has become known as the "Carrington Event" and is recognized by the scientific community as the first time a solar flare was ever observed and recorded (Cliver and Svalgaard 2004). In an amazing coincidence, the Carrington Event is also widely considered to be the largest solar flare to have occurred within the last 500 years (NASA Science, Science News 2008). The solar flare Carrington observed was soon followed by reports of strange phenomena all over the world: auroras as far south as the Caribbean and Hawaii, widespread failures of telegraph systems, and induced currents in wires that had been disconnected from their power sources (Cliver and Svalgaard 2004). Not only was the Carrington Event significant as the first observation of a solar flare, it was also the first documented case of solar weather impacting human industry and society.

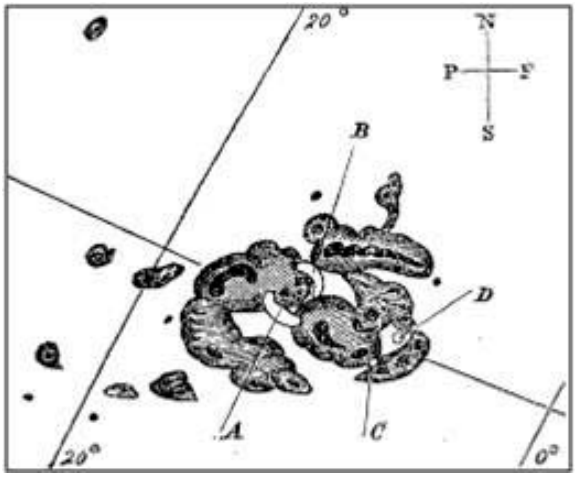

Figure 1-1: Sunspots sketched on Sept 1, 1859 (Carrington 1860)

In the 151 years since Carrington's first solar flare observation, mankind's knowledge of the Sun, solar weather, the solar cycle, and their combined impacts on human activities has grown significantly. Solar science is driven by mankind's need to understand how the Sun affects the various infrastructures which form the basis of our industry, economy, and everyday life: electric power, communications, navigation, and satellites. Solar weather, specifically solar storms present a very real and ever-present danger to the foundations of modern society. Much like terrestrial weather forecasting, solar forecasting is equal parts art and science. Despite access to state-of-the-art monitoring architectures which provide 24-7 coverage of solar activity, solar forecasters are challenged to reliably predict the timing and magnitude of solar storms, let alone the exact effects they will have on modern terrestrial infrastructures.

Solar storms represent a particularly significant hazard to manned space missions in the form of potentially lethal high-dosage exposure to radiation. The solar weather threat to manned spaceflight was first identified during the Apollo program. On August

2nd, 1972, the Sun erupted with a series of major solar flares that lasted for 10 days, which just so happened to occur between Apollo 16 in April 1972 and the scheduled Apollo 17 in December 1972. This unexpected series of major solar flares during an otherwise quiet period of the Sun caught NASA by surprise and kicked off decades of studies which analyzed what might have happened had an Apollo mission been in progress during a solar storm. While no one can know for sure how the Apollo spacecraft hardware would have fared, it is widely accepted that the radiation doses absorbed by the astronauts would have been fatal (Carlowicz and Lopez 2002). Even more alarming, the only mitigation would have been to move the crew into the Command Module, which offered some radiation shielding by virtue of its construction. Of course, this assumes the flares could have been identified and the astronauts warned in a timely manner.

Since the termination of the Apollo program, manned space missions have not ventured beyond Low Earth Orbit (LEO), and there is currently no ongoing requirement to warn manned missions operating outside the immediate vicinity of the Earth. However, based on increasing scientific and public discussions of manned missions to return to the Moon, explore near-earth asteroids, and even visit Mars, a deep-space solar weather warning requirement will exist within the next few decades. Specifically, a manned mission to Mars has been part of the official United States Space Policy during the last two presidential administrations (NASA 2004) (White House 2010). NASA has also developed and regularly updated a Mars mission reference design for over a decade (NASA 1997). More recently, the US Human Space Flight Plans Committee identified Mars as the best opportunity for meaningful manned space exploration in its 2009 annual

report. The Committee even recommended two possible roadmaps to Mars: "Moon First" and "Flexible Path" (Review of U.S. Human Spaceflight Plans Committee 2009). Given the current scientific enthusiasm and renewed interest in manned spaceflight beyond LEO it is almost certain that a manned mission to Mars will take place within the next 50 years. But what if another high-magnitude solar flare and associated radiation storm, like those of 1859 and 1972, were to occur while the manned mission was transiting deep space, outside the relative protection offered by the Earth's magnetic field? The immediate consequences to the crew and mission would be dire, including the rapid onset of debilitating radiation sickness and potentially death.

Over the last 15 years, the United States and other nations around the world have integrated a vast network of solar sensors and communications to evolve a solar warning architecture which enables solar weather forecasting and timely warnings to potentially affected terrestrial and orbital infrastructures. Despite recent efforts such as the STEREO program to expand coverage of the Sun, Earth's solar monitoring architecture is highly Earth-centric and limited to detecting and tracking solar storms aimed in the vicinity of Earth. Simply stated, manned interplanetary missions shall require more robust solar surveillance and warning systems than currently exist, the architectures of which must be selected – ones that can provide accurate forecasting and timely warnings beyond the "Sun-Earth corridor".

Space radiation is widely recognized within the space community as one of the main challenges to human exploration of space, and there are several research efforts underway to analyze mitigation methods for both the immediate (deterministic) and long term (stochastic) risks of space radiation to humans. Current lines of research include

physical hardening, electromagnetic shielding, anti-radiation drugs, and possibly even genetically engineered radiation resistance. While several of these mitigation concepts are either passive or preventative measures, most are reactive and will require the crew to take action in response to warning of an impending radiation threat. Whether the crew must activate some type of radiation deflector field, don special space suits, ingest special anti-radiation medicines, or simply relocate to a heavily shielded portion of the spacecraft as is currently done on the International Space Station, the astronauts will require sufficient warning of the radiation storm's arrival to have time to activate their protective countermeasures. Compounding the issue is the likelihood that no single mitigation concept will provide 100% protection and multiple countermeasures will likely have to be activated in conjunction to maintain the survival and health of the crew. Provision of warning is a baseline requirement for any conceivable concept or architecture involving the protection of astronauts from solar radiation storms in deep space.

Due to the foundational significance of providing radiation storm warnings, this thesis will examine a total of 14 candidate solar warning architectures developed from functional requirements, and evaluate the effectiveness and cost of each in the context of a planned human mission to Mars. The primary objective is to identify a reference architecture which maximizes performance, in this case both warning time and solar coverage, and minimizes cost, represented by the total dry mass that must be launched into Earth orbit.

1.2 Problem Statement

Solar radiation storms are a significant threat to interplanetary manned spaceflight within our solar system, specifically any planned missions to Mars. The United States, in coordination with other countries, has established a global solar weather monitoring architecture that provides Earth-centric solar warnings. However, only limited analysis has been conducted to define and analyze architectures which can provide radiation storm warnings for proposed interplanetary missions. Candidate architectures that can monitor solar weather, detect hazardous solar events, and warn threatened interplanetary assets must be defined, analyzed, and assessed to identify a reference architecture that optimizes warning time and solar coverage while minimizing deployment cost.

1.3 Research Focus

Providing timely solar storm warnings to manned missions bound for Mars will require a complex system of systems consisting of sensors, data processing nodes, and control centers, interconnected via a deep space communications network. This research project focuses on applying model-based systems engineering (MBSE) and analysis to determine how to best arrange these various component nodes into an architecture that maximizes warning time, maximizes solar coverage, while minimizing the total dry mass-to-orbit cost required to deploy the architecture. This study does not focus on the design of detection or protection systems or their underlying technologies. Characteristics of nodes used in modeling the candidate architectures are functionally identical to space capabilities that are currently in use or on orbit today. For example, all solar monitoring nodes have been assigned mass and sensor capabilities identical to the

suite of solar sensors current deployed aboard the Solar Terrestrial Relations Observatory (STEREO) missions (NASA 2006). Leveraging existing technologies and capabilities accomplishes two things: it demonstrates the feasibility of implementing a candidate architecture, and it ensures the research is focused at the appropriate level, namely the architecture's arrangement and the interactions of its nodes to function as whole.

1.4 Methodology

The analysis began by researching the threat, specifically the history and science of solar weather and solar forecasting. This background study enabled identification of key parameters required to model a radiation storm scenario, such as the fact that radio-spectrometry signals provide initial indications of potential solar storms, and that storm particles travel at about 75,000 km/sec (Poppe 2006) between the Sun and Earth. Next, a review of current manned Mars mission plans was conducted. This review included both government and private proposals, and had the goal of identifying a suitably feasible Mars mission scenario against which to "play" the solar warning architectures and assess their performance. The NASA Design Reference Mission 5.0 (NASA 2009) was selected as the simulation scenario due to its maturity, feasibility, and status within the space mission planning community.

The next phase was to develop a set of candidate solar warning architecture concepts. First, a set of baseline functional requirements was developed and defined, to include the capabilities to monitor solar weather, identify and track solar radiation storms, and communicate a warning to threatened spacecraft. From these functional requirements, Warning Time and Solar Coverage were identified as the most significant

performance parameters, and a cost metric was also identified as Dry Mass to Orbit. Then, by examining relevant options for sensor, communications, and processing node locations and links, a set of 14 candidate architectures was iteratively developed via permutation. Each architecture was illustrated and formatted to simplify incorporation into modeling and simulation.

Detailed modeling and simulation was accomplished using AGI's Satellite Tool Kit (STK). Each of the 14 architectures was "played" against the full epoch of a manned Mars mission scenario based directly on the previously selected NASA Design Reference Mission 5.0. Since the locations of all architecture nodes and the spacecraft were dynamic across the entire epoch, dynamic performance values of Warning Time and Solar Coverage were characterized by measuring how the given architecture would perform if a solar storm occurred every 24 hours (an artificially high frequency used to normalize the randomness of solar storm timing). An interval of 24 hours was selected because it ensured generation of a large data set from across the three-year mission epoch. A shorter interval such as 12 hours would proportionally increase the already-massive data sets generated without providing a corresponding improvement in characterizing performance. Total Dry Mass cost budgets for each architecture were developed parametrically by obtaining mass data on current state-of-the art solar monitoring missions and sensor suites, and applying historic mass-budget % breakdowns from past satellite programs.

Warning Time over the mission epoch was calculated by determining the time delta between when the Mars mission spacecraft first received a warning by the fastest path of the architecture being measured and the point in time at which the respective solar

radiation storm actually "hit" the spacecraft, measured in minutes. Fastest warning time was calculated by extracting from STK the distances between architecture nodes, the Sun, and the Earth at each simulated 24 hour storm interval. Based on the architecture configuration, these links formed various warning paths from the Sun to the spacecraft transited by electromagnetic signals including solar signatures, processed data, and communications. Path timings were then calculated by assuming all EM signals traveled at the speed of light and by then adding in estimated time delays for each node transited. The "fastest" path at each 24 hour mission interval was then used in the Warning Time calculation. Solar radiation time was calculated by assuming the worst-case solar storm scenario at each 24 hour interval with the primary axis of the storm being aimed directly at the spacecraft. The distance between the spacecraft and the Sun at every 24 hour interval was extracted from STK and the initial radiation storm arrival time was calculated using the typical solar radiation velocity of 75,000 km/sec (Poppe 2006).

Before dynamic Solar Coverage performance could be calculated, general sets of equations for multi-sensor coverage of the Sun had to be developed. To simplify the equations, only circumferential coverage of the Sun was considered, and a single sensor was assumed to provide 180 degrees or 50% coverage at any point in time, regardless of distance or field of view. From this starting point, a set of percent coverage equations was developed for each individual architecture concept, based on the number of solar sensors present and their relative angles to a baseline sensor. The relative angles between sensors over time were calculated within STK, extracted into MS Excel, and then converted into percent coverage values based on the previously developed equations.

The final step of the analysis was converting the calculated data into usable results. Efficient frontiers analysis was leveraged by plotting the cost (Dry Mass) versus performance (Warning Time and Solar Coverage) for each architecture on the same two-axis graph. The resulting efficient frontier of architectures was then examined to determine the "best-value" architecture solution and observe performance trends.

1.5 Primary Assumptions

The following are the primary assumptions used in this research, modeling, simulation, and analysis. The assumptions are divided into two main categories: Architecture and Analysis. Architecture assumptions were those used in developing the candidate architectures themselves, whereas Analysis assumptions were directly incorporated into the modeling and simulation work.

1.5.1 Architectural Assumptions

1. More warning time is always better. Because solar radiation countermeasure timeline requirements are undefined, warning time is an open-ended requirement with no upper bound, and candidate architectures can be compared with this performance metric as an absolute.

2. Mission planners will have developed emergency countermeasures for the crew in the event of a solar storm which will allow them to survive if provided sufficient warning.

3. The solar warning architecture will be optimized for a Mars mission only and does not need to consider supporting missions to other planetary bodies or near-Earth-objects.

4. All sensors have a 100% probability of detecting a given flare and all satellites or other nodes have a 100% uptime, meaning there are no failures over the course of the scenario epoch, and all systems work 100% as designed.

5. Any satellites placed at libration points will have sufficient fuel to maintain their positions throughout the duration of the mission epoch. Furthermore, satellites placed at the Sun-Earth L4 and L5 libration points will be sufficiently hardened or otherwise protected to survive at these locations for extended periods of time. For reference, Sun-Earth L4 and L5 orbit the Sun at a distance of 1 AU, 60 degrees ahead of and behind the Earth, respectively (see Figure 2-6).

6. Any Mars mission will have a baseline communications (specifically the Deep Space Network) architecture used to ensure connectivity between the Earth, Mars, and any spacecraft in-transit. A deployed solar warning architecture will have priority access to this communications network and will leverage it as required.

1.5.2 Analysis Assumptions

1. Past patterns of solar storm activity (frequency and intensity) will remain valid throughout the period of the manned Mars mission.

2. Communications among architecture nodes will occur at the speed of light.

3. Node processing times for solar warning will be identical to current capabilities.

4. Solar flare indications originate from the outer radius of the Sun at the speed of light.

5. Solar radiation storms originate from the outer radius of the Sun at the exact same time as their associated signatures, but only travel at 75,000 km/sec (Poppe 2006).

6. The epoch and trajectories of the simulated Mars mission scenario are based on NASA DRM 5.0 and the POTUS-stated objective to send a manned mission to Mars in the 2030's timeframe.

7. Any terrestrial processing nodes involving human interactions will incur a 10 minute time delay. This delay shall be adjustable pending more accurate data regarding the timing of current space weather forecasting and warning C2.

1.6 Implications

Mankind must face and overcome the challenges of solar weather and the ever-present threat of solar radiation storms to achieve interplanetary spaceflight. Since warning time is a foundational requirement to any mitigation strategy or protection concept under consideration, the amount of warning time provided by a solar warning architecture will logically drive and define performance requirements for the countermeasures themselves. Likewise, countermeasure performance and cost limitations will, in turn, drive minimum warning time requirements for a reference architecture. This chicken versus egg requirements loop is a common interaction between sensor and execution architectures, but the cycle must be started somewhere. This initial study of solar warning architectures also serves as an excellent starting point for more detailed examinations of the trade spaces involved, or perhaps an expansion of the architectural performance factors requiring consideration. This project also implies there is a long-term issue to be resolved whether mankind should deploy a system-wide

solar monitoring architecture or continue to focus on mission-specific point solutions. Finally, as several of the architectures utilize the manned spacecraft itself as a sensor/processing node, there may also be implications to crew manning and training requirements if the utility of onboard solar weather monitoring is demonstrated.

1.7 Thesis Overview by Chapter

Chapter 1.0 has served as an overview of the project. It introduced the challenge of protecting manned spaceflight from solar radiation; provided a brief background on the myriad of sub-topics involved in analyzing such a problem; described the main assumptions applied to both the candidate architecture development and the comparative effectiveness analysis; summarized the methods involved in candidate solution development, analysis, and assessment; and outlined some of the potential implications.

Chapter 2.0 provides background on a diverse set of topics central to the project including: solar weather, physiological radiation effects, Mars mission plans, Earth's solar warning architecture, solar monitoring capabilities, and architecture placement options to include libration points. Of particular note is the fact that a review of published literature yielded only a single paper on the specific topic of providing radiation storm warnings to manned interstellar space flights, thus necessitating a decomposition of the problem into component areas of interest.

Chapter 3.0 discusses the methods used to accomplish the project. After identifying as much information as possible about the solar radiation storm threat, primary performance and cost metrics were identified by which to compare any candidate architecture solutions developed, specifically Warning Time and Solar Coverage for

performance and Dry Mass to Orbit for cost. Then by examining relevant options for sensor, communications, and processing node locations and links, a set of 14 candidate architectures was iteratively developed via permutation. Next, detailed modeling and simulation was accomplished using AGI's Satellite Tool Kit (STK). Each of the 14 architectures was "played" against the full epoch of a manned Mars mission scenario based directly on NASA's official Design Reference Mission 5.0. Since the locations of all architecture nodes and the spacecraft were dynamic across the entire epoch, dynamic performance of each candidate was characterized by measuring how the given architecture would perform if a solar storm occurred every 24 hours (an artificially high frequency used to normalize the randomness of solar storm timing). Dry Mass to Orbit cost budgets for each architecture were developed parametrically by obtaining mass data on current state-of-the art solar monitoring missions and sensor suites, and applying historic mass-budget percentage breakdowns.

Chapter 4.0 focuses on the results of the research, with a primary emphasis on the modeling and simulation outputs. Relative performances and costs of each architecture candidate are compiled on efficient frontier charts for both Warning Time and Solar Coverage. Efficient frontier charts are similar to cost-benefit analysis charts and can be used to "rack-and-stack" architecture candidates in a number of ways based on performance and cost. In this case, the efficient frontier charts enabled identification of candidate architectures which maximized Warning Time and Solar Coverage while minimizing Dry Mass to Orbit cost. Associated outputs depicting the relative performances of each candidate across the entire mission epoch are also provided and discussed.

Finally, Chapter 5.0 discusses main conclusions from the results of the analysis, including any implications to this and related fields of study. Recommended best-value solutions based on each individual performance metric, plus a composite "best-of-both-worlds" recommendation is provided. Any trends or clustering of candidate results are also discussed along with potential explanations. The chapter concludes with how the "best value" determination might change based on alternative planning assumptions, effectiveness metrics, or cost versus performance priorities, providing some direct references to future avenues of research.

2.0 Background

2.1 Introduction

The challenge of developing a solar warning architecture with coverage beyond Earth-Moon space is unique in that there is very little background material available on this specific topic. The minimal amount of published research is surprising given the renewed interest in Mars exploration and the well-known radiation hazards of space weather and space travel. Since there was limited information on the specific problem of providing solar radiation storm warnings to a manned mission to Mars, it became necessary to decompose the problem into sub-topics to compile a body of background information suitable for analysis. By examining the challenge from an architectural perspective, the following topics were identified as the primary items of interest: radiation effects on humans, space radiation, solar weather, Earth's solar warning architecture, Mars mission planning, and libration points. In addition, the limited previous analysis on this problem was mined for information.

2.2 Radiation Effects on Humans

In 1958 the United States launched its first-ever satellites, the Explorer series, in an attempt to catch up with the Soviet Union at the outset of the Space Race. The Explorer satellites included small scientific payloads which allowed Dr. James Van Allen to discover the presence of vast quantities of high-energy radiation in belts orbiting the Earth. After an instrument failure during one particular mission, it was determined that the radiation detector onboard had failed due to complete saturation. One of Dr. Van

Allen's colleagues exclaimed "My God, space is radioactive!" and from that point on, it became widely known that space was highly radioactive and the mandate to protect astronauts from the hazards of space radiation was born (Poppe 2006).

As a result, the scientific and medical communities have conducted extensive research on radiation and its effects on living organisms. High energy radiation (HER) is extremely harmful to humans and most living organisms. HER causes two primary categories of damage at the cellular level: cell death and genetic damage. Cell death happens when the HER ruptures the cell or destroys one of its internal components. Researchers refer to the symptoms associated with cell death as "deterministic effects" because there are direct, quantifiable relationships between HER dosage and the onset of symptoms collectively labeled as radiation sickness. Genetic damage occurs whenever a HER particle happens to hit the cell's DNA strand, resulting in partial or complete severing (Geard 1982). By harming or altering the cell's DNA, HER genetic damage can eliminate a cell's ability to reproduce, thus impacting an organ's ability to self-repair. Genetic damage can also result in cell mutation and uncontrolled cell reproduction which are associated with cancer. Finally, genetic damage to cells within the reproductive system can lead directly to birth defects. Genetic damage is collectively referred to as "stochastic effects" because they are characterized by probability: either the chance a given health issue will occur within a long-term time span after a radiation exposure, or the chance an effect will manifest after low-level dosages over a period of time, typically years or decades.

Deterministic effects are commonly known as radiation sickness or acute radiation syndrome (ARS), with the exact symptoms and severity determined by total

dosage, how quickly the dosage is received, and the dosage distribution within the body (Young 1987). Deterministic effects begin 30 minutes to 2 hours after a high dose of radiation is received within a short span of time, which is the exposure profile an astronaut will likely face in the path of a solar storm of high-energy particles. Even more alarming from a space mission standpoint is that the initial radiation dosing is painless and undetectable to human senses (Young 1987). ARS consists of a wide range of symptoms and ailments that appear in various combinations and sequences depending on the variables above, any of which can incapacitate an astronaut and likely place the entire mission at risk. These deterministic effects typically include nausea, vomiting, diarrhea, fatigue, dizziness, disorientation, bleeding, fever, infection, ulcers, dehydration, headaches, fainting, and even death in as little as 32 hours for high-end radiation doses (Young 1987). Acute radiation sickness is due to the radiation damaging or killing off large numbers of cells, which result in tissue and organ damage, overwhelming the body's ability to repair itself. Also, deterministic effects do not always manifest all at once, but can build up over a period of hours or days, as the various parts of the body are overwhelmed and shut down (Young 1987).

Stochastic effects, also referred to as "low-level" or "late" effects, represent long term health risks, such as cancer, cataracts, growth and development changes, or damage to the reproductive system which can cause birth defects (Devine and Chaput 1987). Stochastic effects are probabilistic in nature, but because the health issues listed above occur naturally in a given population, it is difficult to quantify the exact contribution of radiation exposure to the total probability of a given health effect occurring. However, it has been repeatedly proven through animal testing that "the probability of late effects

increases with dose, dose rate, and linear energy transfer" (Devine and Chaput 1987). Little is known about the exact probabilities and timelines of stochastic effects because there is such a small pool of subjects from which to draw data, which include Japanese survivors of the WWII nuclear bombs, Russians who secured the Chernobyl reactor, and US and Soviet astronauts who have ventured into space. While a concern to the long term health of astronauts, the stochastic effects of radiation do not represent an immediate threat to a space mission in progress, and mitigation of long term radiation exposure is not the objective of this architecture.

2.3 Space Radiation

There are two primary sources of high-energy radiation in deep space: galactic cosmic rays (GCR) and solar cosmic radiation (SCR). Galactic cosmic rays are high energy particles transiting free space in all directions, having originated from stars in other solar systems and galaxies. GCR flux varies according to the 11-year solar cycle, due to the variations in the strength of the solar magnetic field. GCR flux is minimized during the solar maximum because the Sun's magnetic field disperses more of the particles. Likewise, GCR flux is at a maximum during solar minimum. GCR is considered background radiation because it only accounts for about 5-10% of the total radiation dosage astronauts receive on any given mission, and it's very difficult to shield against due to the high energies involved (Tascione 1994). Until more effective or mass-efficient shielding is developed, long term GCR exposure can be minimized by planning interplanetary missions for periods of solar maximum.

SCRs are heavy particles accelerated to high energies (10^7 to 10^9 eV) during large solar flares and coronal mass ejections (Tascione 1994). These particle storms can represent a 1000 times increase in radiation dosage over a very short period of time, which means they can be highly lethal. The frequency and magnitude of solar events causing SCR have been correlated to the 11 year solar cycle; however, the timing and direction of the resulting solar storms remain highly unpredictable. For this reason, astronauts transiting deep space shall require the means to detect and track solar radiation storms, determine the threat they pose, and have sufficient time to enable any countermeasures that will ensure their wellness and survival.

To understand how lethal these SCR events can be, some background in deterministic radiation effects on humans is required. Radiation absorbed dose (rad) is defined as the amount of ionizing radiation required for 1 kg of material to absorb 0.01 joule. For reference, 100-200 rads has a high probability of killing a cell and in turn causing radiation sickness. However, the total amount of energy absorbed is not the only factor in damage caused. The source of the radiation changes the damage profile as well, with larger particles such as high energy protons causing more damage than smaller particles even at the same energy levels. RBE stands for relative biological effectiveness and indicates the relative effect of a radiation source on biological tissue compared to a 200 keV beam of x-rays. Finally, the rem (Roentgen equivalent man) unit of measure relates absorbed dose to total biological damage based on dosage and RBE, where rem = rad × RBE. For reference, the Roentgen is a basic unit of radiation energy where one roentgen is the amount of energy required to deposit 2.58E-04 coulombs per kg in dry air.

Extensive research in the field of radiation biology has yielded insight into the deterministic effects of radiation on humans. Table 2-1 shows the RBE of various particles, Table 2-2 estimates rem dosages across a range of typical space missions, and Table 2-3 summarizes the grim effects of radiation on a sample population, organized by rem dosage levels.

Table 2-1: Relative biological effectiveness (Bueche 1981)

Radiation Source	RBE
5 MeV gamma rays	0.5
1 MeV gamma rays	0.7
200 keV gamma rays	1.0
Electrons	1.0
Protons	2.0
Neutrons	2-10
Alpha Particles	10-20

Table 2-2: Predicted radiation doses (Bostrom, et al. 1987)

Orbital Inclination/Altitude	Shielding Thickness	Predicted Dose
28.5 deg / 450 km	1.0 g/cm^2	
- Trapped Radiation		7.3 rem
- GCRs		0.4 rem
- Solar Flare Cosmic Rays from Anomalously Large Flare (SCR/ALF)		0.0 (shielded by geomagnetic field)
57.0 deg / 450 km	1.0 g/cm^2	
- Trapped Radiation		4.7 rem
- GCRs		0.7 rem
- SCR/ALF		4-40 rem
90.0 deg / 450 km	1.0 g/cm^2	
- Trapped Radiation		4.2 rem
- GCRs		0.9 rem
- SCR/ALF		29-420 rem
Geostationary Orbit	2.0 g/cm^2	
- Trapped Radiation		4.3 rem
- GCRs		1.8 rem
- SCR/ALF		105-1100 rem

Table 2-3: Probable radiation effects (Cladis, Davidson and Newkirk 1977)

Dose (rem)	Probable Effect
0-50	No obvious effect except, possibly, minor blood changes.
50-100	Radiation sickness in 5-10% of exposed personnel. No serious disability.
100-150	Radiation sickness in about 25% of exposed personnel.
150-200	Radiation sickness in about 50% of exposed personnel. No deaths
200-350	Radiation sickness in nearly all personnel. About 20% deaths.
350-550	Radiation sickness. About 50% deaths.
1000	Probably no survivors.

Closer inspection of Tables 2-2 and 2-3 helps to quantify the threat of solar radiation to astronauts in deep space. Table 2-2 indicates a human behind 2.0 g/cm² of shielding in GEO (which approximates deep space outside the Earth's proactive magnetic field) can receive 105 – 1100 rem to various parts of the body during a typical SCR event. For reference, g/cm² is a standard measure of radiation shielding thickness used to compare the relative effectiveness of different materials. According to Table 2-3, a 1000+ rem dose leads to 100% mortality, with as little as 105 rem yielding 20% radiation sickness. With the capacity to kill or disable the crew aboard a deep space planetary mission, SCR storms represent a dire threat to manned space travel, especially since they can come at any time with little or no obvious warning.

2.4 Solar Weather Events

The topic of solar weather occupies volumes upon volumes of research and study. However, there are two primary categories of solar weather associated with SCRs: solar flares and coronal mass ejections. A solar flare is a "highly concentrated, explosive release of energy within the solar atmosphere which appears as a sudden, short-lived

brightening of a localized area in the chromosphere (Tascione 1994). Solar flares are characterized by total energy released, specifically size and intensity.

Classification of the size of a flare in area is expressed as a fraction of the Sun's surface. More importantly, solar flares are named in terms of their intensity classification or observed x-ray flux. A letter is assigned based on the flare's X-ray flux order of magnitude, and a number is then given based on the first digit of the peak flux measured. Several much-debated theories exist about the solar mechanics behind how and why solar flares occur, and their timing and direction are difficult to predict. However, one popular theory holds that flares are large scale releases of energy that take place during the collapse of magnetic loops within the Sun's atmosphere.

While the origins of solar flares are still debated, it is well-known based on historical observation that the Earth is affected by flares that appear in the solar longitudinal band of 25 deg east to 120 deg west relative to the Earth. In fact, based on the Sun's spiral magnetic field lines, 50 deg west is the longitudinal "sweet spot", with flares originating from that point creating the most significant effects on the Earth (Tascione 1994). The historical observations of solar flare origination may have some utility, since flares originating from 25 deg east to 120 west relative to a manned spacecraft in deep space are likely to be "in range" of causing an SCR event that will affect the ship.

Solar proton events (SPE) are a special category of solar flare that involve the release and acceleration of large quantities of highly energetic protons which can reach the Earth in as little as 30 to 90 minutes (Tascione 1994). These radiation storms typically travel at 75,000 km/sec, which is about one-fourth the speed of light (Poppe

2006). Currently, radio-spectrometry is used to detect and identify SPEs. The large, brilliant flares associated with SPEs create a unique radio signal signature, which is picked up by Earth ground stations and solar monitoring satellites. The actual solar proton flux is then confirmed and measured by spacecraft at the Sun-Earth L1 point. Typically, an SPE is declared when the solar proton flux reaches 4 times that of the normal background flux level.

Coronal mass ejections (CME) are relatively slow-moving eruptions of enormous quantities of solar material into space. CMEs are associated with solar flares and sometimes SPEs, however it is not clear whether CMEs cause the flares, flares cause the CMEs, or if there is another mechanism producing both. CMEs are much slower than flares, only moving at 14 km/sec to 1800 km/sec, with CMEs moving faster than 400 km/sec possibly causing interplanetary shocks. While the actual CME material is not a fast-moving radiation threat, and tends to largely dissipate by the time it reaches the radius of Earth orbit, the CME bow-shock itself can accelerate particles it encounters to extremely high energy levels and velocities, potentially creating a dangerous deep-space radiation wave-front.

2.5 Earth's Solar Warning Architecture

Strangely enough, solar weather forecasting has its origins in warfare (Poppe 2006). During World War II, long-haul directional HF radio communications were absolutely vital to just about every aspect of the forces engaged in the conflict, from operations, intelligence, weather reporting, and logistics to espionage. HF radio provides long-haul communications by bouncing signals off the ionosphere. The higher the

frequency, the clearer the signal, but only up to a point – any higher and the signal will pass through the ionosphere and be lost into space. It was discovered prior to WWII that the Sun and certain aspects of solar weather caused disturbances in the ionosphere, which in turn could cause loss of messages, and in some cases re-direction of the signal into enemy locations. Out of military necessity, solar forecasting, specifically predicting when and how solar weather would affect military radio transmissions became a life-or-death requirement. As radar, various navigation aids, and other electromagnetic technologies were invented and applied throughout WWII, it became increasingly clear that understanding and predicting solar weather were vital to military success. After WW II, a number of Allied country organizations who had led wartime advances in the science of solar weather forecasting came together to form a number of international and national-level organizations dedicated to just that purpose. Over the following decades, the National Aeronautics and Space Administration (NASA), the National Oceanic and Atmospheric Administration (NOAA), and the US Air Force all played significant roles in establishing the solar monitoring architecture relied upon today.

Earth's modern solar monitoring architecture consists of an extensive network of sensors, communications, and command and control nodes, which operate around the world to provide near-real-time monitoring of the Sun, 24 hours per day, and seven days per week. Sensor nodes include various ground observatories, and solar observation satellites in Earth orbit, positioned at Sun-Earth L1, and in deep space. Communications include all forms of terrestrial landlines, satellite communications, and the Deep Space Network for relaying solar data from the deep space solar monitor satellites. Command and control of individual satellites, observatories, and communication hubs are performed

by the various agencies which own and operate them, but the premier organization responsible for worldwide solar forecasting is the Solar Environment Center (SEC) located in Boulder, Colorado. Supported by NASA, NOAA, the US Air Force, the Jet Propulsion Laboratory, and dozens of other solar-monitoring organizations around the world, the SEC conducts around-the-clock monitoring of solar weather and conditions, and issues both periodic forecasts and near-real-time alerts during hazardous space weather conditions. In this case hazardous refers to both human safety, and various industries and infrastructures which can suffer space weather damage, such as telecommunications, satellites, and the power grid. Relying on the Internet, "the SEC processes over 1,400 data streams in real time and distributes data and forecasts in real time that are available anywhere from once a second to once a day" (Poppe 2006). Depending on the type of solar storm or its emission effect (X-ray, Radio, Energetic Particles, or Solar Plasma), the SEC can identify hazardous solar weather and disseminate warnings to affected activities minutes to hours ahead of time, allowing them to take action to safeguard their personnel and systems. In the case of energetic particle storms, the SEC issues a warning at T+1 minute after the event is detected, and an alert by T+15, enabling on-orbit manned space activities such as the International Space Station (ISS) sufficient time to take protective measures, such as moving astronauts into more heavily shielded compartments to weather the storm. (Poppe 2006)

No discussion of the Earth's current solar monitoring architecture would be complete without descriptions of the primary satellite missions that are currently monitoring the Sun and are relied upon daily by solar weather forecasters. Located in geosynchronous orbits, the Geostationary Operational Environmental Satellite (GOES)

series of satellites provide the "most widely used data with longest-running data records in the space community" (Poppe 2006). Built by NASA and operated by NOAA, GOES missions are primarily for terrestrial weather monitoring, but include instruments that provide continuous measurement of the flux of solar protons, electrons, and x-rays. Various GOES missions have been operational for decades and at least two are maintained on orbit at all times to provide continuous monitoring. GOES-11 and GOES-12 are currently operational on orbit, with GOES-13 is already in storage on orbit as a backup.

The Solar and Heliospheric Observatory (SOHO) was jointly built by NASA and the European Space Agency (ESA) and launched in 1995 into orbit at Sun-Earth L1. Its payloads are "designed to study the structure and dynamics of the solar interior, the solar corona, and the source and acceleration of the solar wind" (Fleck, et al. 2006). SOHO includes the Large Angle and Spectrometric Coronagraph (LASCO) imager which creates images of the solar corona, which is used to monitor the solar halo and to identify "halo CMEs" which are aimed directly at the Earth. While still active, SOHO is a single spacecraft with no direct backup, however many of its instrument capabilities have been replicated on subsequent spacecraft.

Designed to continuously monitor various characteristics of the solar wind, the Advanced Composition Explorer (ACE) was the first satellite to enable accurate warning of geomagnetic storms, to include magnitude, arrival time, and duration (Poppe 2006). ACE was built and launched by NASA in 1997 and occupies a halo orbit at Sun-Earth L1. To enable its primary mission to measure the composition of energetic particles from the Sun and the heliosphere, ACE instruments measure particle type, charge, mass,

energy, direction of travel, and time of arrival (Stone, et al. 1998). ACE is expected to remain operational until 2019.

The Wind Spacecraft is another solar monitoring mission located at Sun-Earth L1. Jointly funded by USAF and NASA, and launched in 1994, the Wind mission is to gather data about the magnetosphere and conditions of space "upwind" of Earth. Specifically, it carries a suite of 8 instruments that measure solar wind particle speed and energy, magnetic fields, radio waves, and gamma waves (Szabo and Collier 2010), which provide detailed information on the associated particle-field interactions. Wind serves as a third source of correlation data for the STEREO mission by enabling stereoscopic solar wind structure and radio triangulation studies. Wind also plays a small role in solar forecasting by providing real-time space weather warning data for 2-3 hours each day during its daily telemetry downlink via DSN. Finally, Wind mutually supports ACE by providing instrument calibration information.

Launched in 2006, the Solar Terrestrial Relations Observatory (STEREO) mission is one of the most recent additions to NASA's Living with a Star program. Its multi-year mission is to track the flow of energy and matter from the Sun to the Earth by providing the first-ever stereoscopic 3D images of the Sun and solar weather. Its primary objective is to study CMEs by documenting their true 3D structures and evolution, with the ultimate goal of understanding why they occur. STEREO consists of two identical solar monitoring satellites that have been placed into pro-grade and retrograde orbits in relation to Earth's orbit around the Sun. According to mission plan, the STEREO satellites have been separating from the Earth at a relative angular rate of ~22.5 degrees per year, and

will continue to do so until they "meet" on the far side of the Sun (NASA 2006). NASA is then planning to use STEREO for other missions such as a potential fly-by of Mercury.

The newest cornerstone of the NASA Living with a Star program is the Solar Dynamics Observatory (SDO). Launched by NASA in 2010 into an inclined geostationary orbit, the SDO is designed to study multiple aspects of the Sun, solar activity, and the resulting solar weather affecting the Earth. Focused on analysis of the Sun's interior and magnetic field, SDO instrumentation is also dedicated to measuring both plasma of the solar corona and solar ultraviolet irradiance. SDO's mission capabilities include providing near-real-time solar storm warnings, seeing inside the Sun past its outer layers, and producing 24-7 high-definition movies of the solar surface (NASA 2010). SDO is currently the most advanced suite of instrumentation available to solar forecasters.

Often overlooked, one of the most significant components of Earth's solar monitoring architecture is NASA's Deep Space Network (DSN). The DSN consists of three networked ground complexes, located approximately 120 degrees apart longitudinally around the Earth in California, Australia, and Spain. The California Goldstone complex is located on the US Army's Fort Irwin Military Reservation near Barstow; the Australia complex is located near Canberra; and the Spanish complex is west of Madrid. These locations ensure that any spacecraft located in deep space anywhere in the solar system is within line-of-sight (LOS) of at least one of the three ground stations at all times, providing continuous communication links (Jet Propulsion Laboratory 2005). Each complex includes at least four ground stations, each operating an ultra-sensitive set of directional, parabolic dish antennas ranging from 26 to 70 meters in

size, enabling simultaneous contact with multiple space missions. The ground stations themselves are linked via dedicated landline and satellite communications to ensure smooth and timely handoff's of deep space connectivity between sites.

2.6 Mars Mission Planning

Planning for manned missions to Mars has been underway, both officially and unofficially, within the space community since the beginning of the space age. Portree (2001) provides an exhaustive and detailed review of these efforts. The Encyclopedia Astronautica also provides a short description on 61 various Manned Mars Mission proposals (Wade 2011). While it relies on Portree's work for much of its information regarding U.S. missions, the Encyclopedia Astronautica adds information on Russian and former Soviet Union missions not covered elsewhere. The United States and Russia have produced most of the Mars Mission studies in existence (particularly during the early years of the space age). However, many other nations (Laurini, et al. 2009), private organizations (Wilson and Clarke 2006), (Mars Society 1999), (Ashworth 2007), and industries (Zubrin, Baker and Gwynne 1991) have produced studies of their own. All of these mission planning efforts can be divided into two distinct categories of mission profile: conjunction class and opposition class.

2.7 Opposition vs. Conjunction Class Missions

The terms "conjunction" and "opposition" refer to the relative position of Mars compared to the Earth and Sun at the mid-point of the mission. In a conjunction class mission, Mars has moved behind the Sun (i.e. Mars and the Sun are conjoined) as viewed from Earth, while in an opposition class mission Mars is on the opposite side of Earth

from the Sun (i.e. in opposition) (Portree 2001). Figures 2-1 and 2-2 illustrate the differences between the two types of missions.

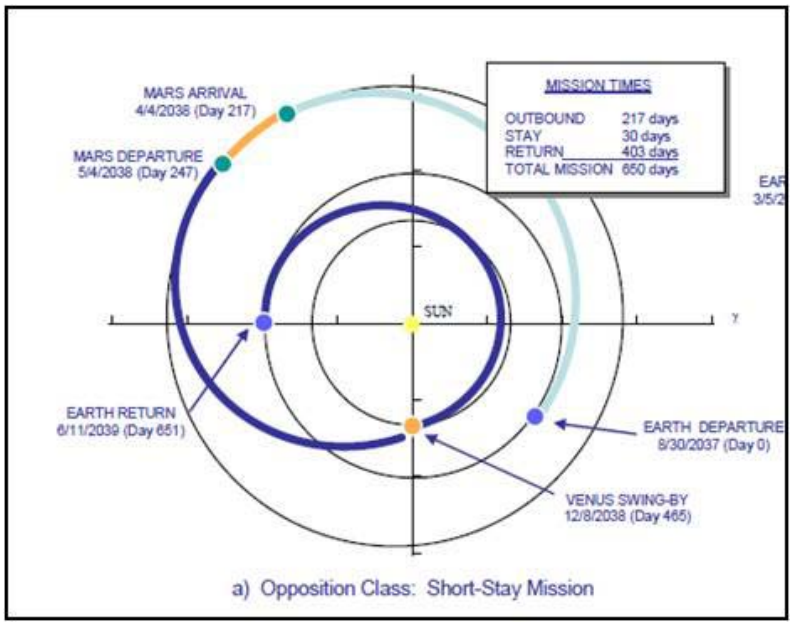

Figure 2-1: Opposition Class Mission (NASA 2009)

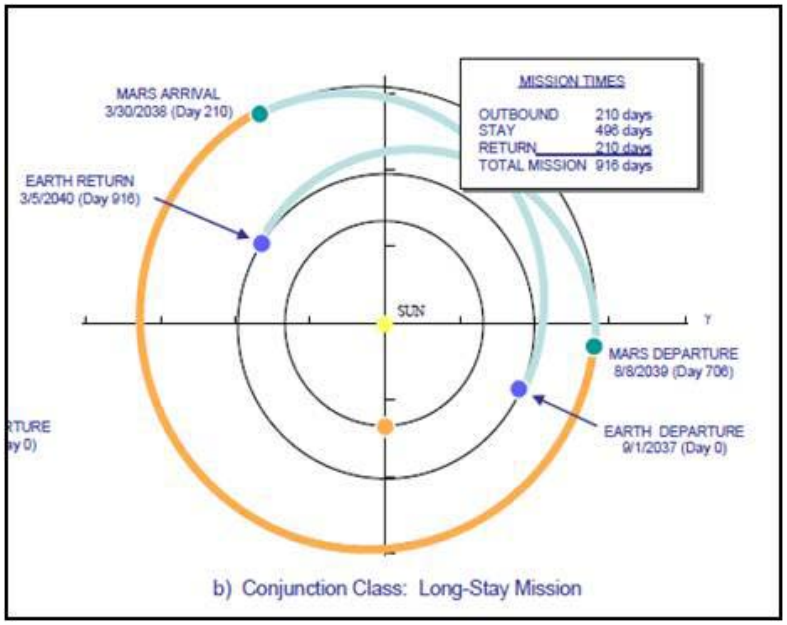

Figure 2-2: Conjunction Class Mission (NASA 2009)

It is interesting to note, that the preferred mission type has shifted over time. Although Von Braun's work in the late 1950's used a conjunction class mission to minimize fuel required (Portree 2001), with only a few exceptions the rest of the studies conducted up until the 1980's all focused on opposition class missions. However, in the early 1980's the conjunction class missions began to receive more attention until the point where it became the mission planning standard, backed by the Mars Direct proposal in 1990 (Portree 2001) and the development of NASA's Design Reference Mission (DRM), published in 1993 (Portree 2001). The DRM has evolved over the past two decades into NASA's most current manned Mars mission proposal: the Design Reference Architecture (DRA) 5.0, published in 2009 (NASA 2009). The ascendance of the conjunction class missions is due to three primary reasons: reduced fuel (delta-V) requirements, longer stay times on the surface of Mars, and reduced radiation risks.

Lower fuel requirements for conjunction class missions was initially noted by Von Braun when he developed the first serious manned Mars mission plans in 1950 (Portree 2001). In fact, this fuel efficiency advantage was one of the main reasons cited as justification by Robert Zubrin and his fellow authors in their 1991 "Mars Direct" paper (Zubrin, Baker and Gwynne 1991). NASA's DRA 5.0 provides a detailed discussion of the differences in fuel requirements for both mission classes. Figures 2-3 and 2-4 are from the DRA 5.0 appendices and illustrate both the lower delta-V requirement and the increased consistency of the required delta-V during a full mission for conjunction class profiles (NASA 2009).

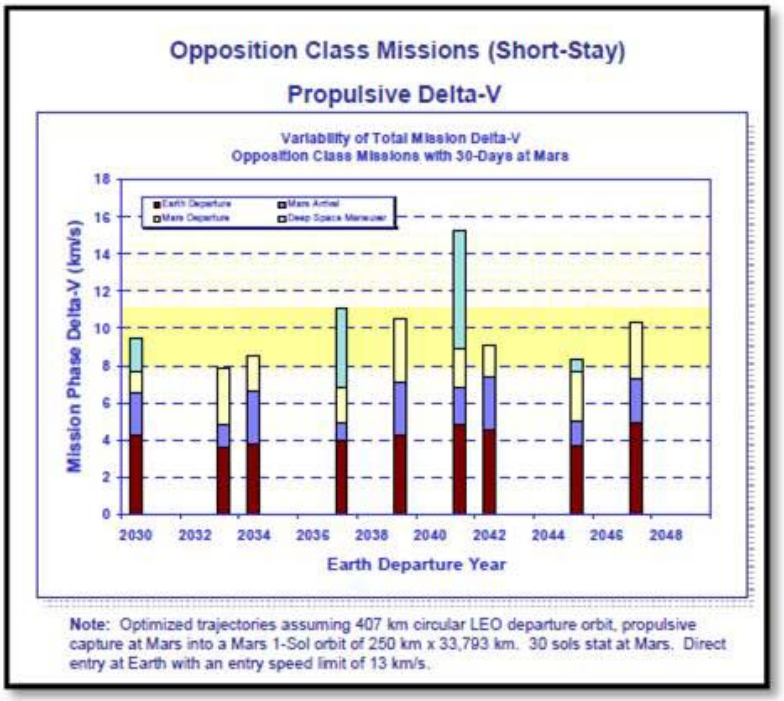

Figure 2-3: Opposition Class Propulsive Requirements (NASA 2009)

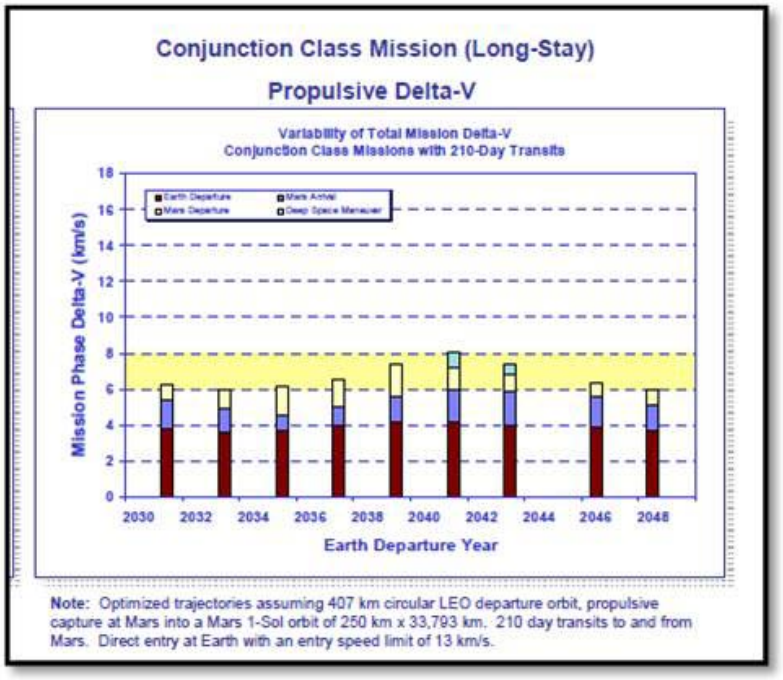

Figure 2-4: Conjunction Class Propulsive Requirements (NASA 2009)

The second major benefit of the conjunction class missions is the much greater time (both absolute and as a percentage of the total mission) that can be spent at Mars. Opposition class missions have been estimated to provide stay times on Mars as short as 20 days (Zubrin, Baker and Gwynne 1991) and as long as 90 days (NASA 2009). With total round trip times of 500-650 days for an opposition class mission, this results in a percentage range of mission time at Mars between only 3% (650 day mission and 20 day stay) and 18% (500 day mission and 90 day stay), which represents an exceedingly low scientific return on investment. Conjunction class missions provide stay times of about 500 days, with total mission durations of around 900 days (NASA 2009). This ratio equates to approximately 55% of the mission time being spent in Mars orbit or visiting its surface. This greater dwell time allows for significantly more research and exploration to be accomplished.

The third advantage of conjunction class over opposition class missions is the lower overall expected radiation exposure (NASA 2009). Despite the fact that conjunction class missions have longer overall durations, all opposition class missions have one transit leg which is significantly longer than the other, and which passes inside the orbit of Venus. The Figure 2-1 illustration of an opposition class mission depicts this return leg. Zubrin et al. explains the significance:

> "Finally, the opposition class mission must spend part of its flight in a swing into the inner solar system to a distance of about 0.65 astronomical units from the Sun. At this distance, the radiation dose experienced from a solar flare would be 2.4 times that felt at Earth's distance, and 5.5 times that felt by a spacecraft in orbit about Mars. This is very important, because the effect of high sudden doses of radiation are non-linear, and a single 200 rem dose experienced by an opposition mission crew as they flew within the orbit of Venus would be far more dangerous (severe radiation sickness would result) than 5 doses of 40 rems

> delivered over a 1.5 year period to a conjunction class mission crew hanging in an orbit about Mars (no observable symptoms would be expected)." (Zubrin, Baker and Gwynne 1991)

2.8 NASA Design Reference Architecture 5.0

NASA has been working on Mars mission plans since the Lewis study in 1960 (Portree 2001). The "Human Exploration of Mars Design Reference Architecture 5.0" (DRA 5.0) is the culmination of NASA efforts for planning Manned Mars Missions that began with the publication of the "Mars Design Reference Mission (DRM)" in 1993 (Drake, Hoffman and Beaty 2009). The DRA 5.0 covers the full set of considerations for a Mars mission including scientific objectives, potential methods, vehicle and habitat design, communication considerations, propulsion options, radiation risks, and interplanetary trajectories. These last two items are of direct interest to the project.

2.9 DRA 5.0 Space Weather and Radiation Risks

DRA 5.0 discusses space weather both in terms of being a subject of continued scientific study and a threat to the success for the mission itself. Additionally, the figures of merit used to guide the decisions that define DRA 5.0 specifically identify the risk of radiation exposure for the crew as a potential hazard to be assessed. Within its Key Challenges section, DRA 5.0 goes as far as identifying "…establishment of a space weather forecasting system and implementation of sufficient 'storm shelters' to warn crews against the transitory, but extreme, levels of radiation that would be encountered during solar flares" (NASA 2009) as the third of three categories of goals under radiation protection. DRA 5.0 calls for a system to provide sufficient time for the crew to take mitigating actions such as returning from an extra-vehicular activity (EVA) and entering

a storm shelter and notes that warning times may be as short as 30 minutes. However, it does not discuss or define this warning system's architecture or components. Furthermore, DRA 5.0 does not identify where the "30 minute" requirement was derived from nor does it provide any indication on what minimum warning time would be required to successfully implement mitigating strategies. It does however clearly state that a "…specific warning system will need to be developed." (NASA 2009) Identifying potential options for such a system and recommending a potential solution is the primary objective of this thesis.

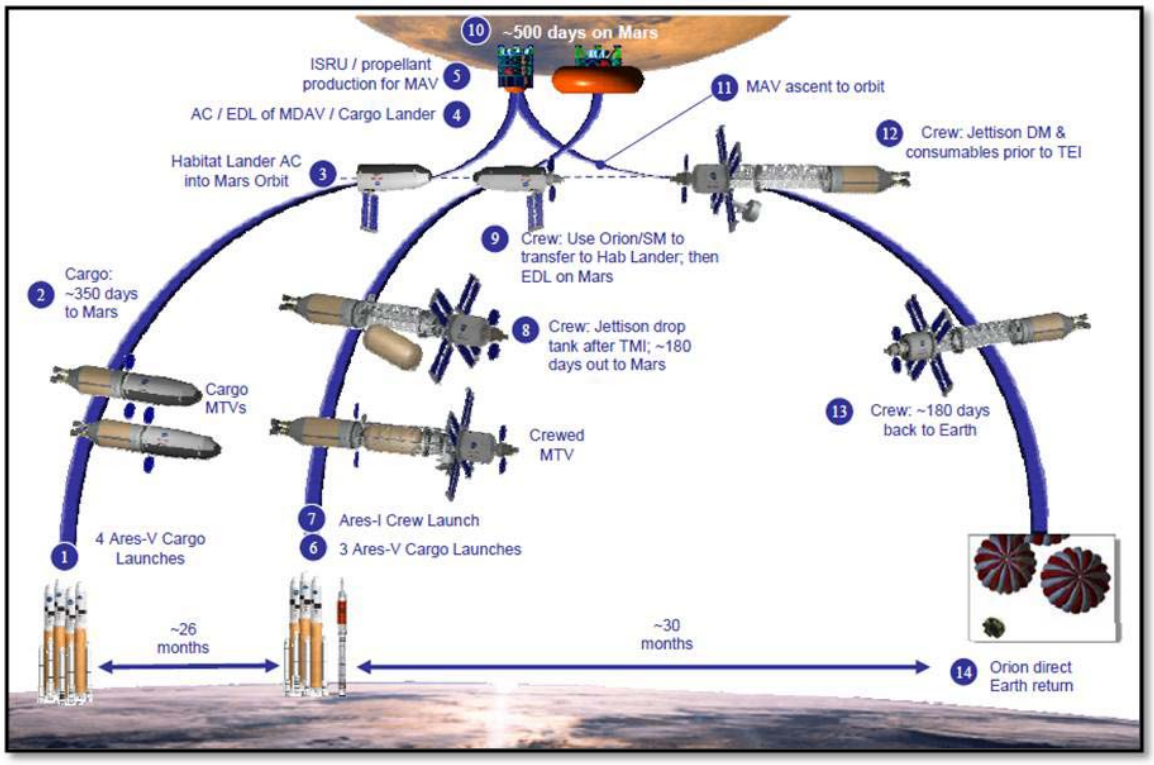

Figure 2-5: Mars DRA 5.0 Mission Summary (NASA 2009)

2.10 DRA 5.0 Mission Parameters

DRA 5.0 is of fundamental importance because in addition to specifying a 30-minute radiation storm warning time requirement, it also serves as an official reference for the details of the Mars mission itself. Identical to challenges faced by terrestrial surveillance architectures, it is impractical and cost-prohibitive to devise a solar storm warning architecture that provides perfect knowledge of the Sun from all angles and can transmit a warning to any point in the solar system, either in deep space or on the surface of a planet. This breadth of requirement scope becomes acceptably constrained when the architecture is designed to provide warning to a specified subset of feasible Mars mission profiles, as defined in DRA 5.0. "Mission Type" is the very first decision outlined in DRA 5.0 (NASA 2009), wherein NASA selects conjunction class missions as the preferred trajectory profile to visit Mars. DRA 5.0 justifies this decision for the reasons discussed above in the comparison of conjunction and opposition class missions (NASA 2009). The other specific mission parameters pertinent to the analysis and defined within DRA 5.0 are discussed in Chapter 3.0.

Another key aspect of DRA 5.0 is that NASA planners intend to leave the Mars Transfer Vehicle (MTV) in orbit above Mars while the crew is on the surface and then reuse it for the return leg. This mission decision directly impacts the cost (in terms of dry mass) of any candidate warning architectures which include placing a solar monitoring sensor suite onboard the MTV. This decision also ensures there is a sensor in orbit at Mars throughout the stay, where it can potentially relay warnings down to the surface. Figure 2-5 above shows the nominal mission profile and reuse of the MTV for the return

flight, while the conjunction example in Figure 2-2 above shows a sample interplanetary trajectory for a DRA 5.0 mission.

2.11 Libration Points

Upon examining the issue of where to potentially position sensors within the solar system to monitor the sun, it became clear there were only three options to consider: in orbit around a given planetary body, aboard the manned spacecraft itself, or at one or more Lagrange (or libration) points. Originally, identified and defined by the Italian mathematician Lagrange as part of his work describing 3-body motion, Lagrange points are a set of 5 points in space about two large masses at which the gravitational pull from the two masses are balanced along at least one axis. As a result, if an object is placed at one of these 5 points, it will maintain its position relative to the two masses with little or no additional energy required over time. These libration points are simply referred to as L1 through L5, and are frequently used to describe points of neutral gravity relative to the Earth and Sun.

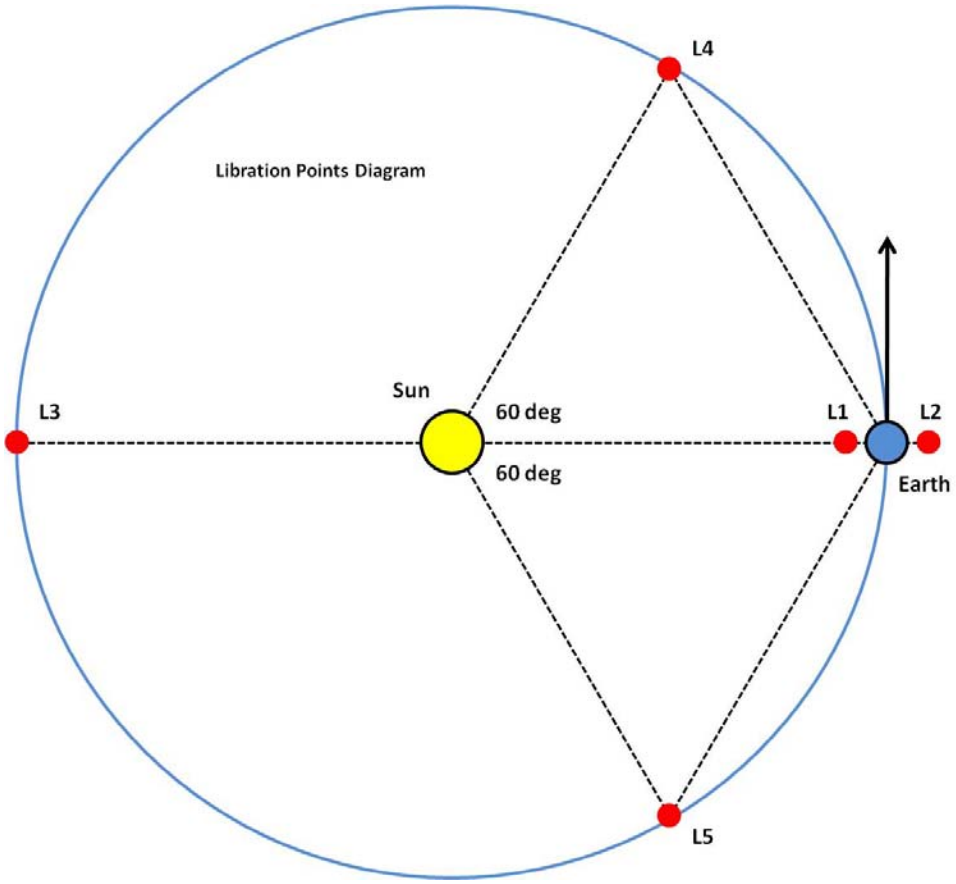

Figure 2-6: Libration Points

As can be seen in Figure 2-6, L1 is located along the Earth-Sun axis about 1/10 the distance between the two bodies. L2 is also located along the Earth-Sun axis, however on the opposite side of the Earth from the Sun. L3 is located exactly opposite the Earth on the far side of the Sun. L1, L2, and L3 are only stable along the Earth-Sun axis. To maintain stability along the other two axes, satellites placed at L1 are inserted into either a halo or Lissajou orbit. A halo orbit is circular about the L1 point, whereas the Lissajou orbit follows a figure-8 shaped path with the crossing near the L1 point (see Figure 2-7).

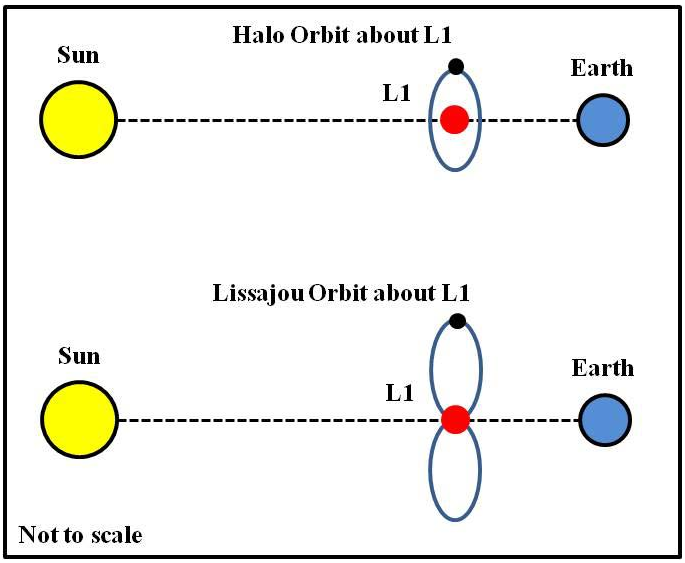

Figure 2-7: Halo and Lissajou Orbits at L1

Slightly closer to the Sun than the Earth with a relatively stable, unobstructed view, L1 makes for an excellent surveillance point, and a number of solar monitoring missions reside there. L4 and L5 are 60 degrees ahead of and behind the Earth, on its orbital path. These two libration points are stable along all 3 axes, leading some to theorize there may be asteroids or clouds of space debris trapped at these locations, presenting a potential hazard to any man-made objects intended to occupy them. It is also interesting to note that the L4 and L5 points form equilateral triangles, and the distance between L4 (L5) and the Earth is approximately equal to the distance between L4 (L5) and the Sun or the Earth-Sun path. Finally, it is important to note there is a libration point set for every Sun-planet pair in the solar system, not just the Sun-Earth pair.

2.12 Previous Analysis

Amazingly, there has been very little published research on developing a solar storm warning architecture to cover manned missions to Mars. In fact, only one published study on that specific topic could be found, but it turned out to be an excellent source of information. "Orbit Selection and Its Impact on Radiation Warning Architecture for a Human Mission to Mars" (Turner and Levine 1998) analyzes both conjunction and opposition class transit missions and presents findings on differences between the two mission classes with regards to the number of monitoring satellites required by each, with the goal of minimizing cost.

In addition to some excellent background on solar proton events (SPEs), the specifics of the SPE threat to a manned mission, and the different types of SPE based on whether they originate from solar flares or CMEs, the Turner and Levine (1998) also provide an overview of the two basic mission profiles to reach Mars: opposition and conjunction.

The analysis of the mission classes was conducted by plotting overlays of 63 conjunction and opposition class mission profiles developed by NASA onto top-down reference frame diagrams where the Earth and Sun remained inertially fixed. One key finding included the fact that opposition class trajectories always make a closer approach to the Sun at some point in their profile, often even inside the orbit of Venus, which significantly reduces the amount of warning and reaction time available to the crew in the event of an SPE.

Turner and Levine (1998) also provide a brief overview of potential options for positioning warning sensor satellites, including on the spacecraft itself, and equilaterally

around the circumference of the Sun spaced every 120 degrees at a range of one astronautic unit (AU) from the Sun. This second option would be similar to the STEREO mission, with satellites located 120 degrees pro-grade (ahead) and retrograde (behind) the Earth, which would also rely on a satellite at Sun-Earth L1 to complete the coverage. Turner and Levine (1998) also acknowledge there will be transmission time issues with transmitting sensor data and warning data across the vast distances involved in a manned mission to Mars, but doesn't cover this topic in detail.

Surprisingly, Turner and Levine (1998) conclude that an opposition class mission profile is preferable because the spacecraft spends the shortest amount of time at risk in space. This conclusion is made despite the fact the spacecraft must pass alarmingly close to the Sun. Turner and Levine (1998) also recommends the opposition class mission because only a single sensor satellite is required to monitor the region of danger posed, and communications distances between the Earth and the at risk spacecraft are relatively shorter.

3.0 Method

3.1 Introduction

The purpose of this chapter is to explain the methods used to generate the results discussed in Chapter 4.0. The initial steps involve defining the problem, deriving functional requirements for potential solutions, identifying solution scenarios, and developing performance metrics and constraints. Once a scenario, architectures, and metrics are defined, a series of models are developed to calculate the performance and cost of each CA, which is then used to generate efficient frontiers and determine the best solutions.

3.2 Problem Definition

One of the first steps in problem-solving is problem definition: looking for key attributes and characteristics from which to derive one or more solutions. Little is known about the threat of solar radiation storms, specifically predicting when and where they will emerge. Only limited quantifiable data is available, including the radiation levels and estimated effects covered in Section 2.3 and the fact that high energy radiation storms travel at speeds as high as 75,000 km/sec (Poppe 2006). As for indications, almost all solar radiation storms are immediately preceded by a particular Type-II radio-spectrometer signature caused by the bow shock of the energetic particles when they erupt from the Sun (Warmuth and Mann 2005). In fact, radio-spectrometers are the primary instruments used to provide early warning of these types of solar storms,

meaning the signature of a just-occurred radiation event originates from the surface of the Sun at approximately the speed of light.

3.3 Functional Requirements Definition

Based on the threat research, two primary functional requirements for the architecture are defined. Functionally, any candidate architecture (CA) needs to monitor the Sun's surface for indications of an erupting solar radiation storm, and provide timely warning to a spacecraft potentially threatened by the storm. Analysis of these functional requirements indicates that any given CA requires a combination of three basic component categories: sensors, communications, and processing. Additionally, the protected asset itself (the spacecraft), the source of the threat (the Sun), and the Earth (a baseline processing and communications node) are common to all CAs.

3.4 Scenario Identification

Since providing solar radiation warnings to manned missions to Mars is the primary objective, scenario identification and analysis were primarily conducted during the background research as described in Chapter 2.0. NASA's Design Reference Architecture 5.0 is selected as the operating scenario based on its feasibility, maturity, and official endorsement by the US government. Selecting DRA 5.0 as the scenario directly leads to a number of other quantifiable factors which are directly applied during the modeling and simulation.

3.5 Constraint Identification

Upon review of potential architecture constraints, cost is recognized as the most significant constraint. Minimizing cost is always of paramount importance when

developing a system or architecture, and cost plays a key role in comparing the CAs. Selection of cost as the primary constraint also drives the requirement to develop both a Cost Metric and Cost Model, as described in Sections 3.9 and 3.11.6.

3.6 Candidate Architecture Development

The next phase is to develop a set of candidate architectures which satisfy the basic functional requirements described above in Section 3.3. The first step is to define the alternatives for each of the three main architecture components previously identified: sensors, processors, and communications. Sensor options include placing solar monitoring satellites in various locations or location sets within view of the Sun or onboard the spacecraft itself. The sensor satellite location options are: Sun-Earth L1, Sun-Mars L1, and a pair of sensors at Sun-Earth L4 and L5. Sun-Mars L4 and L5 are ruled out because they are so far away from both the Sun and Mars that any alert they provide will come after the arrival of the radiation storm. Processing options are limited to the current Earth-bound solar forecasting architecture and onboard the spacecraft itself. Finally, communications are asserted to be integrated into all sensor and processing nodes. However, there are two communications strategies identified, each associated with the location of the processing node: all monitoring data is routed back to Earth, processed, and any required warning data transmitted from Earth to the spacecraft (Earth Relay); or all monitored sensor data is sent directly to the spacecraft and processed directly onboard (Direct). Via permutation, all possible combinations of the sensor, processing, and communication options are identified and all nonsensical or impractical configuration options are eliminated. This process results in a total of 14 CAs, which

satisfy the functional requirements to some degree and are further documented as DoDAF Operational Concepts (OV-1s).

3.7 Baseline Candidate Architecture (BCA)

From the set of 14 CAs, Candidate A1 is identified as the Baseline Candidate Architecture (BCA) due to its high degree of similarity to the Earth's current solar warning architecture. The BCA is defined as the "do nothing" architecture, meaning little to no additional resources will be required to implement or maintain it beyond what current solar forecasting organizations and governments are currently investing. In fact, if a manned mission to Mars were to take place in the very near future, Candidate A1 provides the most accurate representation of an ad-hoc solar warning architecture.

3.8 Performance Metric Definition

The next challenge is to define architecture performance metrics based on the previously defined functional requirements. With a total of 14 potentially viable CAs, further analysis is required to find a set of metrics by which the CAs can be measured and compared. Examination of the functional requirements yields performance metrics of Warning Time and Solar Coverage. Warning Time is assessed to be twice as important as Solar Coverage because the warning metric pertains to the primary functional requirement of the architecture. While important, Solar Coverage is not weighted equally, since any architecture with at least one solar sensor must provides some minimum amount of solar coverage. Once defined, each of the performance metrics is further specified in quantifiable, measurable terms.

3.8.1 Warning Time

Warning Time is defined as: the amount of time a crew has to react to an impending radiation storm and take protective measures. A key concept with Warning Time is that it exists as a requirement independent of the protective countermeasures themselves. It will likely be the case that various countermeasures have a warning time requirement, but those requirements are unknown at present and are not the focus of the thesis. Therefore, Warning Time is deemed an unconstrained metric, with no upper bound, meaning infinite Warning Time is "perfect" and more Warning Time is always better. Warning Time is defined in mathematical terms as:

$$Warning\ (t) = Radiation\ (t) - Alert\ (t)$$

Radiation Time is defined as the amount of time it takes a radiation storm originating from the surface of the Sun to reach a spacecraft. Alert Time is defined as the total path time required for an indication of a radiation storm to travel from the Sun, be detected, and then communicated to the spacecraft. Radiation Time is calculated by taking the distance of the spacecraft from the surface of the Sun, at any given point in time, and dividing by the high-end (worst case) speed of high energy radiation, 75,000 km/sec (Poppe 2006). Alert Time is calculated by adding up the total path time for a radiation storm signature to travel from the Sun to one or more sensor nodes, on to the processing node, and then to the spacecraft. The solar EM signature indicating high energy radiation and all communications links are defined as operating at *c*, the speed of light. Furthermore, constant node delays are assessed and added for each sensor or processing node transited. Sensor nodes are assigned a 4 minute delay based on current

solar monitor satellite refresh rates, and Earth processing is assessed a 10 minute delay based on current solar warning timelines involving the International Space Station. Processing aboard the spacecraft is assessed as 0-30 seconds and not factored into the overall delay. This sub-minute delay time is derived from the SEC warning timeline during which the SEC typically issues its first solar weather warning at T+1 minute after the solar event signature data first reaches an Sun-Earth L1 satellite (Poppe 2006). This warning includes a formal warning order and other administrative tasks that are not applicable to an autonomous or monitored warning system providing an alert to its astronaut crew.

3.8.2 Solar Coverage

Solar Coverage is defined as: the total percentage of the Sun's surface in view of a given CA's set of solar sensors at a given point in time. Even though the Sun is a three-dimensional, roughly spherical object, any sensor with an unobstructed field of view and sufficiently far away sees the Sun as a flat disc and can view approximately 50% of the Sun's surface at any time. If the solar coverage concept is translated into two dimensions with a top-down perspective, then each sensor can be considered to cover 180 degrees of the Sun's 360 degree circumference from any given angle. See Figure 3-1.

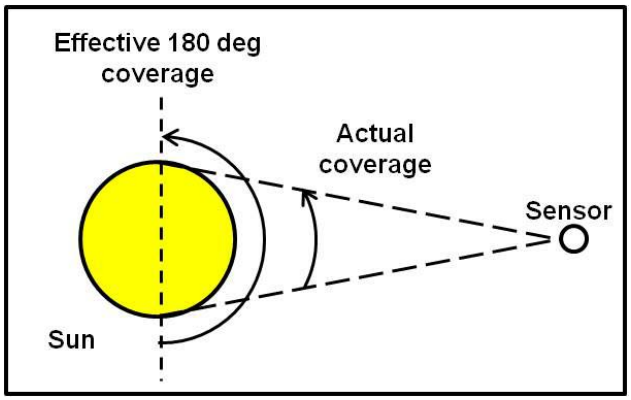

Figure 3-1: Single Sensor Coverage Approximation

Adding one or more sensors at fixed angles relative to a baseline sensor expands the angular coverage by a fixed number of degrees equal to the angular separation of the sensors.

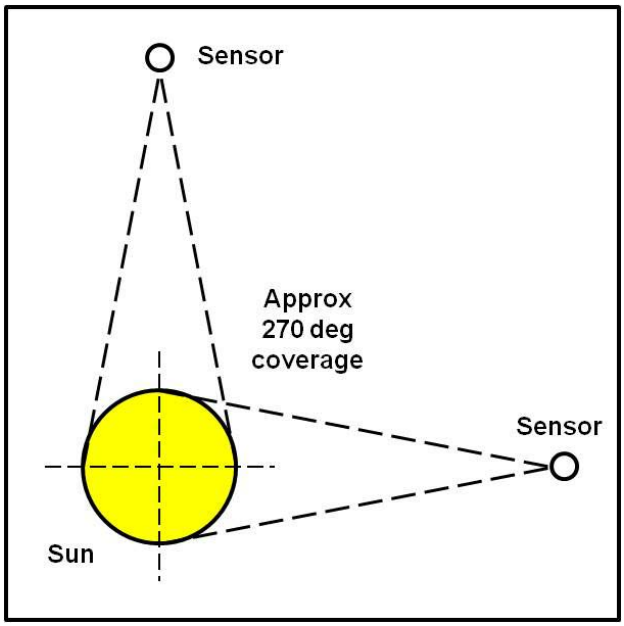

Figure 3-2: Multi-Sensor Coverage Approximation

For example, in Figure 3-2 adding a sensor 90 degrees ahead of the baseline sensor will expand solar coverage from 180 degrees to 270 degrees. If an additional sensor varies in its angular location relative to the baseline sensor, then this dynamic sensor creates a time-based variation in solar coverage. Applying knowledge of potential relative sensor configurations and the coverage concepts described above, a general set of solar angular coverage equations is developed as shown in Table 3-1. Because sensor view overlaps must be considered, the variables in an equation are determined by the number of sensors present. As described in Section 3.11.5, these equations are assigned to individual CAs, and some of the multi-variable equations are simplified due to the particular mission epoch and profile for the selected Mars mission scenario.

Table 3-1: General Coverage Angle Equations

Sensor Configuration	General Solar Coverage Equations A1 = Relative angle between Primary Sensor and Dynamic 1; A2 = Relative angle between Primary Sensor and Dynamic 2					
1 sensor (primary)	180 degrees, constant					
3 sensors (60 deg spacing)	300 degrees, constant					
1 sensor + dynamic 1 (A1)	1 < A1 < 180 180 + A1 181 to 360 deg			181 < A1 < 360 180 + (360 - A1) 359 to 180 deg		
3 sensors + dynamic 1 (A1)	1<A1<60 Constant 300 deg	61<A1<120 300+(A1-60) 301 to 360 deg	121<A1<240 Constant 360 deg		241<A1<300 300+(300-A1) 359 to 300	301<A1<360 constant 300 deg
1 sensor + dynamic 1 (A1) dynamic 2 (A2)	A2, A1 → 1 < A2 < 180 181 < A2 < 360		1 < A1 < 180 180 + max(A1,A2) min(360, 180 + A1 + 360 – A2)		181 < A1 < 360 min(360, 180 + A2 + 360 – A1) 180 + (360 – min(A1,A2)	
3 sensors + dynamic 1 (A1) dynamic 2 (A2)	A2, A1 → 1<A2<60 61<A2<120 121<A2<240 241<A2<300 301<A2<360	1<A1<60 300 deg 300+(A2-60) 360 deg 300+(300-A2) 300 deg	61<A1<120 300+(A2-60) 300+max(A1,A2)-60 360 deg min(360,180+A1+360-A2) 300+(A1-60)	121<A1<240 360 deg 360 deg 360 deg 360 deg 360 deg	241<A1<300 300+(300-A1) min(360,180+A2+360-A1) 360 deg 300+300-min(A1,A2) 300+(300-A1)	301<A1<360 300 deg 300+(A2-60) 360 deg 300+(300-A2) 300 deg

3.9 Cost Metric

Relative cost of each CA is required to make informed cost benefit analyses and comparisons. Because cost is identified as the primary constraint metric, it must be defined. An examination of the Space Mission Analysis and Design handbook (Wertz

and Larson 2007) reveals that delta-V is a common proxy used for cost comparison of space mission alternatives. However, delta-V is a function of the timing, duration, and trajectory of asset maneuvers. Because it focuses on quantifying "how" objects are positioned, delta-V is too complex with too many open-ended variable assumptions to be of objective use. Further analysis of the constraints results in adoption of Total Dry Mass as a quantifiable cost metric for each CA. Total Dry Mass is defined as the total un-fueled (dry) mass of all the architecture components which must be launched into space to form the architecture. Launch mass costs are a primary driver in most space acquisition costs and serve as an excellent benchmark for comparing competing space solutions. Fuel costs are not considered because there are so many variables in placing a given object in a given orbit with respect to mission epoch, mission duration, delta-V, thrusters, and actual trajectory selection. The problem of how to place multiple architecture components into multiple locations with the most efficient delta-V or fuel budgets and within sufficient time to support a Mars expedition exceeds the scope and purpose of this thesis. In fact, entire research papers have been allocated to the delta-V analysis of a single insertion mission alone (Carrico, et al. 2001). For CAs which include hardware onboard the spacecraft, the total mass of the spacecraft itself is not counted; only the antennas, sensor suite, and processing/display station are considered. Furthermore, ground station and Deep Space Network costs are not considered, as these are common to all architectures. A description of the mass estimation process is in Section 3.11.6 which discusses formulation of the Cost Model.

3.10 Analysis Strategy

Due to complex time-space dynamics of the scenario and architecture component interactions, modeling and simulation (M&S) is the most suitable means to measure CA performance. The M&S strategy is to "play" or test each CA against the NASA DRA 5.0 Mars mission scenario as an objective baseline. The challenge of characterizing CA performance is complicated since warning time and solar coverage are variable and dynamic, based on the relative motions and locations of all nodes, planetary bodies, and the manned spacecraft itself. Therefore the analysis approach is to profile the performance response of each CA over time by stimulating the CA with false radiation storms at an artificially high rate of once per 24 hours over the entire mission epoch. Each CA is measured every 24 hours in terms of Warning Time and Solar Coverage, and the results compiled, as shown in Chapter 4.0.

3.11 The Five-Model Approach

Leveraging the requirements, performance, cost, and architectural analysis described above, a series of five models, each building on the previous model, are developed that ultimately provide the tools and data required to assess the CAs and recommend a solution. Developed to optimize the balance between cost and performance in selecting a CA, these five model sets are referred to as the Architecture Models, the Mission Model, the Performance Models, the Cost Model, and the Value Model. Figure 3-3 below depicts the five model sets and how they interact within the analysis.

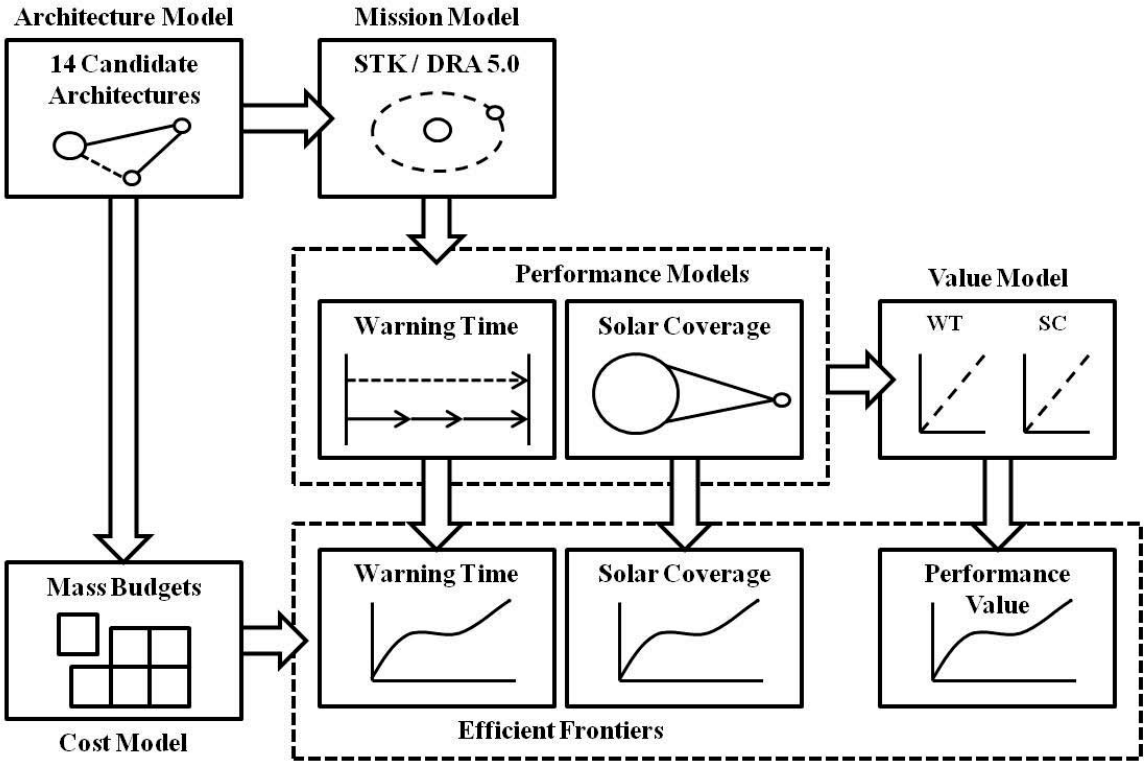

Figure 3-3: Five Model Approach

As described in Section 3.6, the CA models define 14 different configurations of sensors, processing nodes, and communications strategies. A total of seven objects are identified providing 13 potential links, which are then organized into eight relevant data paths. Collectively labeled as the Architecture Models, these CA models are documented as OV-1s and serve as a reference source for the development of later models. The Mission Model, built using Satellite Tool Kit (STK), provides the dynamic location versus time of each CA component during the scenario. Location is in terms of three-dimensional space relative to the Sun, Earth, and Mars Traveler (the manned spacecraft). Mission Model outputs are directly used in both the Link Model and the Coverage Model, which are together referred to as the Performance Models. The Link Model uses

the list of components identified by each Architecture Model and the distances calculated at each interval by the Mission Model to quantify the Warning Time for each CA. The Coverage Model uses the relative angles of each CA sensor set to calculate the total number of solar degrees "covered" versus time, and converts these values into percentages. The Cost Model parametrically estimates the relative costs of the various CAs by assessing the combined dry mass of the various components. Finally, the Value Model combines the Warning Times and Solar Coverage performance metrics to obtain a single weighted Performance Value for each CA. When graphed against the results of the Cost Model in an efficient frontiers chart, the Value Model enables a "best-value" analysis of the entire set of CAs.

3.11.1 Model Term Definitions

For ease of reference and communication, shorthand nomenclature is defined to refer to different architecture elements, as listed in Table 3-2.

Table 3-2: Architecture Element Nomenclature

SE-L1	Sun-Earth L1 Point
SE-L4	Sun-Earth L4 Point
SE-L5	Sun-Earth L5 Point
Mars Traveler (MT)	Mars Transfer Vehicle (MTV) in DRA 5.0
SM-L1	Sun-Mars L1 Point
<>	Signifies a link between two objects

3.11.2 The Architecture Models

Candidate Architecture Models are developed to cover the range of sensor placement options (Sun-Earth L1, Sun-Earth L4 & L5, Sun-Mars L1, and onboard Mars Traveler), processing node options (Earth and Mars Traveler), and communication strategies (Earth Relay and Direct). Since the concept of interfaces is inherent in any

architecture, the Architecture Models further consist of 13 links combined into eight potential data paths. Permutation of these sensors, data paths, and processing options yields a total of 14 feasible architecture options, labeled A1 through H2. Illustrations of each CA can be found in Chapter 4.0, with an example shown in Figure 3-4 below.

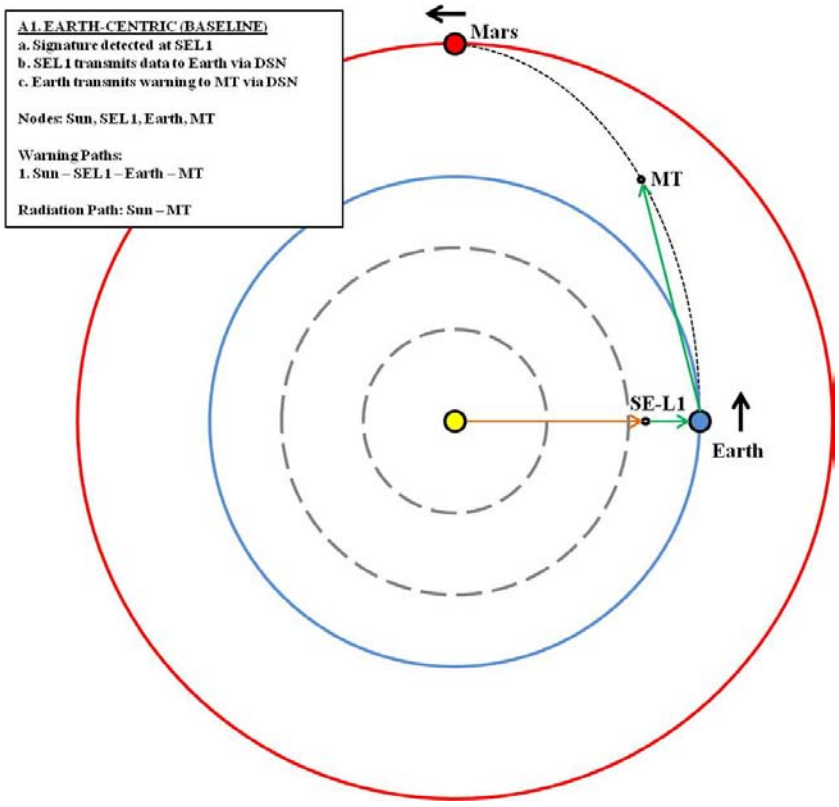

Figure 3-4: Example Candidate Architecture OV-1

CAs are defined as a set of sensors, data paths, and processing nodes organized to provide timely solar warnings to a manned mission (Mars Traveler) during all stages of a manned mission to Mars (Transit, Orbit, and Return). For ease of tracking and discussion, each CA is assigned a shorthand letter-number nomenclature. The letter (A through H) identifies which combination of sensors locations is used, while the number (1 or 2) identifies whether the architecture sends data to Mars Traveler via Earth or also

transmits directly to the spacecraft. Table 3-3 summarizes the CA nomenclatures and descriptions:

Table 3-3: Candidate Architecture Nomenclature

Nomenclature	Name	Sensors	Comm Strategy
A1	Baseline	SE-L1	Earth Relay
B1	Earth-Expanded	SE-L1, SE-L4, SE-L5	Earth Relay
B2	Earth-Expanded, Direct	SE-L1, SE-L4, SE-L5	Earth Relay & Direct
C1	Earth-Mars	SE-L1, SM-L1	Earth Relay
C2	Earth-Mars, Direct	SE-L1, SM-L1	Earth Relay & Direct
D1	Earth-Expanded-Mars	SE-L1, SE-L4, SE-L5, SM-L1	Earth Relay
D2	Earth-Expanded-Mars, Direct	SE-L1, SE-L4, SE-L5, SM-L1	Earth Relay & Direct
E1	Earth-Onboard	SE-L1, MT	Earth Relay
F1	Earth-Onboard-Expanded	SE-L1, MT, SE-L4, SE-L5	Earth Relay
F2	Earth-Onboard-Expanded, Direct	SE-L1, MT, SE-L4, SE-L5	Earth Relay & Direct
G1	Earth-Onboard-Mars	SE-L1, MT, SM-L1	Earth Relay
G2	Earth-Onboard-Mars, Direct	SE-L1, MT, SM-L1	Earth Relay & Direct
H1	Earth-Onboard-Expanded-Mars	SE-L1, MT, SE-L4, SE-L5, SM-L1	Earth Relay
H2	Earth-Onboard-Expanded-Mars, Direct	SE-L1, MT, SE-L4, SE-L5, SM-L1	Earth Relay & Direct

With the CAs defined, the next step is to identify the data elements needed to calculate their performance metrics. These basic elements of CA data are the individual links between each sensor, the Earth, and/or Mars Traveler, as well as the "links" that represent the solar warning signature (at the speed of light) and solar radiation particles (at 75,000 km/sec) between the Sun, the sensors, and Mars Traveler. Analyzing the combined set of 14 CAs identifies 13 links total, listed in Table 3-3. The distance or length of each link (between CA objects) at each 24 hour interval across the mission epoch is required for analysis. This data is output from the Mission Model and feeds into the Link Model.

Individual links are further combined to create specific paths through the CAs, along which travels the indication and warning signals of a solar radiation storm. There are a total of eight of these paths identified across the various CAs. The Link Model uses these defined paths and the link distances provided by the Mission Model to calculate the

propagation times of the indications and warnings signals. These eight paths are listed in Table 3-4 below.

The Architecture Models also illustrate the relative angular spacing of the various sensor satellites in orbit around the Sun for a particular CA. Each OV-1 depicts the CA's solar coverage configuration and the CA models are directly referenced to develop the Coverage Model equations.

Table 3-4: Link and Path Cross-Reference

Links/Paths	S-SEL1 -E-MT	S-SEL4 -E-MT	S-SEL5 -E-MT	S-SML1 -E-MT	S-MT	S-SEL4 -MT	S-SEL5 -MT	S-SML1 -MT
Sun<>SE-L1	X							
Sun<>SE-L4		X				X		
Sun<>SE-L5			X				X	
SE-L1<>Earth	X							
SE-L4<>Earth		X						
SE-L5<>Earth			X					
Earth<>MT	X	X	X	X				
SE-L4<>MT						X		
SE-L5<>MT							X	
Sun<>SM-L1				X				X
SM-L1<>Earth				X				
SM-L1<>MT								X
Sun<>MT					X			

3.11.3 The Mission Model

As described in Chapter 2.0, in the discussion of the evolution of Mars mission planning, the Mission Model scenario is based on analysis of NASA's DRA 5.0. DRA 5.0 calls for a conjunction class mission using a fast transfer (vs. a pure Hohmann transfer) to reduce the amount of time in transit, increase surface exploration time, and minimize radiation risk to the crew during the interplanetary portion of the mission (White House 2010) (NASA 1997). For reference, "the Hohmann transfer ellipse provides orbit transfer between two circlular, co-planar orbits" (Wertz and Larson 2007). NASA's DRA 5.0 authors studied mission window opportunities ranging from 2020 to

2046. For discussion purposes, DRA 5.0 singles out the 2037 mission window in both its summary and full report (Drake, Hoffman and Beaty 2009) (NASA 2009).

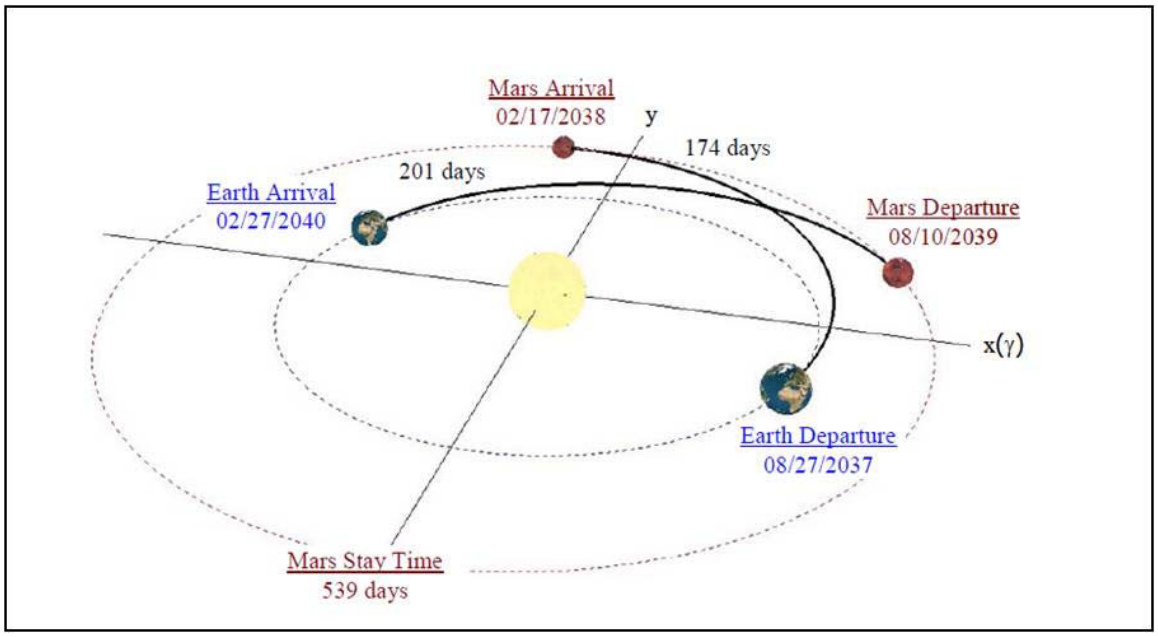

Figure 3-5: Mars Mission Profile from DRA 5.0 (NASA 2009)

In addition to the 2037 example mission, DRA 5.0 provides information on the standard Earth departure and Mars arrival orbits which have been adopted as their baseline. The mission spacecraft always departs Earth from a circular, 407 km orbit; while all Mars arrivals target an elliptical 250 km by 33,793 km orbit, with Earth return being handled by direct re-entry (NASA 2009). For the actual transfer orbits for each mission window opportunity between 2030 and 2046, DRA 5.0 provides the departure inclination from Earth, delta-Vs for transitioning into and exiting the Earth-to-Mars transfer orbit, time of flight for both legs, and the duration of the stay at Mars (NASA 2009).

To accurately determine how much warning time the various CAs will provide a manned mission to Mars, a Mission Model encompassing an Earth-to-Mars transfer, a long-term orbital stay at Mars, and the return trajectory is required. As described above, DRA 5.0 provides the general outlines for the entire mission profile from launch through re-entry at Earth. However, DRA 5.0 does not include the specifics of the orbital trajectory, delta-V on each axis, or inclination/declination of the departure trajectory. Fortunately, it's possible to develop an adequate model of the DRA 5.0 mission profile using just the departure date, arrival date, and time of flight information for each phase of the mission. For purposes of the Mission Model, only the DRA 5.0 Mars Transfer Vehicle (MTV) is tracked, which is referred to as Mars Traveler (MT) or simply Traveler.

Building the Mission Model to approximate the DRA 5.0 mission profile is accomplished in steps. First, the Earth to Mars leg is targeted to arrive as close to Mars as possible using the targeting tool in STK/Astrogator. However, simply targeting an altitude above the surface of Mars results in an interplanetary trajectory which passes beyond Mar's orbit and then comes back in, giving a transit time and shape significantly different from the objective. If STK/Astrogator aims MT at the Mars reference point as defined at the outset of the spacecraft trajectory, it is aimed "behind" Mars and cannot ever catch up, as Mars has moved on in its orbit of the Sun by the time the spacecraft arrives at the targeted point. To correct for this targeting anomaly, the Cartesian coordinates of Mars on 17 Feb 2038 are targeted instead. This adjustment results in a fairly good approximation, but is still not close enough to actually insert Traveler into orbit around Mars. Next, a mid-course trajectory correction burn is added which targets a

specific altitude over Mars (250 km periapsis, per DRA 5.0). This additional targeting places Traveler at point close enough to achieve insertion into orbit around Mars on the targeted day. Finally, an injection burn is added to actually put the Traveler into a stable, elliptical orbit around Mars.

After Mars insertion, the orbit of Traveler is propagated for 539 days, as specified in DRA 5.0. While in orbit at Mars, DRA 5.0 utilizes two additional vehicles beyond the MTV for the Mars mission: a landing vehicle for the crew to reach the surface and a Mars Ascent Vehicle (MAV) for the crew to return to the MTV for the return leg (NASA 2009). For CAs incorporating an "onboard" sensor option, a sensor (and associated processing /communications/display gear) is placed onboard the MTV (Traveler). The MTV remains in orbit during the stay at Mars and communicates with the crew on the surface via the Mars Relay Satellite (MARSAT) in accordance with the communication architecture identified in DRA 5.0 (NASA 2009). While this configuration means any sensor aboard Mars Traveler may be occasionally blocked by Mars, the highly elliptical nature of its Mars orbit (250km by 33,793 km) (NASA 2009) suggests an orbit can be achieved which minimizes or eliminates the periods of sensor blockage. Since DRA 5.0 does not specify the inclination or any other Mars orbital elements for the MTV, the analysis is simplified by inserting MTV into an orbit that maintains almost continuous view of the Sun, using as constraints only the perigee and apogee parameters provided.

Upon Mars departure at the conclusion of the surface mission, the return flight to Earth is built in the same manner as the trajectory from Earth to Mars, with the exception that Mars Traveler does not enter Earth orbit upon return, because DRA 5.0 calls for a

direct Earth return (NASA 2009). The final Mission Model profile is illustrated in Figure 3-6.

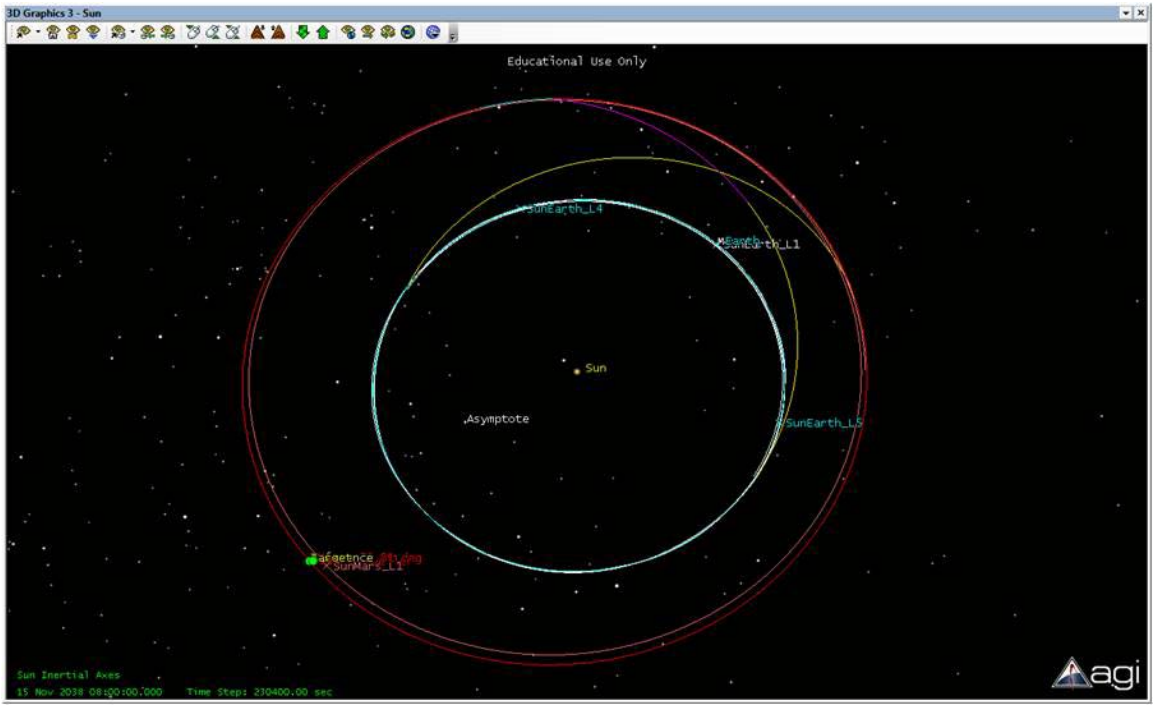

Figure 3-6: Full Mission Profile within STK

The final step in building the Mission Model is adding in the satellites which comprise the range of sensor location options available to the family of CAs. Simple sensor satellites are instanced at Sun-Earth L1, Sun-Earth L4 & L5, and Sun-Mars L1 by using the STK/Astrogator Vector Geometry Tool to define the appropriate coordinate reference systems for each point. Each satellite is created with the Sun as its central (orbit) body using the appropriate coordinate system to govern its location. Building this portion of the Mission Model is critical to developing the ability to extract data relevant to both of the Performance Models.

3.11.4 Designing Reports

The STK reports provide the data bridge from the Mission Model to the Performance Models, specifically the Link and Coverage Models. For the Link Model data, a link report is generated for each of the 13 links defined by the CAs. For each link report, the Vector Geometry Tool is fused to create a custom vector from one object to another (e.g. SE-L4 to Mars Traveler), then the Reports & Graphs Manager are used to create a custom report using the relevant custom vector. The large number of report options within STK make it challenging to find the correct Data Provider (in this case the custom vectors). For all custom vectors, "Vectors (J2000)" is used as the reference standard and "Magnitude" is the output value. "Time Properties" are set up so as to provide the Magnitude once each 24 hour day at 00:00:00.000 UTCG for the entire period of the mission (27 Aug 2037 to 28 Feb 2040). This report generation process creates an STK output list of the magnitude of the vector connecting the two specified objects once per day at 00:00:00.000 UTCG for the entire period selected (the entire mission epoch). The next step is to export or direct copy the report data into an MS Excel file for further processing within the Link Model.

Likewise, raw data for the Coverage Model is generated within the STK Reports & Graphs Manager. The Vector Geometry Tool is used to define position vectors from the center of the Sun to each solar sensor satellite and Mars Traveler, since it too represents a sensor position. Using the same "Time Properties" for the mission epoch with a report interval of 24 hours, the angle of each position vector relative to the Sun-Earth L1 vector (baseline) is output into Relative Angle reports and transferred into MS Excel for further calculations per the Solar Coverage equations.

In addition to the Magnitude reports for the Link Model and the Relative Angle reports for the Coverage Model, data is extracted from STK using the "Access" tool to determine when links are either obstructed by the Sun or lined up in such a way that the Sun blocks the line of sight of a communications antenna, thus preventing communications. For these reports, a three degree exclusion zone around the bore sight of the antenna is used. Both types of blockage generate what is referred to as a "blackout" day during which certain data paths of a particular CA are block unusable.

3.11.5 Link Model

The link model is constructed within MS Excel and consists of seven tabs. The "STK Data" tab holds the raw data results from the STK reports. The "Distance Data" tab adjusts the distances within "STK Data" to account by subtracting out the radius of the Sun or Earth for all links which have either of those two planetary bodies as one of their endpoints. This step is necessary as STK measures vector distances from center-mass to center-mass, when in actuality the signatures for the solar radiation events originate on the surface of the Sun, and communications relay sites are on the surface of the Earth.

The "Time Data" tab calculates the time (in seconds) required for the data, signature, or radiation particles to propagate along each link. In this case, the radioactive particle propagation from the Sun to Mars Traveler is treated as a link. Various link times are summed and node delays added to calculate the total time in seconds it takes a warning to reach Mars Traveler along each possible path for each day of the mission. It should be noted that the Sun-MT timing link is calculated twice: once for the time it takes

a radiation event signature to reach a sensor onboard Mars Traveler, and once for the time it takes the actual radiation particles to arrive. This double calculation is necessary as the warning signature travels at the speed of light while the particles themselves travel at approximately 75,000 km/sec (Poppe 2006).

Next, the "Minimum Times" tab compares the total propagation times along each path to determine the minimum Alert Time path within each CA at each 24 hour interval. For example, CA B2 includes three possible paths: Sun-SEL1-Earth-MT, Sun-SEL4-Earth-MT, and Sun-SEL5-Earth-MT. On Mission Day 1, it takes 1342, 1833, and 1850 seconds respectively for an alert to reach Mars Traveler along each of these paths. The smallest (minimum) of these is 1342 seconds for the Sun-SEL1-Earth-MT path, so this is the value for Alert Time associated with CA B2 for Mission Day 1.

The "Warning Time" tab calculates the Warning Time provided by each CA to Mars Traveler at 24 hour intervals by subtracting the daily Alert Time from the Radiation Time calculated previously. Additionally, this tab converts the Warning Time from seconds into minutes. This conversion makes the graphs and other outputs more readable and easier to understand. This tab is the basis for the "Warning Time vs. Mission Date - All Architectures" chart found in Chapter 4.0.

The "Statistics" tab analyzes data from the "Warning Time" tab to generate warning time performance statistics for each CA relevant across the entire mission epoch, not including blackout days. The statistics include minimum, maximum, and average Warning Time. Minimum and maximum values are calculated because they define the performance envelope of the architecture over time, and are useful if a given architecture must be rated against any critical performance thresholds, such as the minimum warning

time required to activate a particular countermeasure. Average values are useful architecture-to-architecture comparisons as general indications of performance across the entire mission epoch. Standard deviations on the data are not used because no probability functions are used within the Mission Model. The randomness of solar storms with regards to their timing, direction, magnitude, and duration is controlled to focus on architecture performance. The minimum, maximum, and average data is combined with data from the Cost Model to create efficient frontier analysis charts, from which CA observations and recommendations are made. Of note, the minimum warning time calculated on this tab is based on the times calculated in the "Warning Time" tab and should not be confused with the minimum time to provide an alert calculated on the "Minimum Times" tab. That value represents the shortest time it takes a CA to propagate an alert, while the minimum warning time on the "Warning Time" tab calculates the difference between the arrival times for the alert and the particles. On the "Minimum Times" tab, lower propagation times indicate better performance, whereas on the "Warning Time" and "Statistics" tabs, higher values indicate better performance.

The "Results" tab provides a consolidated view of the values for each CA from the "Statistics" tab as well as the Cost and Coverage Models which are contained in the same MS Excel file.

3.11.6 Coverage Model

The Coverage Model is built in a series of steps starting with establishment of angular coverage equations and concluding with the calculations performed in MS Excel on the Relative Angle outputs from STK. The first step is development of a set of

general equations (Table 3-1) using angular math, which relates the relative angles of sensor sets to the total angular range of solar coverage. The next step is to assign the proper solar coverage equation to each CA according to its particular sensor set. The general set of equations for each CA is shown in Table 3-5.

Table 3-5: Candidate Architecture Solar Coverage Equations

Architecture	General Solar Coverage Equations A1 = Relative angle between SEL1 and SML1; A2 = Relative angle between SEL1 and MT				
A1	180 degrees, constant				
B1, B2	300 degrees, constant				
C1, C2	1 < A1 < 180 180 + A1 181 to 360 deg			181 < A1 < 360 180 + (360 - A1) 359 to 180 deg	
D1, D2	1<A1<60 Constant 300 deg	61<A1<120 300+(A1-60) 301 to 360 deg	121<A1<240 Constant 360 deg	241<A1<300 300+(300-A1) 359 to 300	301<A1<360 constant 300 deg
E1	1 < A2 < 180 180 + A1 181 to 360 deg			181 < A1 < 360 180 + (360 - A1) 359 to 180 deg	
F1, F2	1<A2<60 Constant 300 deg	61<A2<120 300+(A2-60) 301 to 360 deg	121<A2<240 Constant 360 deg	241<A2<300 300+(300-A2) 359 to 300	301<A2<360 constant 300 deg
G1, G2	A2, A1 → 1 < A2 < 180 181 < A2 < 360		1 < A1 < 180 180 + max(A1,A2) min(360, 180 + A1 + 360 – A2)	181 < A1 < 360 min(360, 180 + A2 + 360 – A1) 180 + (360 – min(A1,A2)	
H1, H2	A2, A1 → 1<A2<60 61<A2<120 121<A2<240 241<A2<300 301<A2<360	1<A1<60 300 deg 300+(A2-60) 360 deg 300+(300-A2) 300 deg	61<A1<120 300+(A2-60) 300+max(A1,A2)-60 360 deg min(360,180+A1+360-A2) 300+(A1-60)	121<A1<240 360 deg 360 deg 360 deg 360 deg 360 deg	241<A1<300 300+(300-A1) min(360,180+A2+360-A1) 360 deg 300+300-min(A1,A2) 300+(300-A1)	301<A1<360 300 deg 300+(A2-60) 360 deg 300+(300-A2) 300 deg

The position vector angle of Sun-Earth L1 is defined as the baseline reference vector and forms the basis of the relative angular reference frame, always representing zero (0) degrees in position and 180 degrees of solar coverage. Angles 1 and 2 are then defined as the position vector angles of Sun-Mars L1 and Mars Traveler respectively, as measured relative to the baseline SE-L1 vector, as shown in Figure 3-7.

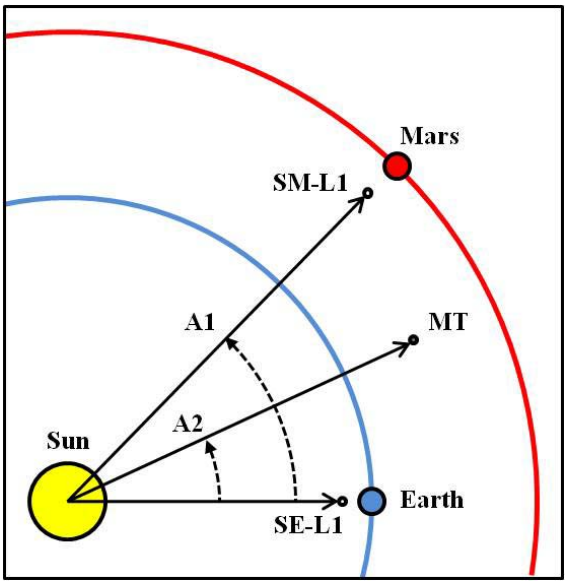

Figure 3-7: Relative Angles 1 and 2

Angles 1 & 2 are measured counterclockwise (CCW) relative to SE-L1, so each angle can vary 1-360 degrees. Within STK, two new user defined angles are created named "Angle(SEL1_SML1)" and "Angle(SEL1_MT)", and reports are run which output the values of these angles versus mission time at 24 hour intervals. However, STK only outputs the magnitude of relative angles, meaning the user-defined angles only vary 0-180 degrees from the SE-L1 vector. Some minor equation changes enable conversion of 1-360 degrees CCW into 0-180 degrees regardless of direction. The actual angles and time values for both Angles 1 and 2 are then copied into MS Excel as raw data for the Coverage Model. The general Coverage Model equations have multiple variables and are conditional, but are designed to account for any combination of sensors regardless of their relative hemispheric location relative to the object being observed. However, upon further inspection of the scenario, it is observed that Sun-Mars L1 and Mars Traveler always share the same hemisphere throughout the entire mission epoch. This limitation greatly simplifies the multi-variable general equations as shown in Table 3-6. Using

these simplified equations and the raw Angle 1 and 2 data extracted from STK, the tab "Coverage Degrees" is used to calculate the total degree coverage of each CA versus mission time. Tab "Coverage %" is used to convert these degree coverage values into percent coverage by dividing by 360 degrees.

Table 3-6: Scenario-Limited Solar Coverage Equations

Architecture	Coverage Equations (Scenario Limited) A1=Angle 1; A2=Angle 2
A1	180 deg
B1 / B2	300 deg
C1 / C2	180 + A1
D1 / D2	min(360, 240 + max(60, A1))
E1	180 + A2
F1 / F2	min(360, 240 + max(60, A2))
G1 / G2	180 + max(A1, A2)
H1 / H2	min(360, 240 + max(60, A1, A2))

3.11.7 Cost Model

Built to define the relative cost of each CA, the Cost Model is fundamental for developing the efficient frontier charts which show the relative cost-benefit of the entire set of CAs. The Cost Model is unique in that it does not rely on data outputs from STK, but instead relies entirely on parametric analysis of the CAs. The Cost Model consists of four tables: the CA Master Component Table (Table 3-7), the STEREO/MRO Factsheet Table (Table 3-8), the Subsystem Percent Mass Budget Allocation Table (Table 3-9), and the CA Mass Table (Table 3-10).

Table 3-7: Candidate Architecture Master Component List

Parameter	SEL1 Sat	SEL4/5 Sat	SEL4/5+ Sat	SML1 Sat	SML1+ Sat	MT S-Pkg	MT C-Pkg	MT P-Pkg
Reference	STEREO	STEREO	STEREO/MRO	MRO	MRO	STEREO	MRO	HTPC
S/C Mass (kg)	381	381	381	892	892	0	0	20
P/L Mass (kg)	133	133	133	133	133	133	0	0
Antenna(s)	1.2m HGA	1.2m HGA	1.2m + 3m	3m	3m + 3m	None	3m	None
1.2m (kg)	33	33	33	0	0	0	0	0
3m (kg)	0	0	62	62	124	0	62	0
Tot Mass (kg)	547	547	609	1087	1149	133	62	20
Fuel	Variable	Variable	Variable	Variable	Variable	NA	NA	NA
Proc Delay (sec)	240	240	240	240	240	240	NA	60

The CA Master Component Table includes an entry for each component or component configuration that will have to be deployed to implement one or more of the CAs. For example, there are entries for both an SML1 Satellite and an SML1+ Satellite. The "+" indicates a configuration that can also support direct communications with Mars Traveler, as is required in some of the CAs. Within the Master Component Table, each component is assigned a real-world reference system such as STEREO or the Mars Reconnaissance Orbiter (MRO), which serve as parametric references for technical specifications and mass budget. Total Dry Mass is then divided into three sub-categories: spacecraft, payload (sensor), and antenna (communications).

Table 3-8: STEREO/MRO Fact Sheet (Jet Propulsion Laboratory n.d.) (NASA 2006)

Component	STEREO	MRO
Spacecraft (kg)	414	892
Payload (kg)	133	139
Fuel (kg)	63	1149
Total Wet (kg)	610	2180
Total Dry (kg)	547	1031
Antenna	1.2m	3m
Delay (sec)	240	240

Using NASA Fact Sheets for STEREO and MRO (Table 3-8), and a historical breakdown of past mission mass budgets defined by percentage of total (Table 3-9), the mass budgets of each component are calculated. The spacecraft mass for STEREO-based components is found by subtracting the telecom mass calculated within Table 3-8 from the total spacecraft mass listed for STEREO in Table 3-7 (which did not break out the telecom mass).

Table 3-9: Typical Mass Budget for Interplanetary Satellites (Brown 2002)

Subsystem	Mass Budget (%)	STEREO (kg)	MRO (kg)
Structure	26	142.22	268.06
Thermal	3	16.41	30.93
ACS	9	49.23	92.79
Power	19	103.93	195.89
Cabling	7	38.29	72.17
Propulsion	13	71.11	134.03
CDS	6	32.82	61.86
Payload	11	60.17	113.41
Telecom	6	32.82	61.86
Total	100	547	1031

The spacecraft mass for MRO-based satellites is taken directly from Table 3-8, and the "spacecraft mass" for the Mars Traveler processing package is approximated as the mass of a 17-inch LCD monitor and mini-computer, taken from specifications found on the Internet. The payload masses for STEREO and MRO are taken directly off their respective specification sheets in Table 3-8. Antenna sizes and quantities are then assigned to each CA Master Component based on the link and range requirements as documented in the CA OV-1s. For example the SML1 Sat component only has to communicate back to Earth via the DSN and therefore only requires a single 3-meter antenna. However SML1+ Sat is a component of CAs which must directly communicate with both Mars Traveler and the DSN in parallel, therefore it requires two 3-meter antennas. The mass budgets for the various antenna sizes and quantities are calculated, once again parametrically from Tables 3-8 and 3-9. The total mass budget for each CA Master Component is tallied for use in Table 3-10.

Table 3-10: Candidate Architecture Dry Mass Budgets

Arch	SEL1 Sat	SEL4 Sat	SEL5 Sat	SEL4 Sat +C	SEL5 Sat +C	SML1 Sat	SML1 Sat +C	MT +Sensor	MT +Comm	MT +Proc	Total Mass (kg)
A1	547										547
B1	547	547	547								1641
B2	547			609	609				62	20	1847
C1	547					1087					1634
C2	547						1149		62	20	1778
D1	547	547	547			1087					2728
D2	547			609	609		1149		62	20	2996
E1	547							133		20	700
F1	547	547	547					133		20	1794
F2	547			609	609			133	62	20	1980
G1	547					1087		133		20	1787
G2	547						1149	133	62	20	1911
H1	547	547	547			1087		133		20	2881
H2	547			609	609		1149	133	62	20	3129

The end result of the Cost Model is Table 3-10, which calculates the total dry mass of each CA by summing the mass contributions of each component present in a given CA. For example, CA-D1 includes an SEL1 Sat, SEL4 Sat, SEL5 Sat, and an SML1 Sat, all of which amount to a total dry mass of 2728 kg. The Cost Model dry mass outputs for each CA are then transferred to the "Results" tab for incorporation into the efficient frontier charts.

3.11.8 Value Model

When considered in isolation, the analysis results for each performance metric may recommend a different CA as the optimal solution. This situation shall require some form of relative valuation to determine an overall solution. Since the purpose of the thesis is to identify an optimal reference architecture, the two performance metrics are combined using the Value Model to obtain a single, weighted performance value (utility) by which to assess each CA. The respective single dimensional value functions (SDVF) of each performance metric are shown in Figure 3-8.

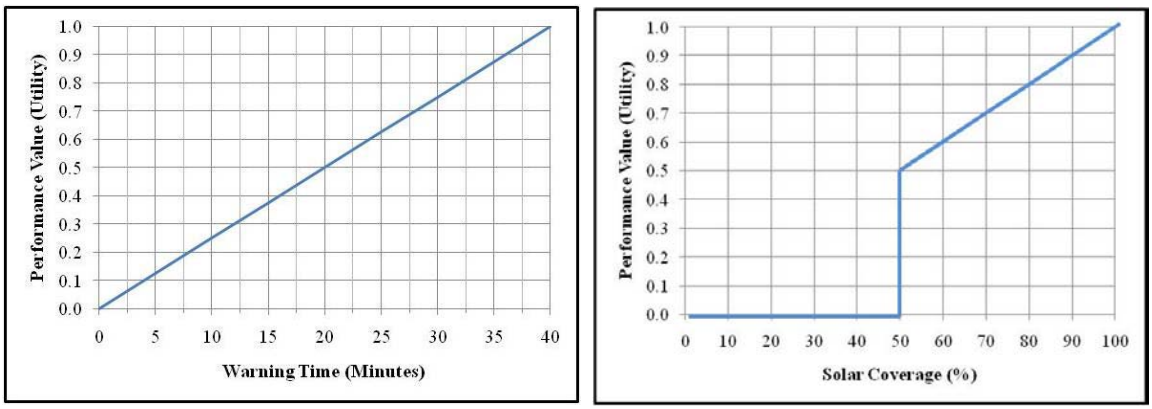

Figure 3-8: Single Dimensional Value Functions

Linear value functions are defined for each performance value, with the range of each based on the potential range of values for each performance metric. For the Solar Coverage SDVF, any coverage percentage less that 50% has a performance value of 0.0, since a CA must have at least one sensor providing a minimum of 50% coverage. As previously discussed in Section 3.8, the Warning Time metric is defined to have twice the importance of the Solar Coverage metric, and is weighted accordingly in the value equations. Value models are user-defined tools, so these performance metric weights and the SDVF curves can be modified based on the values of the user, or further adjusted based on new information. From the two Value Models, the following equations are derived describing the performance metric - value relationships:

$$\textit{Warning Time Value (CA)} = \textit{Warning Time (CA)} / 40, \textit{Warning Time} \leq 40 \textit{ min}$$

$$\textit{Warning Time Value (CA)} = 1.0, \textit{Warning Time} > 40 \textit{ min}$$

$$\textit{Solar Coverage Value (CA)} = \textit{Solar Coverage (CA)} / 100, \textit{Solar Coverage} \leq 100\%$$

$$\textit{Solar Coverage Value (CA)} = 1.0, \textit{Solar Coverage} > 100\%$$

$$\textit{Overall Value (CA)} = (\textit{Warning Time Value (CA)} \times 0.66) + (\textit{Solar Coverage Value (CA)} \times 0.33)$$

The weighted value equations are then applied to the efficient frontier results for the individual performance metrics and enable construction of an Overall Value Efficient Frontier chart as shown in Figure 3-9.

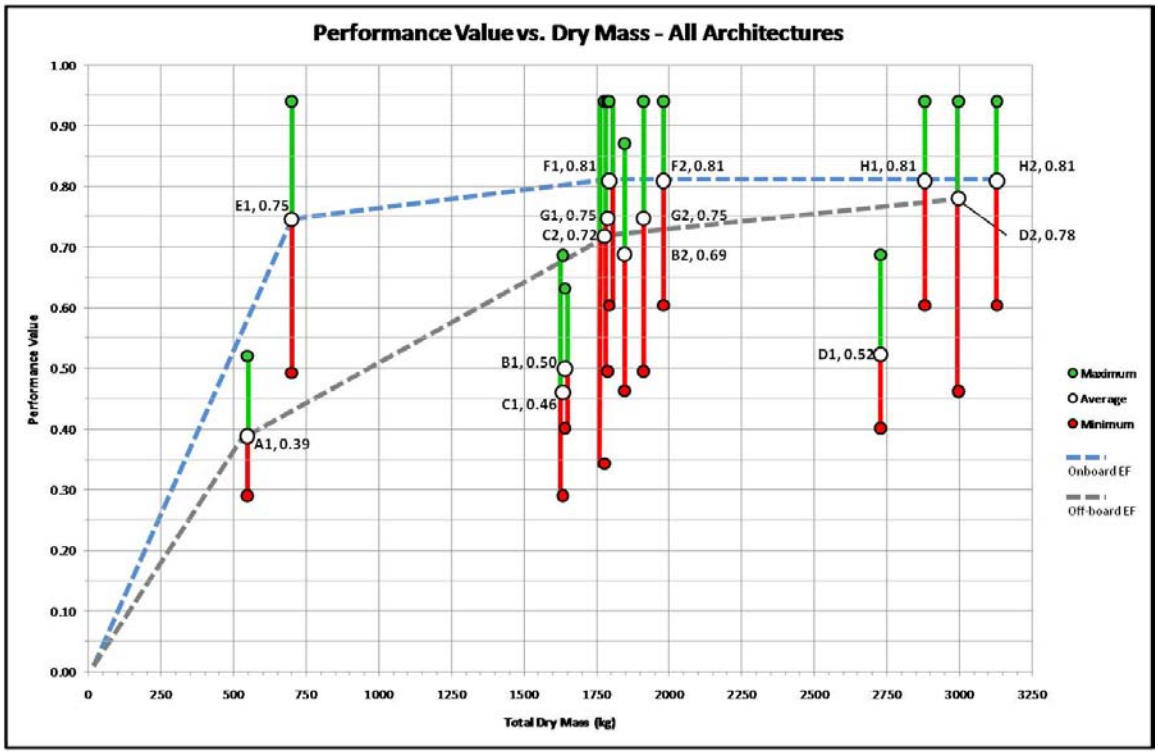

Figure 3-9: Performance Value Efficient Frontier

4.0 Results and Analysis

4.1 Introduction

This chapter examines the outputs from the Five-Models used to identify the best-value CA. It includes analysis of individual warning propagation paths, followed by inspection of the performance of each CA. CAs are then compared using efficient frontier graphs for each performance metric, and these separate performance metric results are combined using a value model to arrive at a final recommended CA.

4.2 Propagation Paths

Within the 14 CAs, there are a total eight unique propagation paths that can provide an alert to Mars Traveler of an imminent solar radiation storm (see Figure 4-1). As depicted in Figure 4-2, each propagation path provides widely varying amounts of warning time, depending on the current date of the mission and relative positions of the CA components involved.

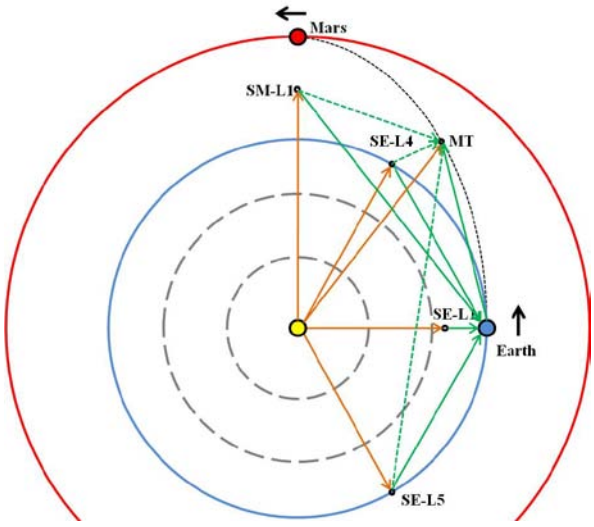

Figure 4-1: Architecture Paths

Each alert propagation path directly affects the performance over time of the various CAs. The first feature of interest is the red (dashed) line (Figure 4-2) which represents the time it takes for a radiation storm to reach Mars Traveler from the Sun. When a given path line is below the radiation line, the amount of warning time provided by a given alert path is represented by the difference between the two lines. When a given path line lies above the radiation line (i.e. Sun-SML1-Earth-MT) the warning time is negative, which means the alert arrives after the radiation. Another notable feature of Figure 4-2 is that several of the path lines show drop outs where the propagation time goes to zero. These drop outs do not represent conditions of instantaneous alert time; instead they indicate blackout periods during which a given path is blocked by the Sun and is unable to provide an alert.

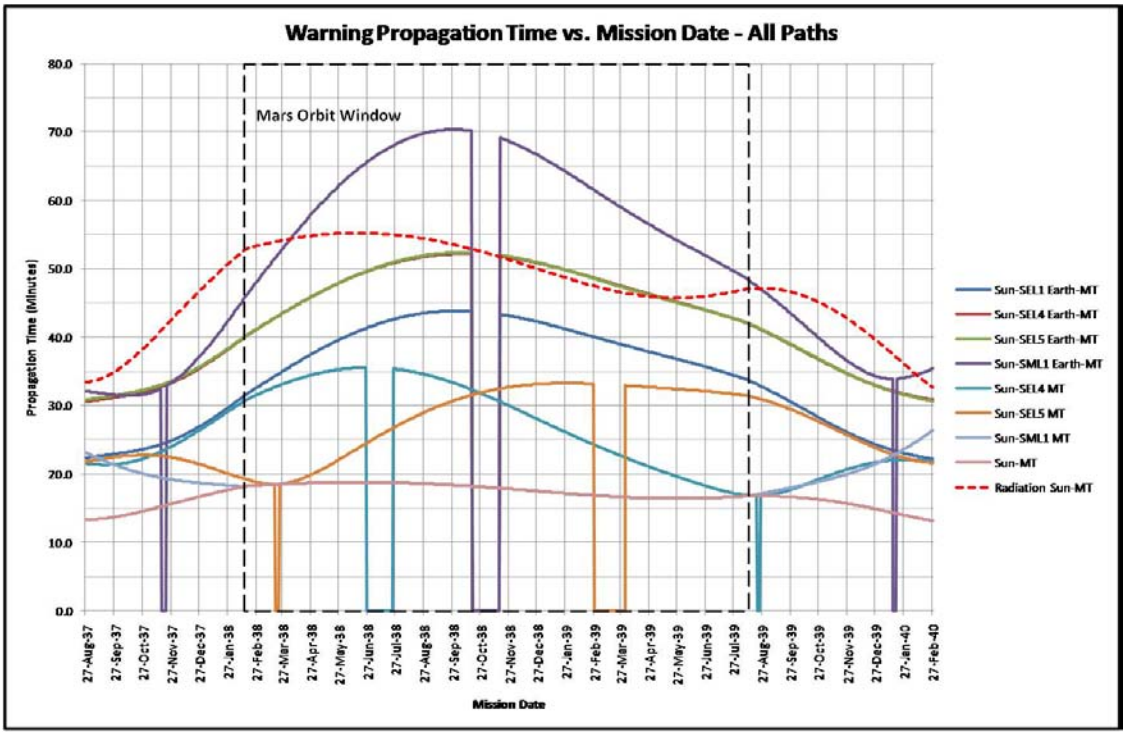

Figure 4-2: Warning Propagation Time vs. Mission Date

4.2.1 Sun-SEL1-Earth-MT:

The Sun-SEL1-Earth-MT path serves as the baseline CA and models a radiation storm indication originating from the Sun and being detected at the Sun-Earth L1 point by a solar observation satellite. The indication data is transmitted to Earth via the NASA Deep Space Network (DSN), and then transmitted to the Space Environment Center (SEC) in Boulder, Colorado via terrestrial communications networks. At the SEC, solar forecasters make a real-time determination to transmit a space weather storm alert, which is sent to Mars Traveler via the DSN. From first indication to when Mars Traveler receives the alert, this path has an average propagation time of 33.8 minutes with a maximum propagation time of 43.8 minutes and a minimum propagation time of 22.2 minutes. This path also suffers a 30-day blackout of its connection to Mars Traveler at approximately the mid-point of the scenario mission epoch, when Mars is in conjunction with the Sun (as viewed from Earth). This blackout period takes place while the Mars crew is performing their surface activities and are somewhat protected by both the Martian atmosphere and (half the time) the mass of Mars itself. This path is included in every CA as baseline.

4.2.2 Sun-SEL4(SEL5)-Earth-MT

The Sun-SEL4-Earth-MT path and its mirror, Sun-SEL5-Earth-MT, rely on sensors at the Sun-Earth L4 & L5 points respectively. These sensors add additional solar surface coverage by extending the arc of coverage by 60 degrees ahead of and behind the Sun-Earth L1 sensor. However, this coverage comes at the cost of reduced warning time compared to Sun-Earth L1, especially for Earth Relay-based CAs, as L4 and L5 are both

as far from the Earth as they are from the Sun, thus requiring about twice the alert propagation time as Sun-Earth L1. This additional delay causes a negative warning time period immediately after Mars moves from behind the Sun as seen from Earth. Additionally, as both of these paths still pass their data to Earth for processing and then transmission to Mars Traveler, both paths suffer from the same communication drop out as the Sun-SEL1-Earth-MT path. From radiation event to alert arrival at Mars Traveler, the L4 and L5 paths average propagation times are both 43.3 minutes, with maximum propagation times of 52.2 and 52.4 minutes, and minimum propagation times of 30.6 and 30.7 minutes respectively. These paths are included in architecture options B1, B2, D1, D2, F1, F2, H1, and H2.

4.2.3 Sun-SML1-Earth-MT

The Sun-SML1-Earth-MT path relies on a solar observation satellite placed at Sun-Mars L1. Solar signature data is then routed to Earth for processing and then transmitted back out to Mars Traveler if an alert is required. As expected, due to the typically extreme distance between Sun-Mars L1 and Earth, this path suffers the long propagation times with the exception of a short period when Mars is directly behind the Earth from the Sun and the Sun-Mars L1 point is actually closer to Earth than the Sun-Earth L4 and L5 points. In fact, as clearly shown in Figure 4-2, this path provides negative warning time over a significant portion of the mission profile. It also suffers from the 30 day blackout window common to all paths that rely on Earth Relay when Mars is in conjunction. This path suffers from two additional, 4-day blackout periods, one early and one late in the mission epoch, when Mars is in opposition to the Sun as

seen from Earth. During these periods, Earth sits in a 3 degree exclusion angle window to Sun-Mars L1 during which radio interference from the Sun drowns out communications signals (NASA 2009). Indication to alert time this path has an average propagation of 50.9 minutes with a maximum of 70.3 minutes and a minimum of 31.5 minutes. This path is included in architectures C1, C2, D1, D2, G1, G2, H1, and H2.

4.2.4 Sun-SEL4(SEL5)-MT

Similar to Sun-SEL4/SEL5-Earth-MT, these paths have sensors located at the Sun-Earth L4 & L5 points. The significant difference is that these paths represent direct data transmission to Mars Traveler for processing, analysis, and first-hand alert notification. Without needing to route data back to Earth, these paths are notably faster in providing alert data to Mars Traveler. Additionally, the removal of the Earth processing node results in significantly different propagation time profiles for the two paths and eliminates the 30 day blackout window due to the Mars-Sun conjunction as viewed from Earth. However, each path still experiences a 30-day communications blackout when due to Mars-Sun conjunctions as viewed from Sun-Earth L4 and L5. These blackouts occur when the solar satellites and Mars Traveler are opposite each other with respect to the Sun, at their farthest separation points when the blocked path is not optimal for alert time. However, since these two paths always exist as a pair within the various CAs, due to the architectural pairing of SEL4 and SEL5, there is actually no blackout period in a given CA, as Mars Traveler is always in view of either SEL4 or SEL5 at any given point in time during the mission epoch. Each path also suffers from a 4-day blackout when Mars Traveler passes behind the solar satellite with respect to the

Sun. As with the Sun-SML1-Earth-MT path this is caused by the 3 degree exclusion angle due to solar interference (NASA 2009). Unlike the 30-day blackout windows, these occur at points where the solar satellites are closest to Mars Traveler and will result in noticeable spikes in propagation times (and corresponding drops in warning times) in at least some of the CA options. For the L4 and L5 paths, indication to alert reception average propagation times are 25.6 and 26.7 minutes, maximum times are 35.6 and 33.3 minutes, and minimum times are 16.8 and 18.5 minutes, respectively. These paths are included in architecture options B2, D2, F2, and H2.

4.2.5 Sun-SML1-MT

Similar to Sun-SEL4/SEL5-Earth-MT, these paths have sensors located at the Sun-Earth L4 & L5 points. The significant difference is that these paths represent direct data transmission to Mars Traveler for processing, analysis, and first-hand alert notification. Without needing to route data back to Earth, these paths are notably faster in providing alert data to Mars Traveler. Additionally, the removal of the Earth processing node results in significantly different propagation time profiles for the two paths and eliminates the 30 day blackout window due to the Mars-Sun conjunction as viewed from Earth. However, each path still experiences a 30-day communications blackout when due to Mars-Sun conjunctions as viewed from Sun-Earth L4 and L5. These blackouts occur when the solar satellites and Mars Traveler are opposite each other with respect to the Sun, at their farthest separation points when the blocked path is not optimal for alert time. However, since these two paths always exist as a pair within the various CAs, due to the architectural pairing of SEL4 and SEL5, there is actually no

blackout period in a given CA, as Mars Traveler is always in view of either SEL4 or SEL5 at any given point in time during the mission epoch. Each path also suffers from a 4-day blackout when Mars Traveler passes behind the solar satellite with respect to the Sun. As with the Sun-SML1-Earth-MT path this is caused by the 3 degree exclusion angle due to solar interference (NASA 2009). Unlike the 30-day blackout windows, these occur at points where the solar satellites are closest to Mars Traveler and will result in noticeable spikes in propagation times (and corresponding drops in warning times) in at least some of the CA options. For the L4 and L5 paths, indication to alert reception average propagation times are 25.6 and 26.7 minutes, maximum times are 35.6 and 33.3 minutes, and minimum times are 16.8 and 18.5 minutes, respectively. These paths are included in architecture options B2, D2, F2, and H2.

4.2.6 Sun-MT

This path places a solar sensor and processing capability directly onboard the Mars Traveler vehicle itself, resulting in the shortest overall propagation distance and correspondingly fastest alert time. Only when Mars Traveler is at Earth or Mars are the other paths comparable to the Sun-MT alert times. While Mars Traveler is near Earth, the additional time required to pass information via the Earth and DSN prevents the Sun-SEL1-Earth-MT path from closing the gap. However, Sun-SML1-MT provides an almost-identical alert time profile while Mars Traveler is at Mars. Indication-to-alert average propagation time is 16.8 minutes, with a maximum of 18.8 minutes and minimum of 13.2 minutes. This path is included in architecture options E1, F1, F2, G1, G2, H1, and H2.

4.3 Architecture Performance

As discussed in Chapter 3.0 there are 14 candidate architectures under consideration. The Warning Time, in minutes, provided by each CA across the mission epoch is shown in Figure 4-3. Due to the high degree of overlapping, and the fact that there are only five Warning Time curves for the 14 CAs, this graph clearly shows that certain propagation paths dominated within CA sets with similar features. Warning Time performance for all architectures is summarized in Table 4-1.

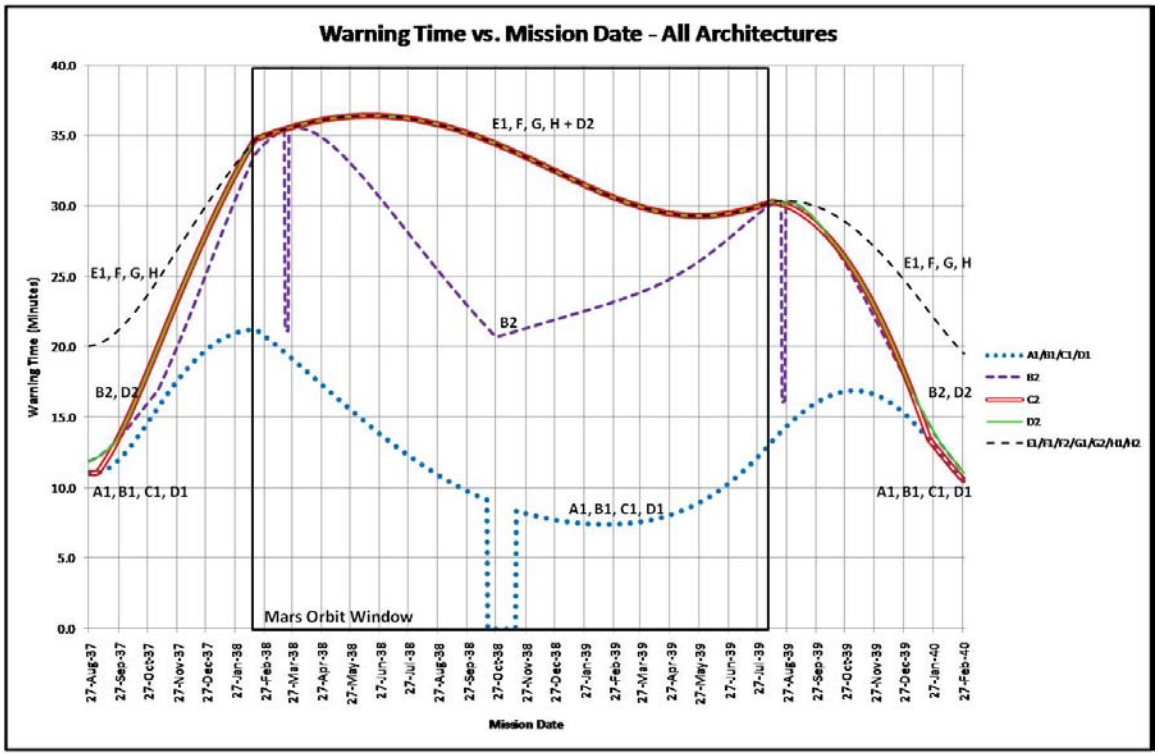

Figure 4-3: Warning Time vs. Mission Date

The Solar Coverage, in percentage of solar surface, provided by each CA across the mission epoch is depicted in Figure 4-4. As with the Warning Time vs. Mission Date graph, there is also a significant amount of profile overlapping among the 14 CAs,

especially during the Mars orbit window. This high degree of overlap simply indicates performance similarities among CAs with the same sensor sets. Solar coverage for all architectures is also summarized in Table 4-1.

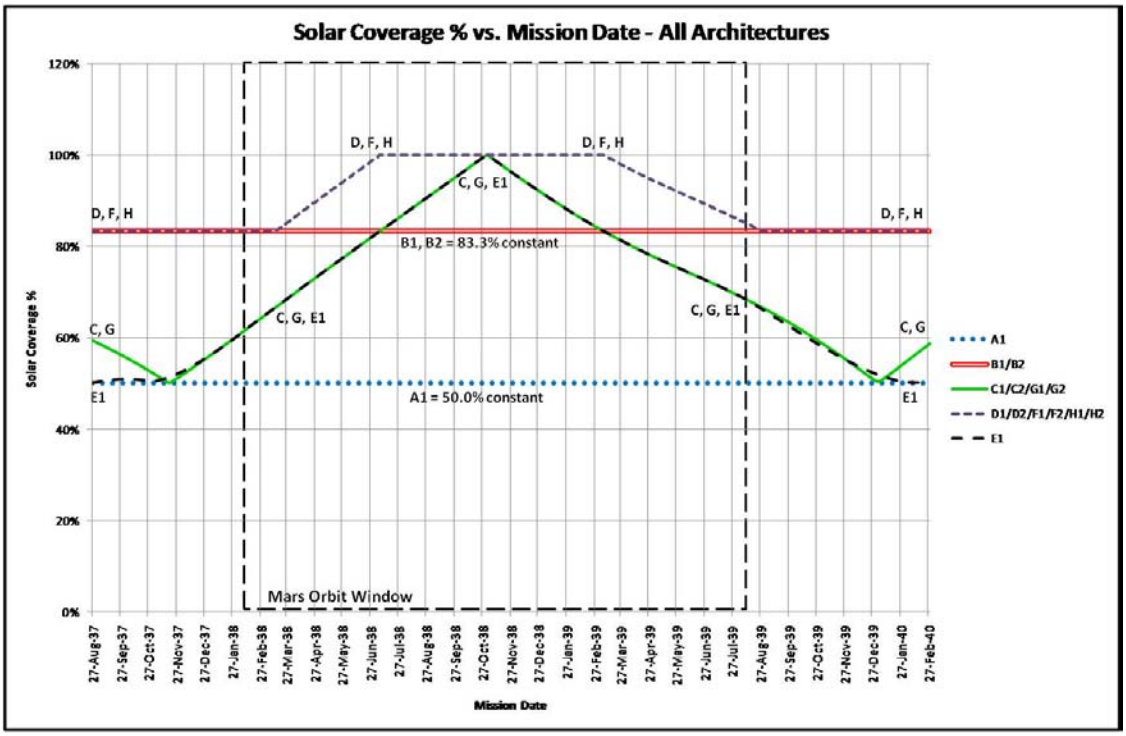

Figure 4-4: Solar Coverage vs. Mission Date

4.3.1 Candidate Architecture OV-1s

The 14 CAs were documented in a series of OV-1s, which are included in the written architecture descriptions below. Each OV-1 depicts a top-down view of the solar system with the Sun (yellow) in the center and Earth (blue) and Mars (red) in their orbits. Mars was placed ahead of Earth in its orbital progression to simplify the Mars Traveler illustration. The dashed parabolic line is a representation of Mars Traveler's trajectory from Earth to Mars. The grey dashed circles represent the orbits of Mercury and Venus, for reference. Also, the radii of the Sun, Earth, and Mars are not to scale. Orange vectors originating from the Sun represent the electromagnetic signature of a solar radiation

storm. Green vectors represent man-made data signals: both processed sensor data and alert communications.

4.3.2 Architecture Candidate A1

Architecture A1 includes only the Sun-SEL1-Earth-MT propagation path (see Figure 4-5). It is the simplest of the architecture options and serves as the baseline. As the simplest option, it also has the lowest mass (cost). A1 provides an average of 13.3 minutes of warning time across the mission epoch, which isn't too impressive. Maximum warning time occurs when Mars Traveler initially reaches orbit at Mars. This CA suffers from the 30-day Earth to Mars communications blackout caused by Sun occultation of Mars as seen from Earth. While in view, the least warning time provided is 7.4 minutes which occurs shortly past the mid-point of the mission when Mars is at its furthest distance from the Earth. Within Figure 4-3, A1 shares the same Warning Time curve as B1, C1, and D1. A1's single sensor at SE-L1 provided a constant 50% solar coverage.

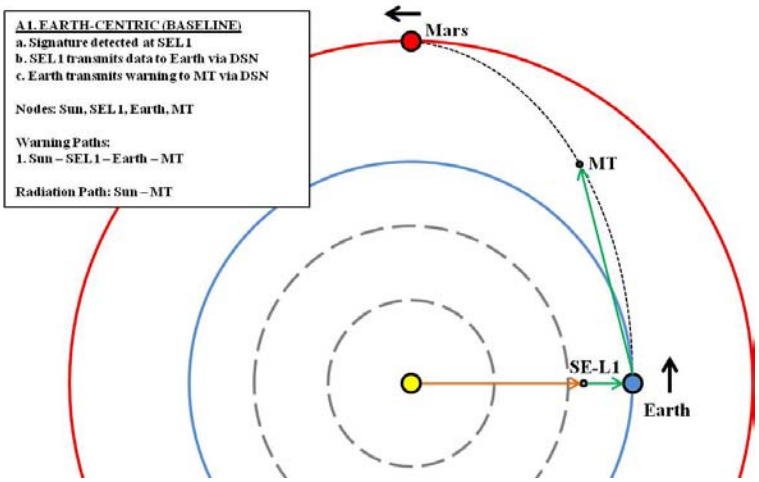

Figure 4-5: Candidate Architecture A1

4.3.3 Architecture Candidate B1

Architecture B1 includes three propagation paths: Sun-SEL1-Earth-MT, Sun-SEL4-Earth-MT, and Sun-SEL5-Earth-MT (see Figure 4-6). This option has over three times the mass of A1 (1641 kg vs. 547 kg), but has the exact same Warning Time profile as A1. This matching to A1 performance is driven by the fact that Sun-Earth L1 is significantly closer to Earth than Sun-Earth L4 and L5, making the Sun-SEL1-Earth-MT path significantly shorter and with a correspondingly shorter propagation time across the entire mission epoch. Since the model assumes a radiation storm signature is in view of all CA sensors at the same instant, the shorter length of the Sun-SEL1-Earth-MT path dominates the longer SEL4 and SEL5 paths. With its two additional sensors, B1 provided a constant 83.3% solar coverage across the mission epoch.

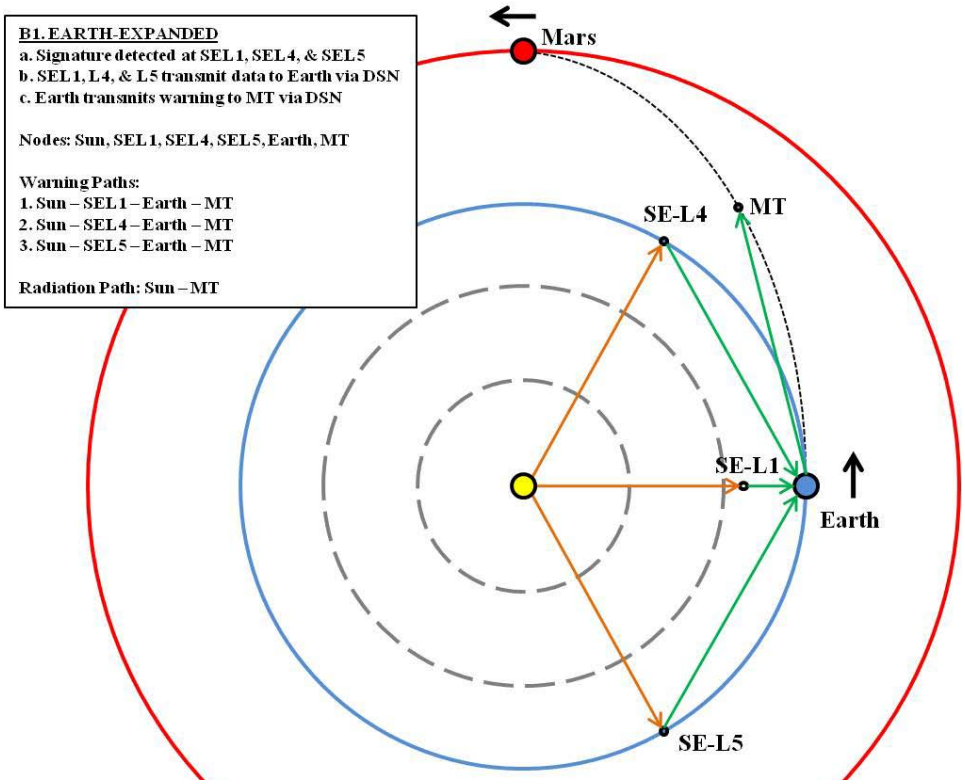

Figure 4-6: Candidate Architecture B1

4.3.4 Architecture Candidate B2

Architecture B2 uses the same sensor paths as B1: Sun-SEL1-Earth-MT, Sun-SEL4-Earth-MT, and Sun-SEL5-Earth-MT, but then adds direct links from the SE-L4 and SE-L5 sensors to Mars Traveler (see Figure 4-7). These additional communications paths increase the estimated mass requirement by approximately 200 kg when compared to B1, however they also radically change the provided warning time profile. Bypassing Earth and sending the data directly to Mars Traveler significantly reduces the average length of the propagation path. As a result, the Sun-SEL1-Earth-MT path no longer dominates the results, and the best path varies between the direct links from Sun-Earth L4 and L5. In this case, the Sun-SEL1-Earth-MT path never dominates due to the delays caused by using the Earth's communications and processing infrastructure. Because of the direct links from Sun-Earth and L5, B2 provides an average of 24.6 minutes of warning time across the mission epoch, with minimum and maximum times of 11.1 and 35.6 minutes, respectively. The direct links from the Sun-Earth L4 and L5 also eliminate the 30-day communications blackout caused by the Sun blocking Earth-Mars line of sight. The B2 warning time profile contains two unique features not exhibited by the other CAs. There are two sudden short drops in warning performance caused by the alignment of Mars Traveler behind Sun-Earth L4 during the outbound journey and Sun-Earth L5 during the return journey, as viewed from the Sun. These alignments place the transmission path from the closer point directly on the Mars Traveler-Sun line, resulting in disruption of the link, which forces Mars Traveler to rely on the other, much further away sensor. Each of these interruptions is approximately 4 days long. In either case the

Sun-SEL1-Earth-MT path is still longer due to the additional Earth delays. Like architecture B1, B2 provides a constant 83.3% solar coverage.

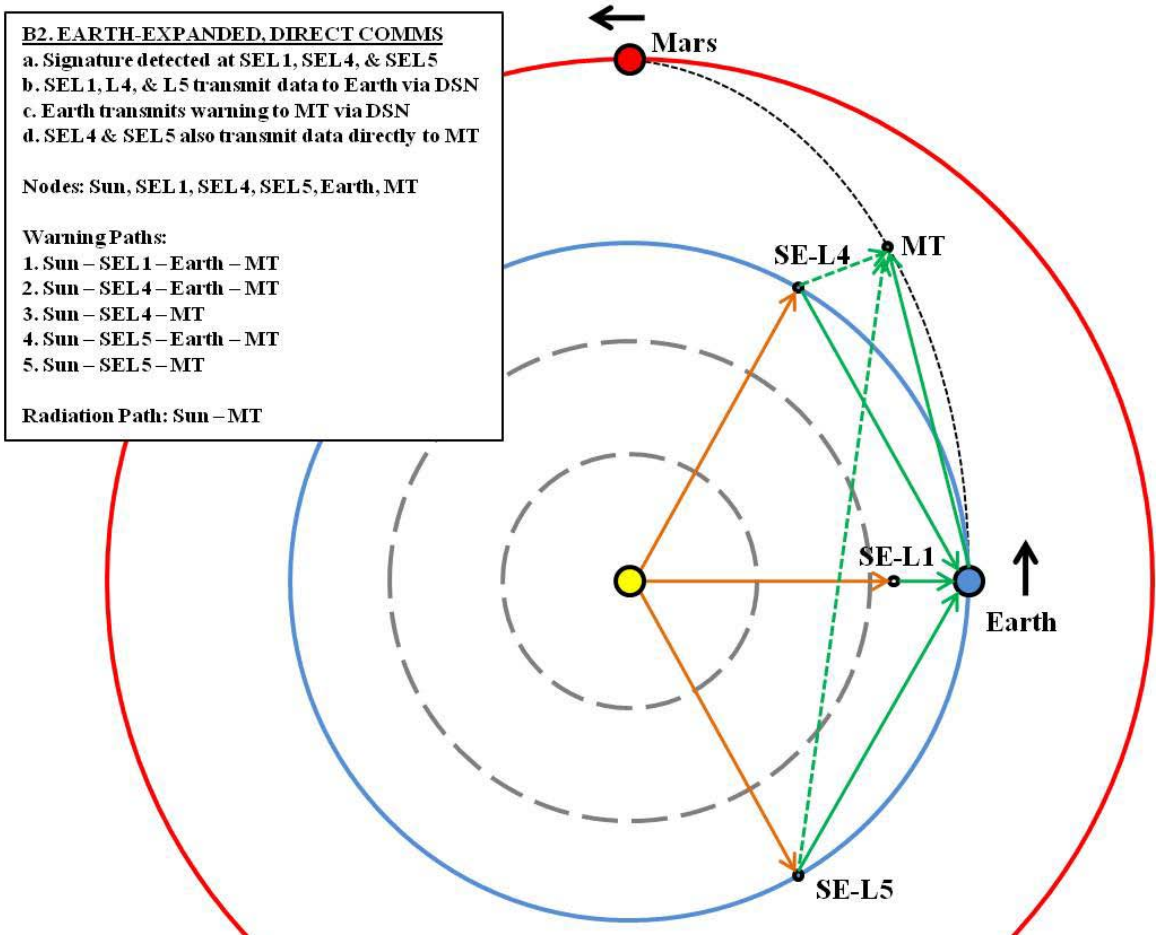

Figure 4-7: Candidate Architecture B2

4.3.5 Architecture Candidate C1

Architecture option C1 adds to A1 by placing a sensor at Sun-Mars L1 (see Figure 4-8). However, this CA does not include data reception and processing capabilities on Mars Traveler, so the data must be relayed to Mars Traveler via Earth. The two propagation paths included in C1 are Sun-SEL1-Earth-MT and Sun-SML1-Earth-MT. C1 has almost the same estimated increase in mass and cost over A1 as compared to B1

(C1: 1634kg, B1: 1641kg, A1: 547lg). However, as with B1, the requirement to route all data through Earth results in the Sun-SEL1-Earth-MT path dominating the warning time results. Despite the additional mass, C1 has exactly the same warning time performance as A1 and B1, likewise suffering from the same 30-day communications blackout. With the addition of a dynamic sensor at SM-L1 relative to the SE-L1 baseline, architecture C1 provides an average of 71.8% coverage.

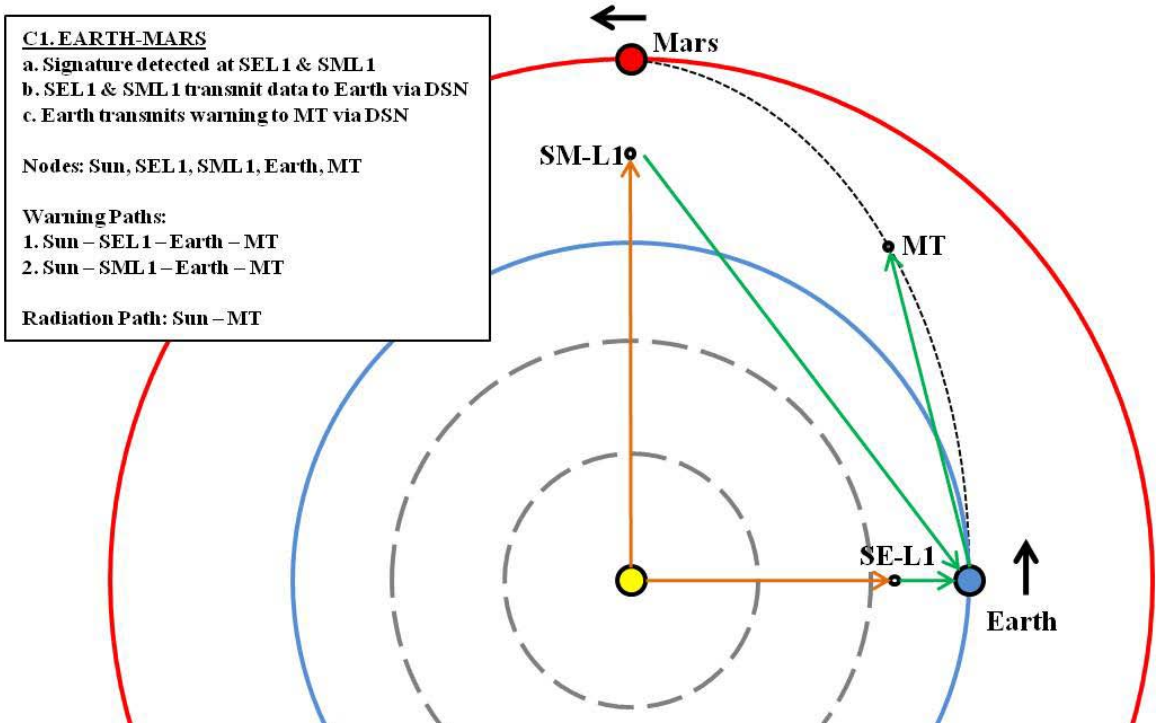

Figure 4-8: Candidate Architecture C1

4.3.6 Architecture Candidate C2

Architecture C2 uses the same two locations for sensors as C1, Sun-Earth L1 and Sun-Mars L1, but adds a direct link from the Sun-Mars L1 sensor to Mars Traveler (see Figure 4-9). This additional path, Sun-SML1-MT, profoundly alters the results as compared to both C1 and A1. C2 provides an average warning time of 28.7 minutes, a minimum warning time of 10.6 minutes, and a maximum warning time of 36.4 minutes.

Additionally, due to the direct link from the Sun-Mars L1 sensor to Mars Traveler, there is no 30-day blackout period. Even better, C2 represents only a small increase in mass over C1 (144kg). On Figure 4-3 the C2 profile is barely visible early and late in the mission epoch, but is otherwise identical to D2 (outbound and return) or H1 (at Mars). Architecture C2 provides an average of 71.8% solar coverage.

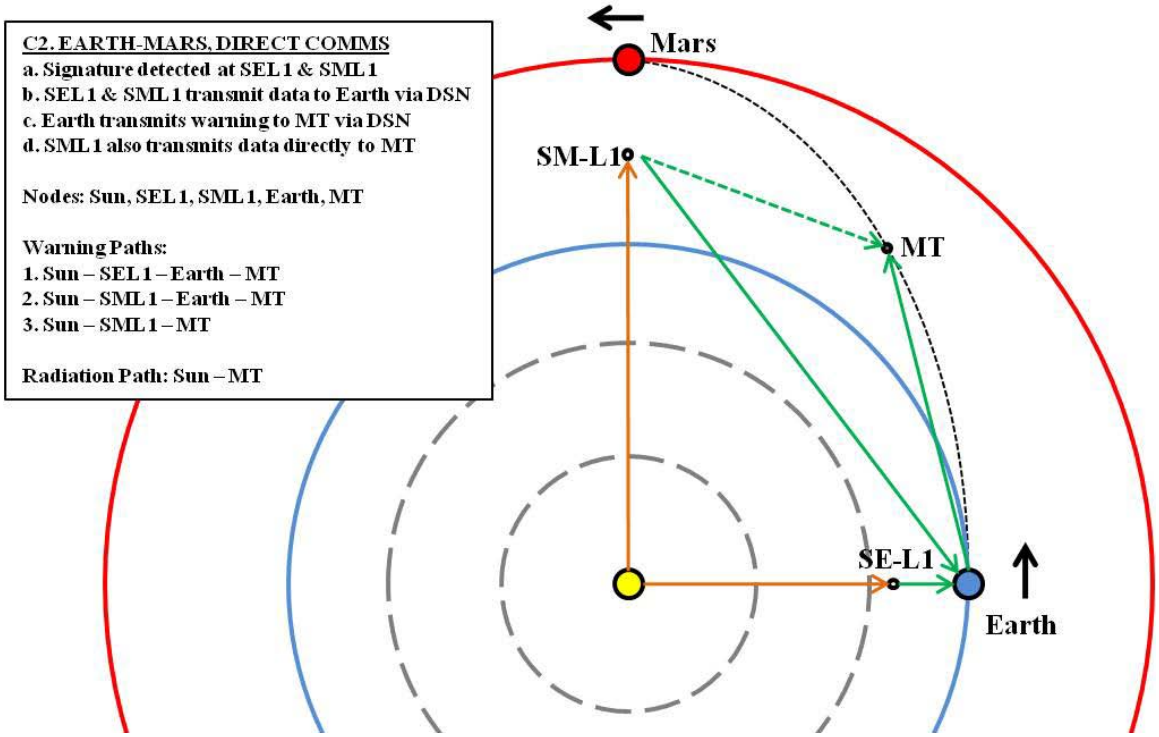

Figure 4-9: Candidate Architecture C2

4.3.7 Architecture Candidate D1

Architecture D1 adds the Sun-Earth L4 and L5 sensors of from B1 and the Sun-Mars L1 sensor from C1 to the A1 baseline (see Figure 4-10). As previously discussed, the Sun-SEL1-Earth-MT path dominates these arrangements, and it is the same case here. The warning time performance for D1 is identical to that of A1, as well as B1 and C1, as

can be clearly seen in Figure 4-3. Unfortunately, D1 is one of the four heaviest options in the CA set, with an estimated mass requirement of 2728 kg. Architecture D1 significantly increases solar coverage to an average of 90.4% due to additional sensors at SE-L4, SE-L5, and SM-L1.

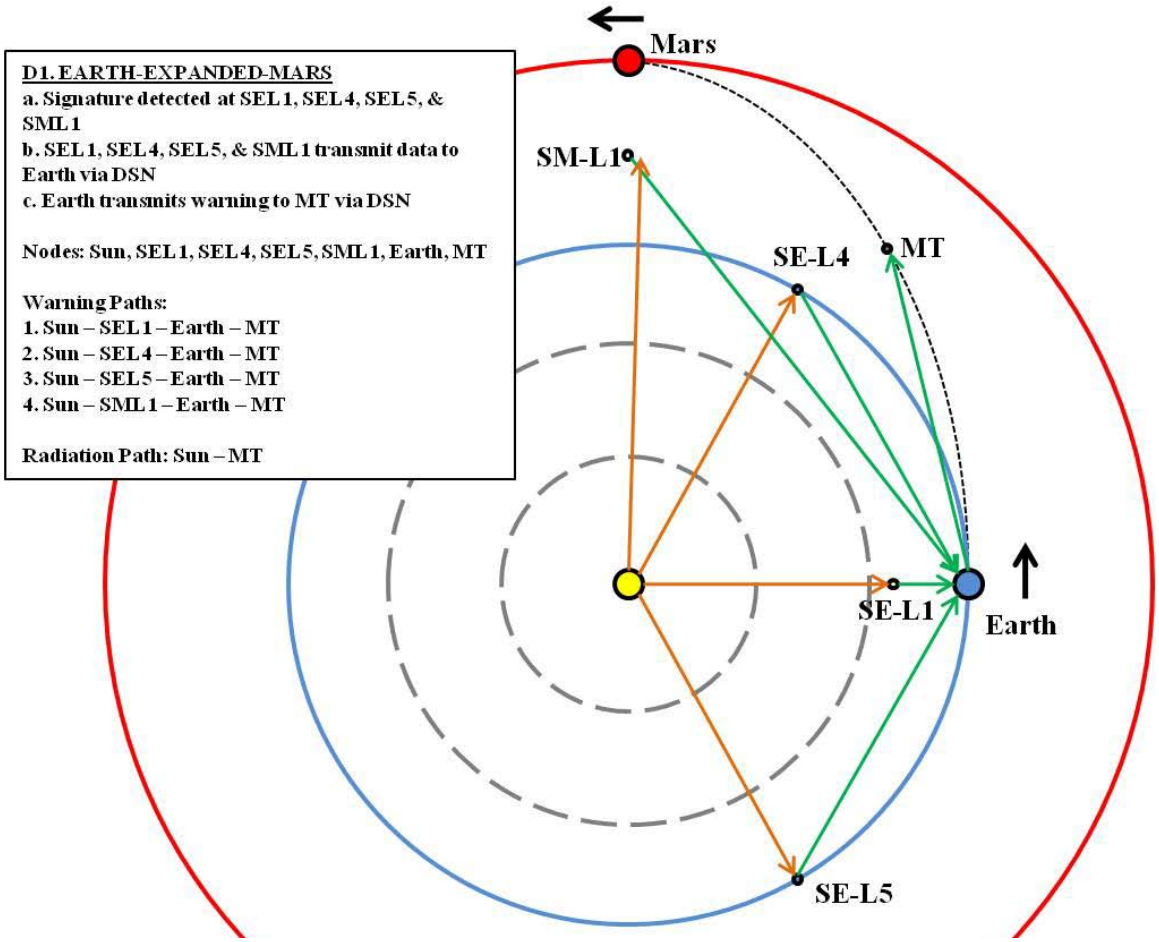

Figure 4-10: Candidate Architecture D1

4.3.8 Architecture Candidate D2

Similar to D1, the D2 architecture adds the sensors and communications links of B2 and C2 to A1 (see Figure 4-11). However, D2 also includes direct links from Sun-Earth L4, Sun-Earth L5, and Sun-Mars L1 to Mars Traveler. D2 mirrors the performance

of C2 over most of the mission epoch with only short periods at the beginning and end where it mirrors B2 instead. D2 provides an average warning time of 28.8 minutes, a minimum warning time of 11.1 minutes, and a maximum warning time of 36.4 minutes. As with the other options with direct links to Mars Traveler there is no 30-day blackout period. Overall, D2 has the second highest mass estimate at 2996 kg. Like D1, architecture D2 provides an extensive 90.4% solar coverage.

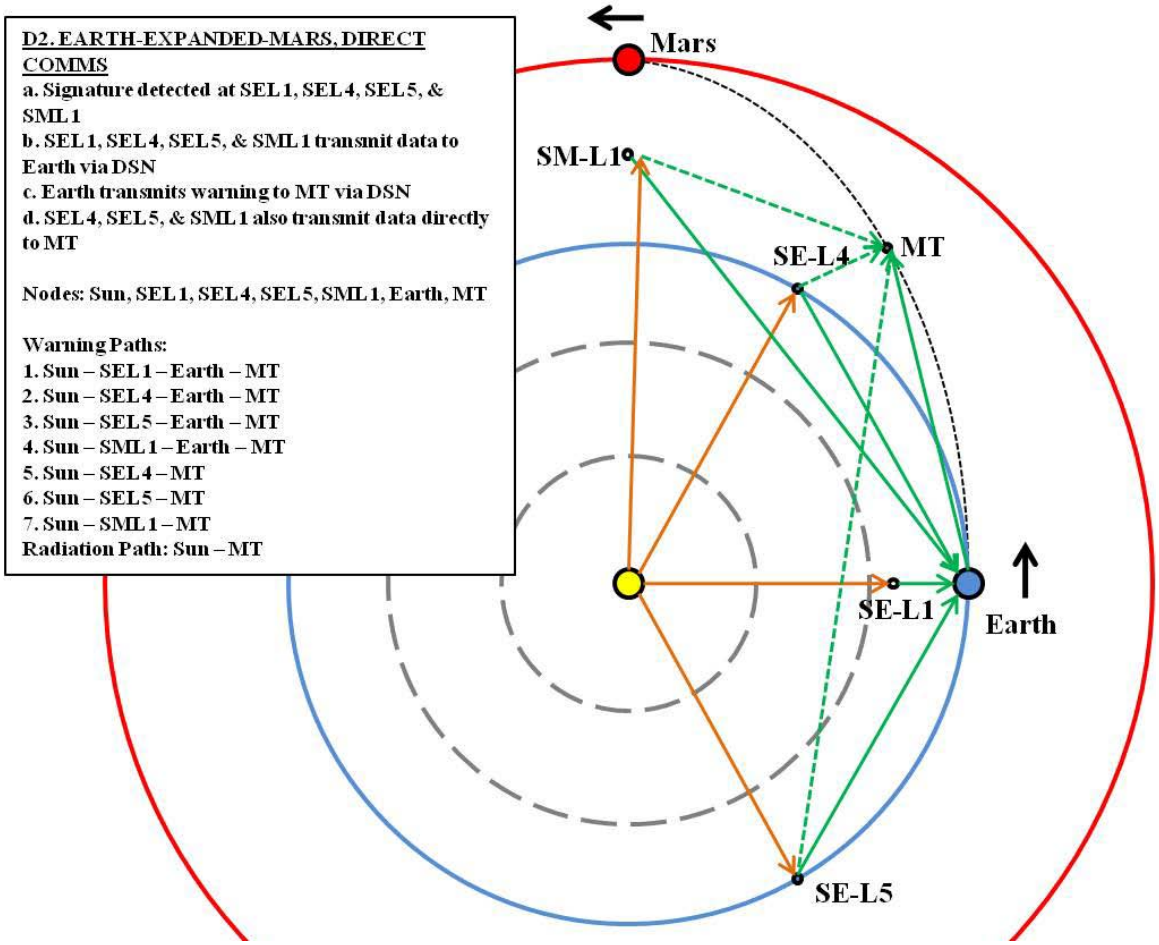

Figure 4-11: Candidate Architecture D2

4.3.9 Architecture Candidate E1

The E1 architecture consists of the A1 baseline with a sensor and processing capability added onboard Mars Traveler itself (see Figure 4-12). E1 provides an outstanding average warning time of 30.5 minutes, with a minimum of 19.7 minutes and a maximum of 36.4 minutes. By avoiding Earth relay delays, the sensor package aboard Mars Traveler provides more warning time than the Sun-SEL1-Earth-MT propagation path across the entire epoch of the mission. In Figure 4-3, E1 shares the exact same warning profile curve as the F, G, and H architectures. Even better, E1 has the second lowest mass estimate at 700 kg; only A1 at 547 kg is lower. Architecture E1 resembles C1 for purposes of providing only a single additional dynamic sensor and provides an average solar coverage of 71.2%.

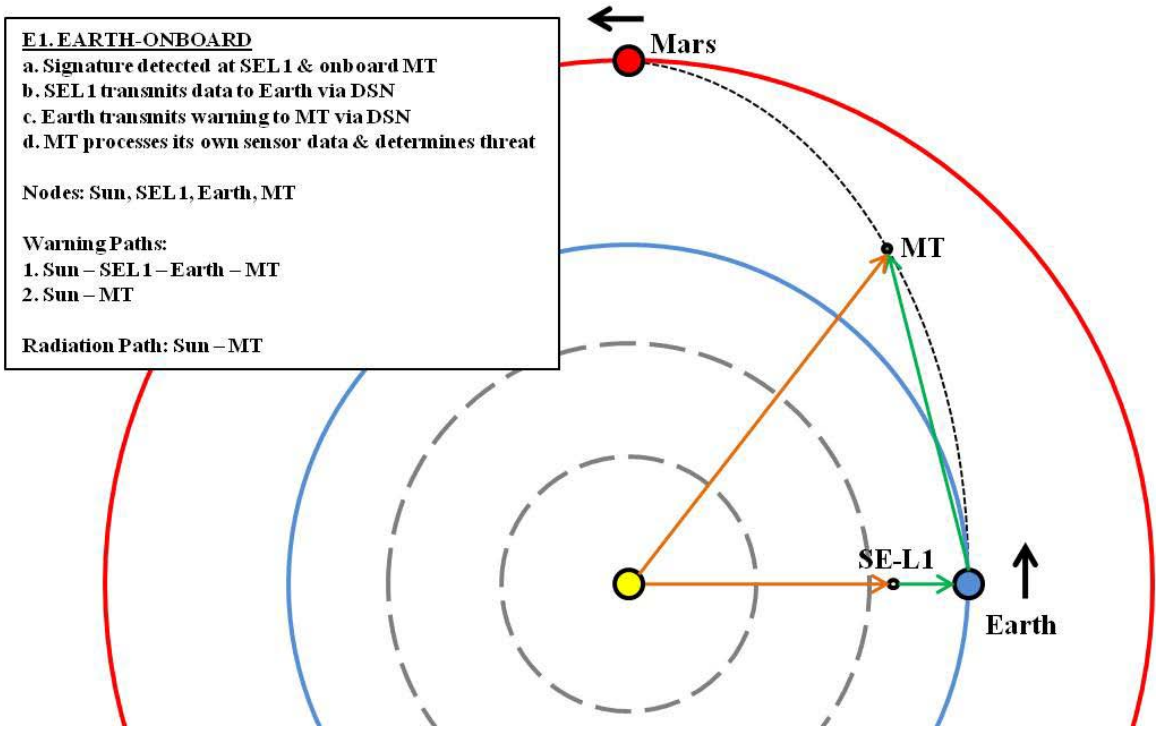

Figure 4-12: Candidate Architecture E1

4.3.10 Architecture Candidate F1

Architecture F1 adds sensors at Sun-Earth L4 and L5 to the E1 configuration and limits data routing to Earth only (see Figure 4-13). As discussed in the B1 section, the Earth data relay does not provide any increase in warning time. This limitation is even more apparent when compared to the Mars Traveler onboard option. Architecture F1 has exactly the same warning performance profile as E1, grows in estimated mass from 700 kg to 1794 kg. Architecture F1 provides an average of 90.4% solar coverage.

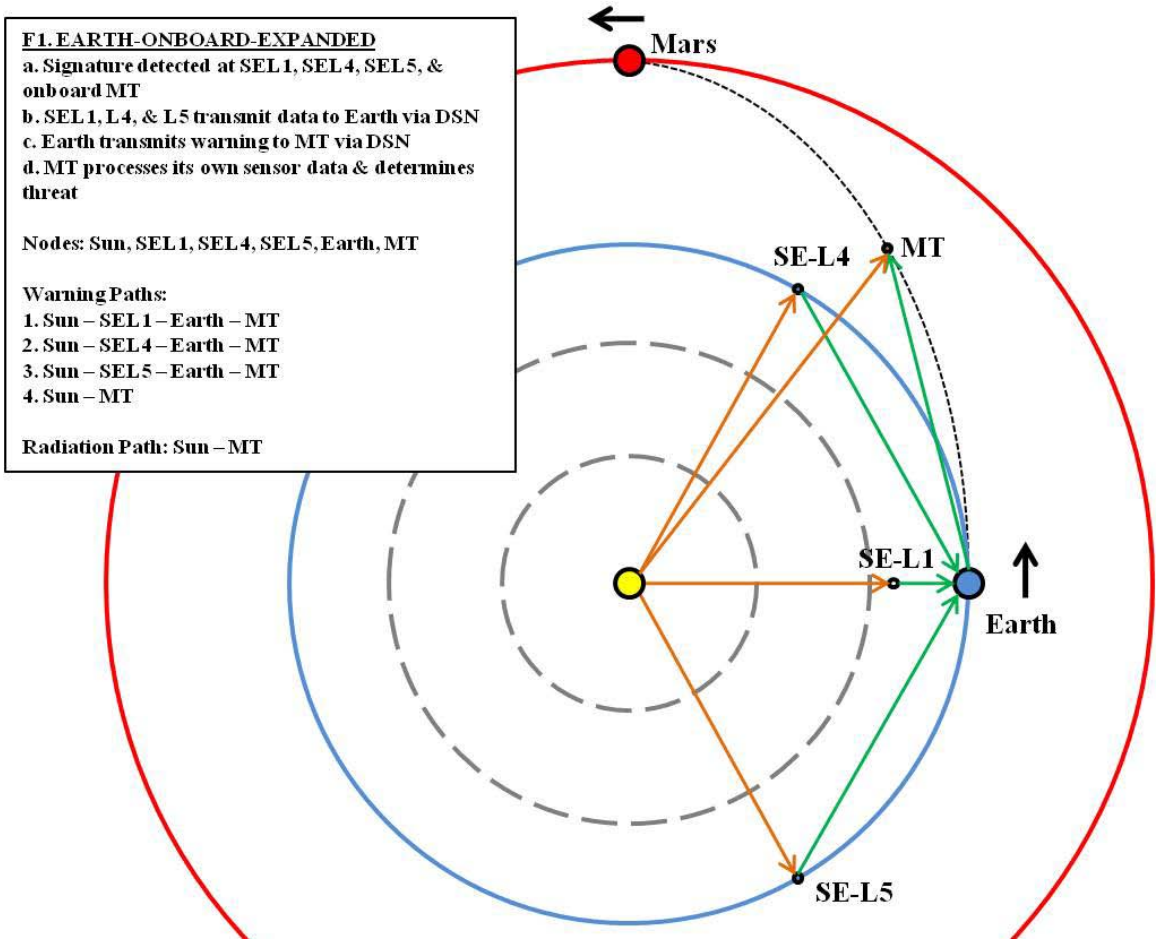

Figure 4-13: Candidate Architecture F1

4.3.11 Architecture Candidate F2

Architecture F2 uses sensor locations identical to F1 with the addition of direct links from the sensors at Sun-Earth L4 and L5 to Mars Traveler (see Figure 4-14). This change results in a mass estimate of 1980 kg, but does nothing for the warning time profile, which mirrors that of E1. Again, the warning time advantage of placing a sensor aboard Mars Traveler is evident. With an identical sensor configuration as F1, candidate F2 also provides 90.4% average solar coverage.

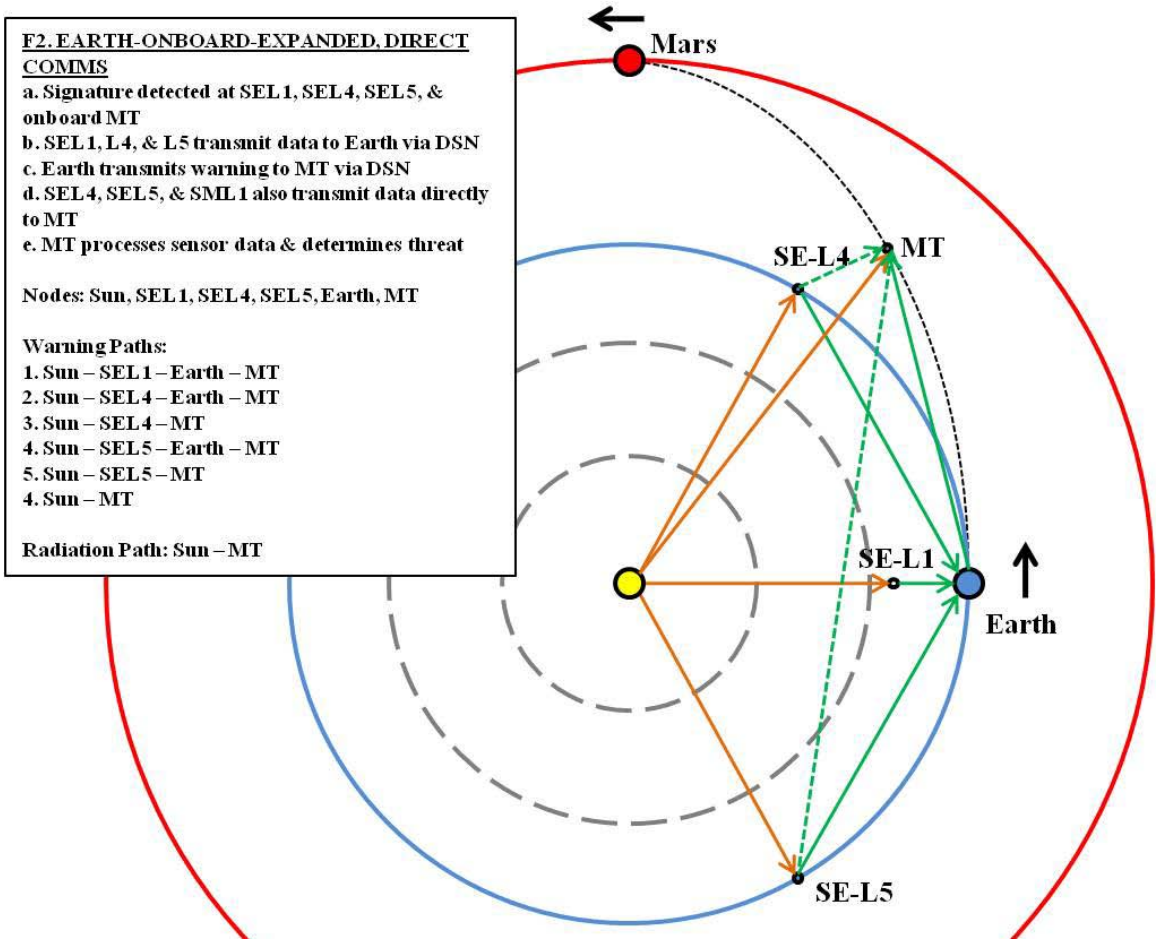

Figure 4-14: Candidate Architecture F2

4.3.12 Architecture Candidate G1

Architecture G1 adds a sensor at Sun-Mars L1 with the data relayed to Earth for processing and re-transmittal, as in architecture C1 (see Figure 4-15). The estimated mass for this configuration is 1787 kg, very close to that of F1. The shortest propagation path over the entire mission profile is again the Sun-MT path, which results in G1 having an identical warning time curve to that of E1. Architecture G1 represents the first in the series with two dynamic sensors relative to the SE-L1 baseline (at MT and SM-L1). However, these two additional sensors do not significantly increase the average solar coverage (71.9%) because MT and SM-L1 share the same vantage point throughout most of the mission.

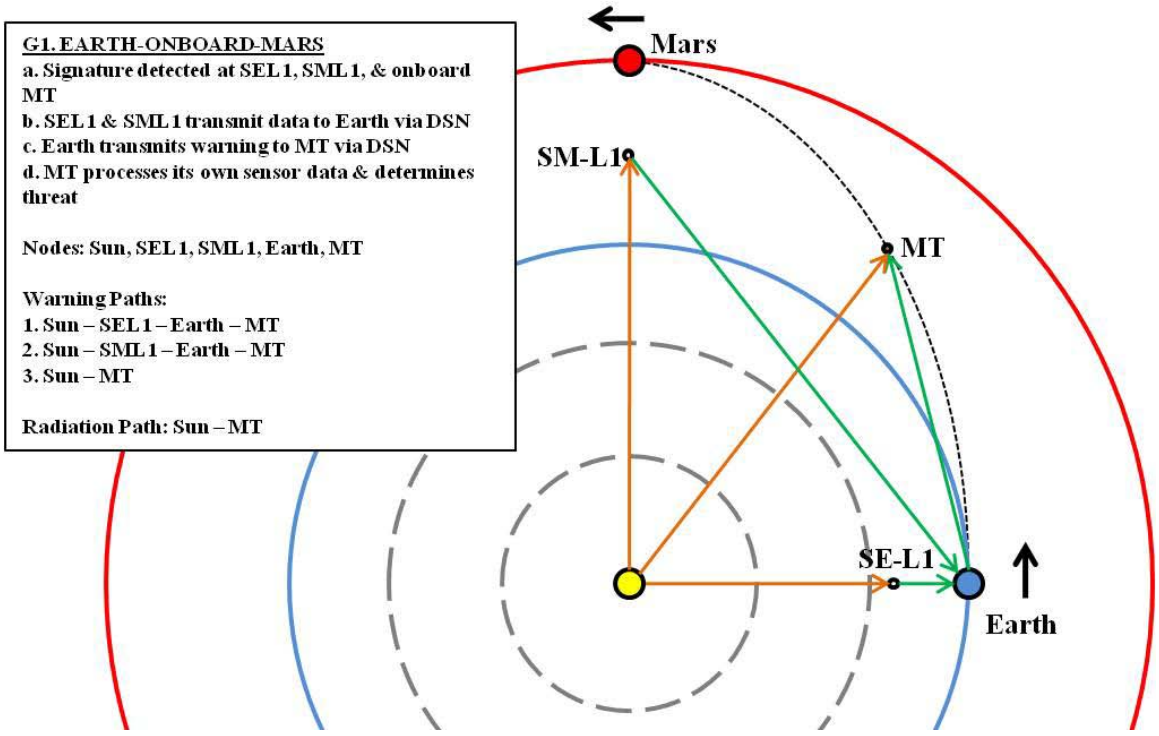

Figure 4-15: Candidate Architecture G1

4.3.13 Architecture Candidate G2

Architecture G2 adds a direct link from the Sun-Mars L1 sensor to Mars Traveler (see Figure 4-16). Only while Mars Traveler is at Mars does this path perform as well as that of E1. This parity is evident in Figure 4-3. The estimated mass for the G2 architecture is 1911 kg. Architecture G2 has the same sensor allocation as G1 and only provides 71.9% average solar coverage.

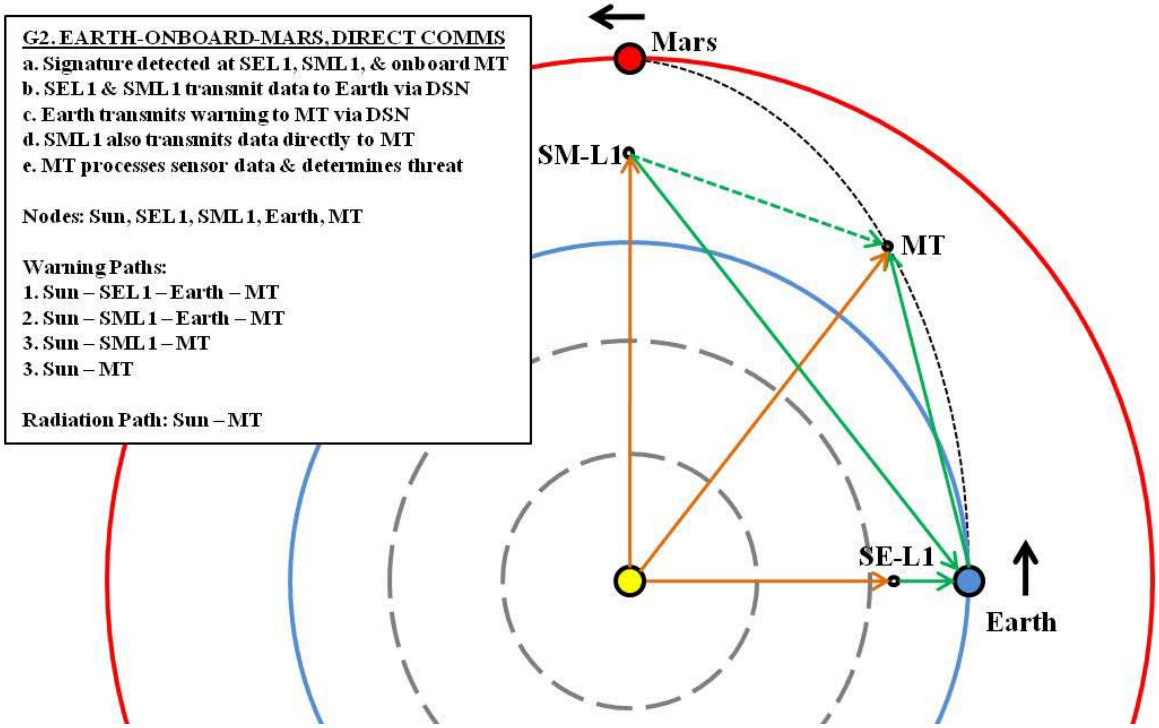

Figure 4-16: Candidate Architecture G2

4.3.14 Architecture Candidate H1

Architecture H1 adds sensors at Sun-Earth L4 and L5 and at Sun-Mars L1 to the E1 configuration (see Figure 4-17). As with architectures F1 and G1, these additional sensors do not provide any better warning time than that of E1, and H1 has the exact same performance profile as E1 on Figure 4-3. H1 has an estimated mass of 2881 kg.

Only architectures H2 and D2 have greater estimated mass costs. With the full complement of solar sensors, H1 provides an average of 90.4% solar coverage.

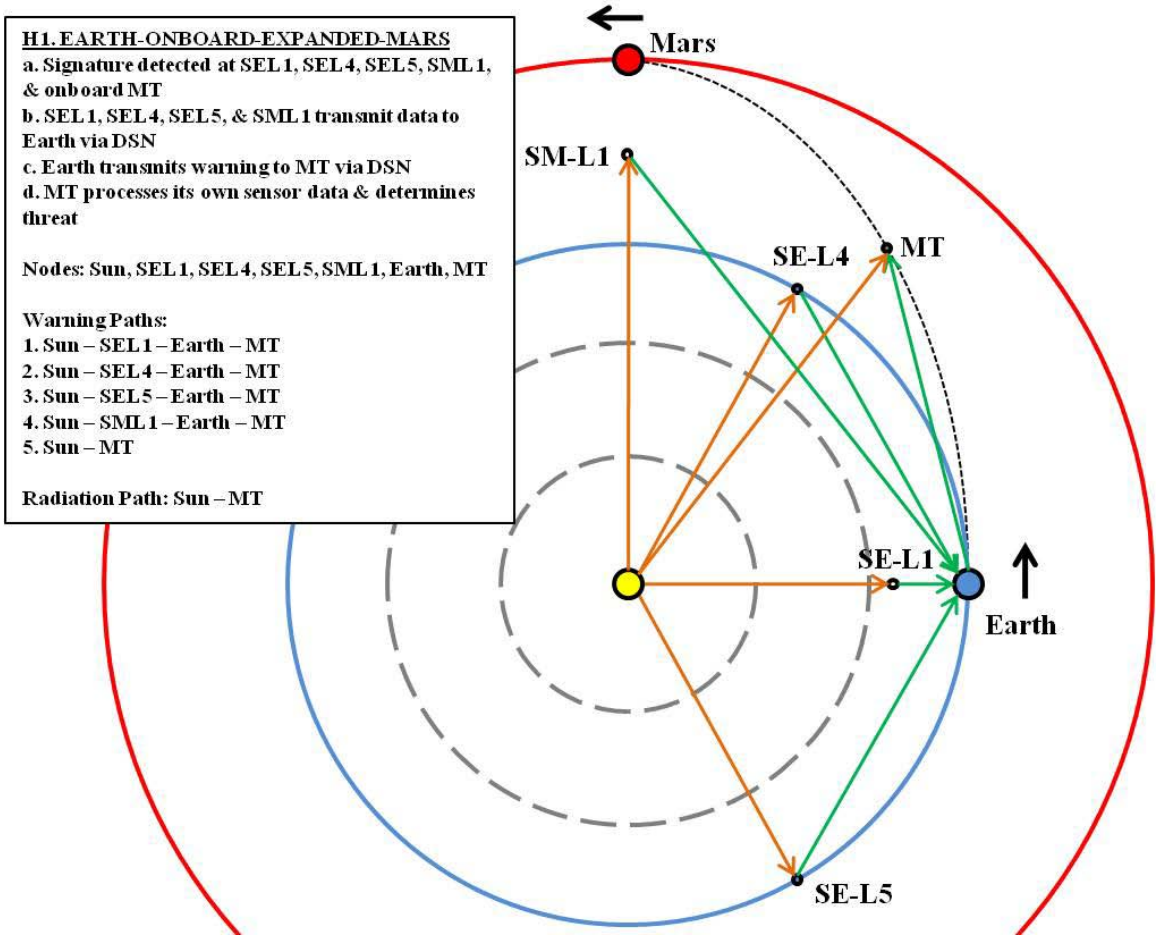

Figure 4-17: Candidate Architecture H1

4.3.15 Architecture Candidate H2

Candidate H2 is referred to as the "All-In" option and incorporates all possible sensors and data paths, both Earth relay and direct (see Figure 4-18). As is the case for F2 and G2, even the inclusion of the direct links does not provide superior warning time to the sensor onboard Mars Traveler. Even with the highest mass requirement (3129 kg),

H2 provides exactly the same performance profile as E1. Like H2, H1 provides 90.4% solar coverage.

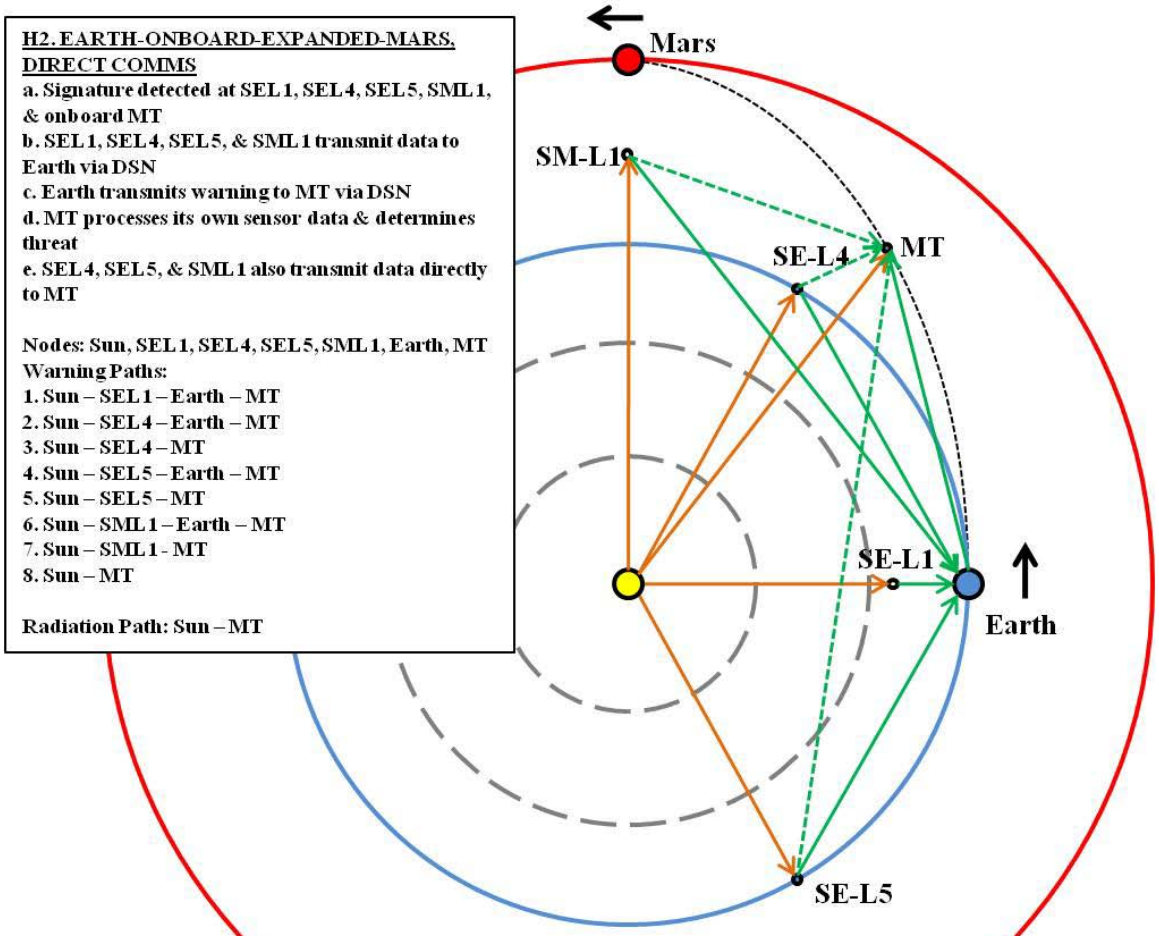

Figure 4-18: Candidate Architecture H2

4.3.16 Summary of Architecture Performance

Table 4-1 summarizes the candidate architectures with regards to Warning Time, Solar Coverage, and estimated Total Dry Mass.

Table 4-1: Candidate Architecture Summary

Candidate Architecture	Sensors	Comm Strategy	Avg Warning Time (min)	Avg Solar Coverage (%)	Estimated Dry Mass (kg)
A1	SE-L1	Earth Relay	13.3	50.0%	547
B1	SE-L1, SE-L4, SE-L5	Earth Relay	13.3	83.3%	1641
B2	SE-L1, SE-L4, SE-L5	Earth Relay & Direct	24.6	83.3%	1847
C1	SE-L1, SM-L1	Earth Relay	13.3	71.8%	1634
C2	SE-L1, SM-L1	Earth Relay & Direct	28.7	71.8%	1778
D1	SE-L1, SE-L4, SE-L5, SM-L1	Earth Relay	13.3	91.4%	2728
D2	SE-L1, SE-L4, SE-L5, SM-L1	Earth Relay & Direct	28.8	91.4%	2996
E1	SE-L1, MT	Earth Relay	30.5	71.2%	700
F1	SE-L1, MT, SE-L4, SE-L5	Earth Relay	30.5	90.4%	1794
F2	SE-L1, MT, SE-L4, SE-L5	Earth Relay & Direct	30.5	90.4%	1980
G1	SE-L1, MT, SM-L1	Earth Relay	30.5	71.9%	1787
G2	SE-L1, MT, SM-L1	Earth Relay & Direct	30.5	71.9%	1911
H1	SE-L1, MT, SE-L4, SE-L5, SM-L1	Earth Relay	30.5	90.4%	2881
H2	SE-L1, MT, SE-L4, SE-L5, SM-L1	Earth Relay & Direct	30.5	90.4%	3129

4.4 Efficient Frontiers Analysis

As described in Chapters 1.0 and 3.0, identification of the "best-value" candidate architecture was accomplished using efficient frontiers analysis. Average Warning Time and Solar Coverage were the two performance metrics against which each candidate architecture was assessed. Minimum and maximum values of each performance metric were also included in order to illustrate the potential range of values around each average.

4.4.1 Warning Time Efficient Frontier

Figure 4-19 depicts the Warning Time vs. Dry Mass efficient frontier for the family of candidate architectures, with Warning Time as the y-axis and Estimated Dry Mass as the x-axis. This figure illustrates a total trade space of 13.3 – 30.5 minutes of warning time and 547 – 3219 kg of dry mass. With the "best-value" objective of minimizing mass and maximizing warning time, the graph organizes the candidate architectures such that the "best" ones are found in the upper left quadrant of the chart.

Those candidate architectures which are furthest to the upper and left edges of the trade space are said to be on the frontier and it is from this subset that the recommended architecture was selected. Within Figure 4-19, there are two obvious groupings of the candidate architecture distribution: one based on average warning time performance and the other based on the mass estimate. This organization resulted in six distinct groups of architectures within the trade space, numbered 1 through 6.

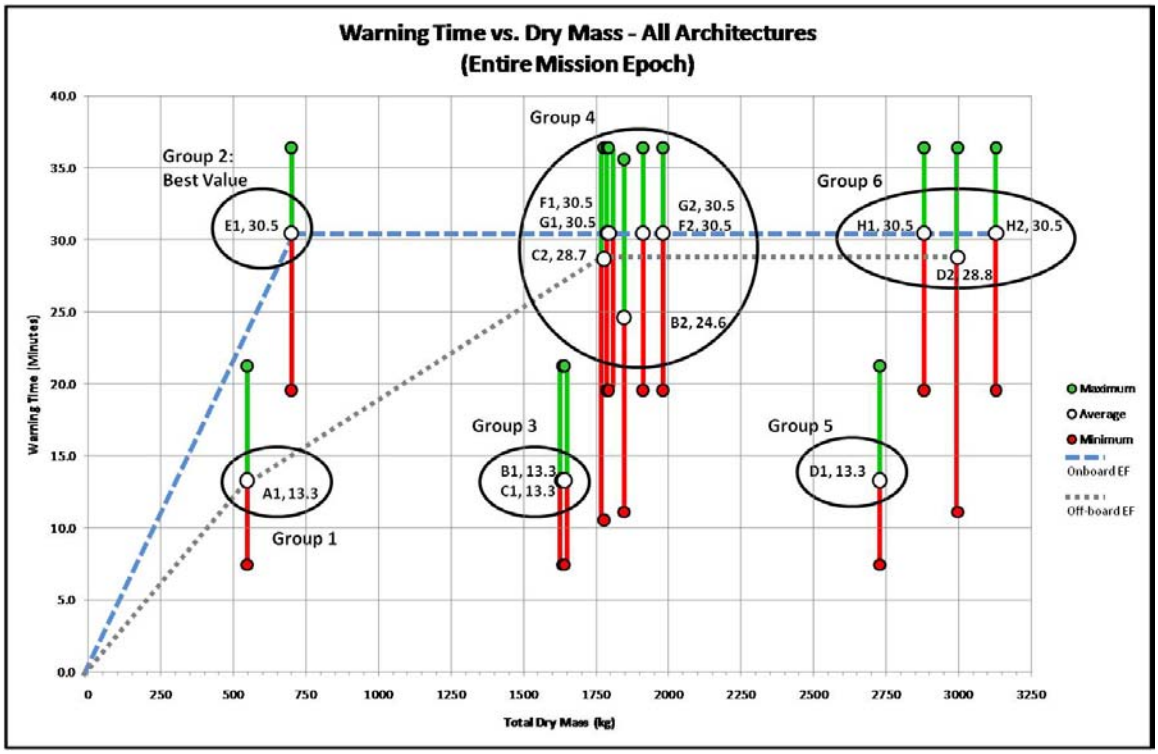

Figure 4-19: Warning Time Efficient Frontier

Based on warning time performance, the candidate architectures are aligned within two distinct horizontal groups. Options A1, C1, B1, and D1 perform at 13.3 minutes of average warning time, while the remaining architectures form a second horizontal group that lines up between 24.6 and 30.5 minutes of average warning time.

The main driver for these horizontal groupings is the difference between the performance of the Earth Relay and Direct Link architectures. Warning time provided by architectures using the Earth Relay are dominated by the Sun-SEL1-Earth-MT path. The average warning time provided by this path is 13.3 minutes and thus these architectures (A1, B1, C1, and D1) all align at 13.3 minutes on the "Y" axis.

A similar mechanic is at play within the second group of architectures aligned between 24.6 and 30.5 minutes. This grouping can be further sub-divided into two parts. The first group is those architectures which incorporate a sensor directly on Mars Traveler: E1, F1, F2, G1, G1, H1 and H2. The second group is those candidates which include use of a direct link from an external sensor to enable data processing aboard Mars Traveler, but not an onboard sensor itself: B2, C2, and D2. Those configurations with a sensor aboard Mars Traveler all align at 30.5 minutes of average warning time. Those without the onboard sensor provide 24.6 – 28.8 minutes of warning on average. While superior to "Earth Relay" solutions, the "Direct Link, No Sensor" set is slightly inferior to the "Onboard Sensor" set. For this last set, in all cases warning time is dictated by the Sun-MT path which is why they all align at 30.5 minutes of average warning time.

Along the x-axis, the architectures form three vertically-aligned groups based on their estimated masses. Architectures A1 and E1 form the first group and have the lowest mass requirements, with 547 kg and 700 kg respectively. Architectures B1, B2, C1, C2, F1, F2, G1, and G2 form the second (most numerous) group with masses varying from 1634 kg to 1980 kg. The jump in estimated dry mass over the first group is driven by the addition of either the Sun-Earth L4 and L5 satellites or the Sun-Mars L1 satellite. Within this group there is some variation based on whether direct communications links to Mars

Traveler are included, but the additional mass for this feature is relatively small compared to the mass required to add an entirely new sensor node. Architectures D1, D2, H1, and H2 form the heaviest group with masses ranging from 2728 kg to 3129 kg. The D and H architectures include both the Sun-Earth L4 and L5 satellites and the Sun-Mars L1 satellite with the only difference being that the H architectures also add a sensor aboard Mars Traveler. As this sensor has the smallest additional mass of any component, its addition is insignificant compared to the mass increase of the direct Mars Traveler link packages on the Sun-Earth L4, L5 and Sun-Mars L1 nodes. The end result is close alignment of the D and H architectures in Figure 4-19.

Based on the described warning time and mass alignments, the 14 architecture options are organized into six groups, each containing one to six architectures:

- Group 1: A1
- Group 2: E1
- Group 3: B1, C1
- Group 4: B2, C2, F1, F2, G1, G2
- Group 5: D1
- Group 6: D2, H1, H2

Groups 3 and 5 are deep inside the trade space and not near the efficient frontier. All of these architectures (B1, C1, and D1) rely on the Earth relay, and it becomes apparent that this communications restriction effectively eliminates any benefit of placing additional sensors beyond the one at Sun-Earth L1. As such, none of these architecture options can be recommended.

Some of the options within Groups 4 and 6 do indeed lie on the efficient frontier. However, both groups require significant additional mass when compared to Group 2 (Architecture E1), but only in return for identical or slightly inferior average warning

times. With no average warning time advantage and a significant cost in terms of estimated mass, neither of these groups can be recommended as the preferred solution.

This leaves only Groups 1 and 2, or architectures A1 and E1, open for consideration. A1 has a much lower mass requirement, but also provides a significantly shorter average warning time of only 13.3 minutes. Conversely, E1 provides 30.5 minutes of average warning time, but requires an additional 135 kg of mass integrated aboard Mars Traveler. This additional mass equates to an increase of only 28% over the 547kg estimated for the baseline A1 architecture, but generates a 129% improvement in warning time (from 13.3 to 30.5 minutes). While the A1 architecture initially appears to provide an excellent value, the E1 architecture represents a superior "best value" solution with regards to warning time. This conclusion is strengthened within Figure 4-19, where it is clear that the E1 architecture sits at the "knee in the curve" for the Warning Time Efficient Frontier.

4.4.2 Solar Coverage Efficient Frontier

Based on the efficient frontier analysis for Warning Time, architecture E1 shows best value. However, that selection rests on a few assumptions, one of those being that the radiation storm event occurs in view of the sensor which enables the shortest path in each CA. Depending on the amount of solar coverage a CA provides, it is possible a radiation storm that threatens MT could erupt outside the CA's field of view. As the Mission Model used did not allow for randomly placing the point of origin and direction of radiation storms, an alternate approach was used. Rather than approach the issue from determining if randomly timed and directed radiation storms are in view, the solar

coverage percentage of each CA was characterized and then compared via efficient frontiers analysis, similar to warning time. Solar coverage was measured as an estimated percentage of the Sun's total surface, and not just limited to the surface area of the Sun that might directly threaten the spacecraft. This metric was defined in terms of total solar surface area because of a requirement to provide warnings to multiple missions simultaneously. The Mission Model was limited to provision of warnings to MT. However, DRA 5.0 identifies additional unmanned and manned missions taking place at various intervals, not to mention the potential for manned missions in parallel to other solar system bodies, such as asteroids. An improved method for characterizing surveillance of the specific threat region of the Sun is briefly discussed in Section 5.5. Figure 4-20 depicts the Dry Mass vs. Solar Coverage efficient frontier for the family of candidate architectures. Some of the candidates, like A1, are represented with a red dot stacked on top of a white one; this depiction simply indicates that solar coverage was constant; with the minimum and maximum values being co-plotted with the average value. Figure 4-20 illustrates a total trade space of 50% - 90% average solar coverage and 547 - 3219 kg of dry mass. With the "best-value" objective of minimizing mass and maximizing solar coverage, the graph organizes the candidate architectures such that the "best" ones are found in the upper left quadrant of the chart. Those candidate architectures which are furthest to the upper and left edges of the trade space are on the frontier and it is from this subset that an architecture should be recommended. Within Figure 4-20, there were three groups of candidates. Group 1, comprised of A1 and E1 appears early in the efficient frontier, having the two lowest masses and relatively low average solar coverage values in the 50% to 71% range. Group 2, consisting of the B, C,

and F families have 2-3 times more mass than the first group, but have higher solar coverage values, ranging from 72% to 90%. Group 3 is composed of the D and H families, which all provide 90% average solar coverage, but are by far the most massive architectures. They show little gain over some of the Group 2 candidates for the mass increase.

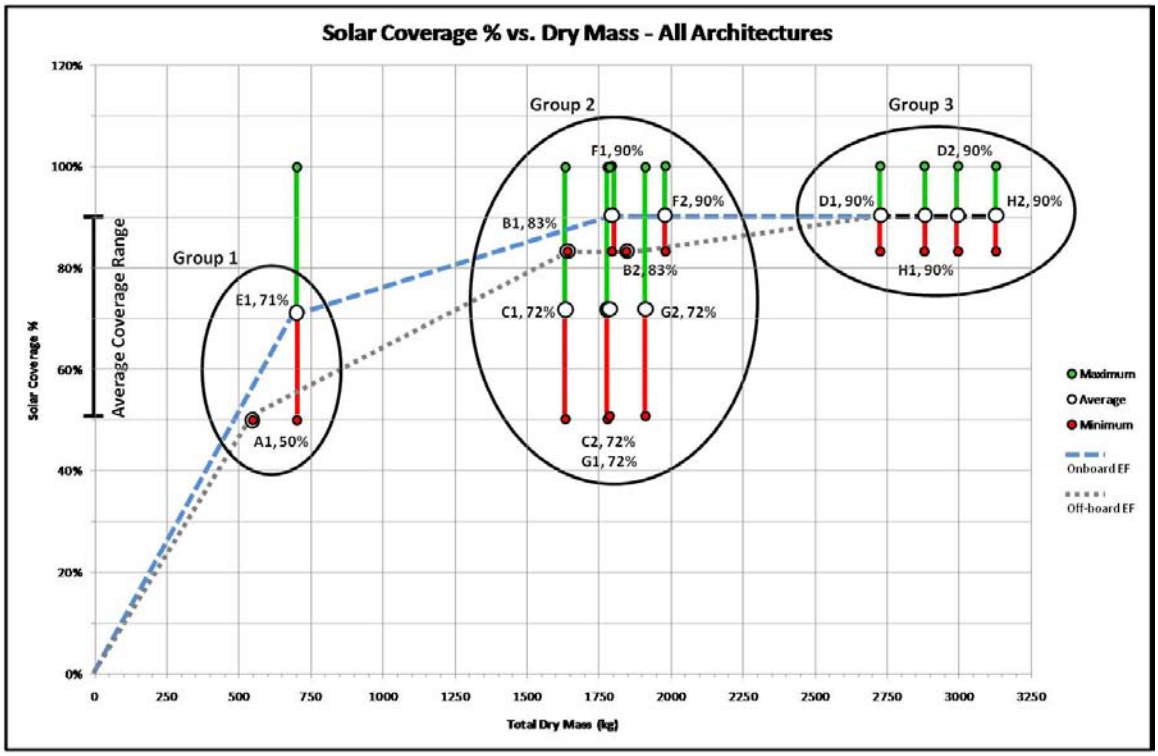

Figure 4-20: Solar Coverage Efficient Frontier

For the A and B architecture options, the solar surface coverage at any given point in time is fixed at 50% and 83% respectively, resulting in the maximum, minimum, and average values being equal. In both architectures, the longitudinal arc of the Sun being monitored is centered with respect to the Earth, thus when Mars and Earth are on the

same side of the sun, the coverage is effective but when Mars and/or Mars Traveler are opposite the Earth, the surface arc covered may not be adequate.

The C and G architectures add a Sun-Mars L1 sensor, while the G architectures go even further with inclusion of the Mars Traveler sensor. The addition of the Sun-Mars L1 sensor increased the average portion of the Sun's surface in view to 72%. More importantly, the Sun-Mars L1 sensor ensures the side of the Sun facing Mars Traveler is always in view, and drives the coverage up to 100% when Mars is in conjunction with the Sun as viewed from Earth. The drawback with this configuration is that the coverage drops to 50% when Mars and Earth are aligned with respect to the Sun. During this stage of the mission, placing a sensor aboard Mars Traveler in architecture G does not provide any additional coverage compared to just adding the Sun-Mars L1 sensor.

Architecture E1 provides almost identical coverage performance as architectures C and G (71% vs. 72%), but at a significantly reduced mass requirement. This similarity of coverage is due to a Mars Traveler sensor covering almost the same arc of the Sun as a Sun-Mars L1 sensor throughout most of its journey.

Architectures D, F, and H add the Sun-Earth L4 and L5 sensors along with one or both a Sun-Mars L1 sensor (D and H) and a Mars Traveler sensor (F and H). All three combinations provide a healthy 90% average coverage of the Sun's surface, with approximately 8 months of the Mars orbit window at 100%. The F architecture does this for significantly less mass than either the D or H options due to the low mass requirement of a Mars Traveler sensor.

As with the efficient frontier analysis for Warning Time, the E1 architecture appears at a "knee in the curve" of the Solar Coverage frontier. However, there is a

second “knee” where the F architectures appear. Although the F architectures require about 2.5 times the estimated mass (1794 kg vs. 700 kg), they also provide a significant boost in both the average and minimum of solar coverage. Average solar coverage is increased by 79% over the E1 architecture and minimum solar coverage is increase by 60% over E1, but it remained questionable as to whether the mass increase was worth the solar coverage gained.

4.5 Value Modeling

Although the Warning Time efficient frontier clearly indicated architecture E1 as the “best value”, the Solar Coverage efficient frontier revealed the F architectures to be competitive with E1 in that performance metric. To resolve the best overall value issue, a Performance Value efficient frontier was required. A value model represented as both a graph and an equation was developed for each of the performance metrics: Warning Time and Solar Coverage. The Warning Time value model (see Figure 3-8) is a simple linear equation relating the range of possible warning times to a number ranging from 0.0 to 1.0. The Solar Coverage value model (see Figure 3-9) maps out the linear relationship between the possible range of solar coverage values and a number ranging from 0.0 to 1.0. One of the strengths of value modeling is that depending on values of a given customer or decision-maker, the relative importance of various performance metrics can be modified as desired.

The next step in the Value Model process was to apply these value model equations to their respective performance metrics, as depicted in the efficient frontiers charts, with the end goal of creating an overall performance value efficient frontier. The

average warning time for each CA was converted to its corresponding value (0.0 to 1.0), the average solar coverage for each CA was then converted to a second value (0.0 to 1.0), and then the two values were weight-averaged together. Recall that Warning Time was earlier assessed to be twice as important as Solar Coverage. Therefore, Warning Time accounted for two-thirds of the overall performance value for each CA. This process resulted in a Performance Value efficient frontier (Figure 4-21) where the y-axis marked out the 0.0 to 1.0 overall value of each architecture, and the x-axis indicated estimated dry mass.

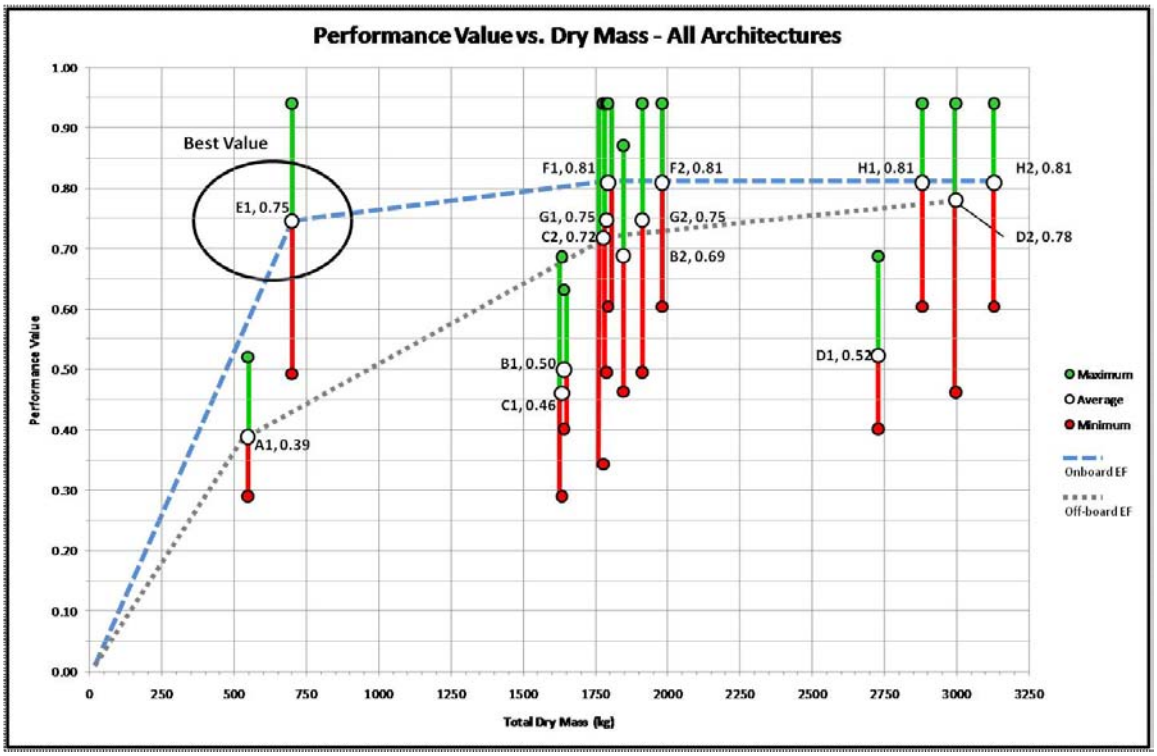

Figure 4-21: Performance Value Efficient Frontier

Inspection of the Performance Value efficient frontier clearly indicates that architecture E1 provides better value than the F-family of architectures, as the E1

architecture continues to define the “knee in the curve” for overall Performance Value. Hence, architecture E1, or placing a sensor/processing/display capability aboard the manned mission to Mars spacecraft itself represents the best value in terms of both Warning Time and Solar Coverage for the estimated cost in dry mass.

5.0 Discussion

5.1 Study Overview

The primary objective of this study was to identify and recommend a solar radiation storm warning architecture for manned missions to Mars. Architectural combinations of five sensor set locations, two data processing node sites, and two communication path strategies (Earth Relay and Direct), yielded a total of 14 candidate architecture configurations. All candidates satisfied to some degree the functional requirements of monitoring the Sun for solar radiation storms and communicating a warning to a threatened spacecraft. Within STK, these 14 architectures were played against a simulation of NASA's DRA 5.0 mission to Mars scenario, and the resulting performance data was analyzed within MS Excel. Link Model and Coverage Model data was correlated with Cost Model data to create efficient frontiers for Warning Time and Solar Coverage. Finally a Value Model was developed to determine an overall Performance Value efficient frontier. The results of all three efficient frontier analyses consistently showed that the "best value" candidate architecture was E1: the placement of a solar sensor and processing capability directly onboard Mars Traveler in addition to the baseline Sun-Earth L1 solar sensor (Figure 5-1).

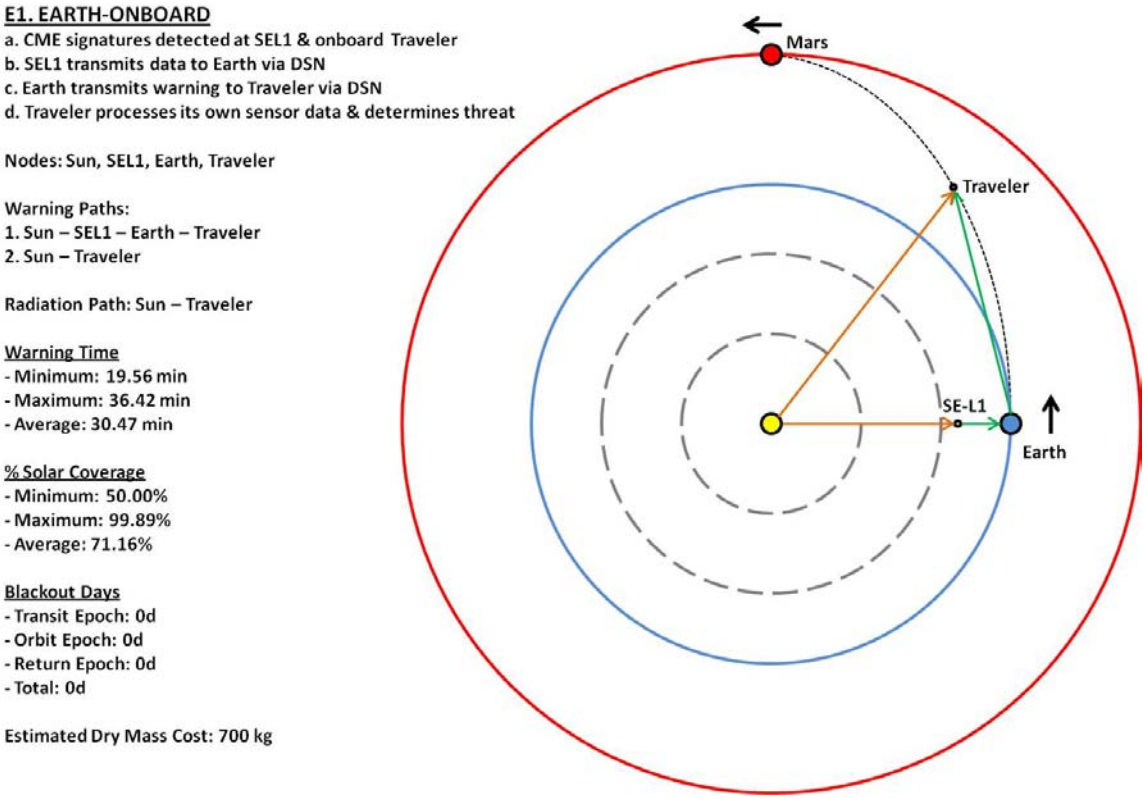

Figure 5-1: Best Value Solar Warning Architecture - Candidate E1

5.2 Model Limitations

As described above, this study primarily relied on a series of interrelated models. While this approach was effective overall, there were some challenges encountered in the development of each model.

5.2.1 Solar Warning Architecture Limitations

For the solar warning architecture candidates there were no limitations placed on sensor or processing node location options. However, the decision was made to simplify the definition of the baseline (Architecture A1), as compared to the current architecture. Currently, Earth's solar forecasting infrastructure includes terrestrial observatories,

observation satellites at Sun-Earth L1 and in Earth orbit, and the unique STEREO mission. All of these assets provide information used by NASA and NOAA to monitor the Sun and provide the raw data required for solar weather forecasting.

For purposes of this study, Earth-based ground sensors were omitted from consideration for two reasons. First, they do not provide any additional warning time beyond the sensors at Sun-Earth L1. Second, identifying, geo-locating, and modeling all the ground sensors would have been a complex project in of itself, not to mention determining their communications infrastructures.

5.2.2 Mission Model Limitations

Because the Mission Model was built using STK, one limitation involved the simulation of the sensors at Sun-Earth L1 and Sun-Mars L1. Instead of using the time-consuming method of developing complex mission profiles to launch each satellite from Earth into a Lissajou (figure-eight) or halo orbit at each libration point, the satellites were simply instanced into the Mission Model at user-defined locations representing the libration points. This method of representing the satellites means that the Mission Model does not account for the small link length variations due to the sensor satellites moving along their realistic orbital paths. However, the scale of typical orbital distance about a given libration point is several orders of magnitude less than the point's distance to the Sun, so any orbital position variation would have negligible effect on link metrics, especially assuming the signatures and data transmissions involved were traveling at the speed of light.

5.2.3 Link Model Limitations

In building the Link Model only one issue was encountered. When calculating the distances between objects in the STK Mission Model, all distances are measured from center mass. This results in distances from the Sun being measured from its center, not its surface where a solar radiation storm signature would originate. The Earth was also modeled as a point rather than its component parts, and all communications links involving the Earth were calculated using the Earth's center as an endpoint. A simple fix was found by subtracting the radius of the respective celestial body from any link distance output by STK for which the Sun or Earth (or both) was an endpoint.

5.2.4 Cost Model

The Cost Model was one of the most challenging models to assemble because it almost entirely relied upon parametric cost estimation analysis. There are relatively few solar observation satellites available to reference to develop the mass budgets of each component for the candidate architectures. As such, the current STEREO mission satellites were used to represent the Sun-Earth L1, L4, and L5 satellites, and the current Mars Reconnaissance Orbiter (MRO) was used to approximate the Sun-Mars L1 satellite. Gaps for additional antennas and missing mass budget entries were filled in by relying on a historical breakdown of deep space satellites by percent mass budget (Brown 2002).

5.2.5 Solar Coverage Model

The primary assumption made during development of the Solar Coverage Model was that each sensor views the Sun as a perfectly flat disc and has perfect access to the full 180 degrees of its latitudinal circumference at any given point in time. In reality, the

arc of the Sun under observation by a single sensor would be slightly less than 180 degrees, and because the Sun is spherical, the performance of a given solar sensor to detect and track radiation storm signatures would likely vary across the sensor's field of view, based on the specifics of its design and implementation.

One factor of the solar coverage that was not taken into consideration was the robustness or redundancy of the solar surveillance capabilities of each CA. No analysis was performed on architecture reliability or backup coverage in a scenario where one or more of the sensors fail. Factoring in reliability would have an impact on the relative value of each CA, which would be determined by integrating reliability with the other performance metrics within the Value Model, based on one or more user-defined SDVFs.

5.3 Research Conclusions

As stated earlier, Architecture E1 was clearly the best value candidate in terms of both Warning Time and overall Performance Value. Co-locating a sensor with the asset (human) it is designed to serve or protect has been demonstrated in other architectural designs to be a highly effective and feasible strategy, and the case for placing a sensor and the associated processing components onboard Mars Traveler is no exception.

The decision to go with the Onboard option for a solar warning architecture in turn suggests at least two new requirement paths for a manned Mars mission: to pursue either an automated or human-operated onboard monitoring system. An automated solar monitoring system must be intelligent enough to perform solar forecasting, which is considered both science and art by current human practitioners. Developing such a system will require detailed quantification of the knowledge solar forecasters leverage

when they make their assessments. A human-operated system will drive an entire host of human factors issues and ramifications. For instance, several (if not all) of the astronaut crew will need to be trained in solar forecasting, continuous monitoring will be required which impacts duty shifts, and personnel engaged in monitoring will not be free to engage in other work.

5.4 Implications

Beyond identification of a potential Mars crew requirement, there are some notable implications to this analysis, and a number of areas stand out as potential avenues for future research. For one, the work performed to date could serve as the introductory analysis required to define a baseline reference architecture for interplanetary missions within our solar system. Although the particulars of the mission and orbital trajectories would change based on the timing, window, and destination, the analysis techniques are equally applicable across a wide range of interplanetary scenarios.

Another critical implication of this work directly impacts the development of solar radiation protection measures. The results of this or similar analyses have direct bearing on the timing requirements for various radiation countermeasures which may be under consideration. For example, the worst-case scenario for architecture E1 (Onboard Mars Traveler) indicated a minimum warning time of 19 minutes. This performance metric could be directly translated into a performance requirement for radiation countermeasures, with some additional margin of error or safety built in. In turn, if there are already radiation countermeasures with quantified activation times, these metrics

could be levied upon the warning architecture as a minimum requirement, affecting the allowable trade spaces accordingly.

5.5 Further Analysis

As is always the case, there are a number of additional analysis efforts possible. The Earth, Mars Traveler, and the various sensor satellites were all modeled as black boxes with assigned delay times. Decomposing the architecture one to three levels and filling out the actual activities involved would result in a more accurate model and potentially impact the warning time results, especially with regards to the performance of Earth's current solar warning and forecasting architectures. As has been mentioned previously, the actual Lissajou and halo orbits of the sensor satellites could be more accurately modeled, but the improvement in precision is discounted. The Mars scenario only considered conjunction class missions, for reasons described in Chapter 2.0. However, it might be insightful to analyze the performance of the architectural candidates against an opposition class mission and quantify any differences in solar radiation hazards. Within the set of candidate architectures, not all combinations were analyzed. For instance, the sensor location options treated Sun-Earth L4 and L5 as a pair, with neither sensor ever operating alone. Using these two sensors as individual options might have further defined the efficient frontiers and perhaps identified one of the pair as more effective than the other.

During analysis of the solar coverage results and their implications, a potentially more effective way to quantify and compare CA monitoring was identified. While solar flares and other radiation-producing phenomena can technically originate from any point on the solar surface, historically, the majority of radiation storms that have affected Earth

originated at approximately 52 degrees east solar latitude, “ahead” of the Earth (Poppe 2006) (Tascione 1994). This pattern is due to the Sun’s spiral-shaped magnetic field lines which channel the highly energetic particles. Thus, it’s highly probable that only radiation storms originating 50-55 degrees ahead of Mars Traveler’s solar radial position will pose a threat to the spacecraft. With this additional (probabilistic) constraint in mind, the solar coverage performance of the various candidate architectures could be re-analyzed based on how much coverage of this particular solar arc is provided. Furthermore, this factor would constrain the origination point of the radiation storm link to the Mars Traveler and solar sensor links, and a path curvature coefficient could be factored in to accurately portray the radiation traveling along the longer spiral distance. These refinements of the solar coverage analysis would lead to a more accurate assessment of the family of candidate architectures. However, the analysis would not change the final recommendation of placing the sensor onboard Mars Traveler. Measuring solar coverage performance in this way will only strengthen the case for an onboard solution for the simple fact that a 5-10 degree solar arc centered at 55 degrees ahead of Mars Traveler will always be in view of the spacecraft across the entire mission epoch.

Bibliography

Ashworth, Stephen. *Three Ways to Mars.* London: British Interplanetary Society, 2007.

Bostrom, C. O., C. L. Fischer, P. Webb, D. J. Williams, P. C. Johnson, and J. Fabian. *Committee to Review Solar Flare Hazards to Man in Space.* Pentagon: USAF Scientific Advisory Board, 1987.

Brown, Charles D. *Elements of Spacecraft Design.* Reston, VA: American Institute of Aeronautics and Astronautics, Inc., 2002.

Bueche, F. *Technical Physics.* New York: Harper and Row, 1981.

Carlowicz, Michael J., and Ramon E. Lopez. *Storms From the Sun.* Washington D.C.: Joseph Henery Press, 2002.

Carrico, John P., Jon D. Strizzi, Joshua M. Kutrieb, and Paul E. Damphouse. *Trajectory Sensitivities for Sun-Mars Libration Point Missions.* Thesis, Monterey: Department of Aeronautics & Astronautics, US Naval Postgraduate School, 2001.

Carrington, R. C. "Description of a Singular Appearance seen in the Sun on September 1, 1859." *Monthly Notices of the Royal Astronomical Society* (Royal Astronomical Society) XX (1860): 13-15.

Cladis, J. B., G. T. Davidson, and L. L. Newkirk. *The Trapped Radiation Handbook.* Santa Barbara: Defense Nuclear Agency, General Electric Company, 1977.

Cliver, E. W., and L Svalgaard. "THE 1859 SOLAR–TERRESTRIAL DISTURBANCE AND THE CURRENT LIMITS OF EXTREME SPACE WEATHER ACTIVITY." *Solar Physics (2004) 224,* 2004: 407-422.

Devine, Robert T., and Raymond L. Chaput. "Low-Level Effects." In *Military Radiobiology,* by James J. Conklin and Richard I. Walker, 379-381. Orlando, FL: Academic Press, 1987.

Drake, Bret G, Stephen J Hoffman, and David W Beaty. "Human Exploration of Mars Design Refrence Architecture 5.0." 2009.

Fleck, Bernhard, Daniel Muller, Stein Haugan, Luis Sanchez Duarte, and Tero Siili. "10 Years of SOHO." *esa Bulletin 126,* May 2006: 25-32.

Geard, Charles R. "Effects of Radiation on Chromosomes." In *Radiation Biology,* by Donald J. Pizzarello, 84-103. Boca Raton, FL: CRC Press, Inc., 1982.

Jet Propulsion Laboratory. "Deep Space Network Factsheet." *Deep Space Network Website.* 2005. http://deepspace.jpl.nasa.gov/dsn/ (accessed January 2011).

—. *Mars Reconnaisance Orbiter*. http://marsprogram.jpl.nasa.gov/mro (accessed 2011).

Laurini, Kathleen C., Bernhard Hufenbach, Britta Schade, Peter Weber, and Andrea Lorenzoni. "From LEO, to the Moon and Then Mars: Developing a Global Strategy for Exploration Risk Reduction." 2009.

Mars Society. *Mars Society Mission.* Encyclopedia Astronautica. 1999. www.astronautix.com/craft/marssion.htm (accessed Oct 3, 2010).

NASA. *Human Exploration of Mars Design Refrence Architecture 5.0.* Hanover, MD 21076-1320: NASA Center for AeroSpace Information, 2009.

NASA. *Human Exploration of Mars: The Refrence Mission of the NASA Mara Exploration Study Team.* NASA, 1997.

NASA. *Mars Design Refrence Architecture 5.0 -- Addendum.* Hanover, MD: NASA Center for AeroSpace Information, 2009.

NASA Science, Science News. *A Super Solar Flare.* May 6, 2008. http://science.nasa.gov/science-news/science-at-nasa/2008/06may_carringtonflare/ (accessed August 29, 2010).

NASA. "Solar Dynamics Observatory (SDO) Press Kit." 2010.

NASA. "Solar Terrestrial Relations Observatory (STEREO) Press Kit." 2006.

NASA. *The Vision for Space Exploration, February 2004.* NASA, 2004.

Poppe, Barbara B. *Sentinels of the Sun: Forecasting Space Weather.* Boulder, CO: Johnson Books, 2006.

Portree, David S.F. "Humans to Mars: fifty years of mission planning, 1950–2000." (NASA History Division) Monographs in aerospace history, no. 21 (2001).

Review of U.S. Human Spaceflight Plans Committee. "Seeking a Human Spaceflight Program Worthy of a Great Nation." 2009.

Stone, E. C., et al. "The Advanced Composition Explorer." *Space Science Reviews*, 1998: 1-23.

Szabo, Adam, and Michael R. Collier. *WIND: 2010 Senior Review Proposal.* NASA Goddard Space Flight Center, 2010.

Tascione, Thomas F. *Introdcution to the Space Environment.* Malabar, FL: Krieger Publishing Company, 1994.

Turner, Ronald E., and Joshua M. Levine. "Orbit Selection and Its Impact on Radiation Warning Architecture for a Human Mission to Mars." *Acta Astronautica* (Elsevier Science Ltd.) 42, no. 1-8 (1998): 411-417.

Wade, Mark. *Mars Expeditions.* 2011. http://www.astronautix.com/fam/martions.htm (accessed Apr 3, 2011).

Warmuth, Alexander, and Gottfried Mann. "The Application of Radio Diagnostics to the Study of the Solar Drivers of Space Weather." In *Space Weather: The Physics Behind A Slogan*, by Klaus Scherer, 51-70. Berlin Heidelberg: Springer, 2005.

Wertz, James R., and Wiley J. Larson. *Space Mission Analysis and Design, Third Edition.* Hawthorne, CA: Springer, 2007.

White House. "National Space Policy of the United States of America, June 2010." 2010.

Wilson, D, and J.D.A. Clarke. "A Practical Architecture for Exploration-Focused Manned Mars Mission Using Chemical Propulsion, Solar Power Generation and In-Situ Resource Utilisation." Proceedings of the 6th Australian Apace Science Confrence, 2006, 2006.

Young, Robert W. "Acute Radiation Syndrome." In *Military Radiobiology*, by James J. Conklin and Richard I. Walker, 165-190. Orlando, FL: Academic Press, 1987.

Zubrin, Robert M., Davis A. Baker, and Owen Gwynne. *Mars Direct: A Simple, Robust, and Cost Effective Architecture for the Space Exploration Initiative.* AIAA, 1991.

REPORT DOCUMENTATION PAGE

Form Approved
OMB No. 074-0188

1. REPORT DATE *(DD-MM-YYYY)*	2. REPORT TYPE	3. DATES COVERED *(From – To)*
06-2011	Master's Thesis	Aug 2010 – May 2011

4. TITLE AND SUBTITLE

Solar Warning Architecture for Manned Missions to Mars

5a. CONTRACT NUMBER

5b. GRANT NUMBER

5c. PROGRAM ELEMENT NUMBER

6. AUTHOR(S)
Bohren, James S., Major, USAF
Howard, John K., Major, USAF

5d. PROJECT NUMBER
N/A

5e. TASK NUMBER

5f. WORK UNIT NUMBER

7. PERFORMING ORGANIZATION NAMES(S) AND ADDRESS(S)
Air Force Institute of Technology
Graduate School of Engineering and Management (AFIT/EN)
2950 Hobson Way
WPAFB OH 45433-7765

8. PERFORMING ORGANIZATION REPORT NUMBER

AFIT/GSE/ENV/11-J01DL

9. SPONSORING/MONITORING AGENCY NAME(S) AND ADDRESS(ES)

Intentionally Left Blank.

10. SPONSOR/MONITOR'S ACRONYM(S)

11. SPONSOR/MONITOR'S REPORT NUMBER(S)

12. DISTRIBUTION/AVAILABILITY STATEMENT
APPROVED FOR PUBLIC RELEASE; DISTRIBUTION UNLIMITED

13. SUPPLEMENTARY NOTES
This material is declared a work of the U.S. Government and is not subject to copyright protection in the United States.

14. ABSTRACT
Solar radiation storms represent a dire threat to manned interplanetary space travel. Earth's current solar forecasting architecture is Earth-focused and insufficient to provide timely warnings to a manned mission to Mars, therefore a "best value" solar warning architecture must be identified. A total of 14 solar warning architectures were developed by varying 5 solar sensor locations, 2 processing locations, and 2 communications strategies. Using Satellite Tool Kit, performance of the candidate architectures in terms of Warning Time and Solar Coverage was quantified during a Mars mission scenario based on NASA's Design Reference Architecture 5.0. Cost of each candidate architecture was estimated by parametrically determining the total dry mass of each. Efficient frontiers graphs for Warning Time and Solar Coverage versus Dry Mass were developed which depicted the relative cost-benefit of each candidate. A value model was also applied to develop an overall performance value efficient frontier. The analysis indicates a solar sensor and processing capability onboard the manned spacecraft itself is the "best value" solution providing the most performance in return for cost.

15. SUBJECT TERMS
Mars, Manned, Solar Weather, Radiation, Warning, Architecture, Efficient Frontier

16. SECURITY CLASSIFICATION OF:			17. LIMITATION OF ABSTRACT	18. NUMBER OF PAGES	19a. NAME OF RESPONSIBLE PERSON
a. REPORT	b. ABSTRACT	c. THIS PAGE			Dr. John M. Colombi (AFIT/ENV)
U	U	U	UU	133	19b. TELEPHONE NUMBER *(Include area code)* 937-255-3355 x3347 john.colombi@afit.edu

Standard Form 298 (Rev. 8-98)
Prescribed by ANSI Std. Z39-18

Form Approved
OMB No. 074-0188